

**AZO DYE TRANSFORMATION
BY ENZYMATIC AND CHEMICAL SYSTEMS**

Sangkil Nam

B.S., University of Kansas, 1994

A dissertation submitted to the faculty of the
Oregon Graduate Institute of Science and Technology
in partial fulfillment of the
requirements for the degree
Doctor of Philosophy
in
Biochemistry and Molecular Biology

November 1998

The dissertation "Azo Dye Transformation by Enzymatic and Chemical Systems" by Sangkil Nam has been examined and approved by the following Examination Committee:

V. Renganathan, Advisor
Associate Professor

Thomas M. Loehr
Professor

Paul G. Tratnyek
Associate Professor

Gebre Woldegiorgis
Associate Professor

ACKNOWLEDGMENTS

I wish to dedicate this thesis to my wife Kabsoon, my son Luke, and my daughter Arin. My wife has constantly supported me with her self-sacrificing love for the last eight and a half years, since I started studying my new major, Chemistry, at the University of Kansas. She provided more love, attention, and support than I deserved. Luke and Arin have been a constant source of joy.

I would like to thank my parents, my wife's parents, and all my family members for their valuable support and encouragement.

I would like to thank my advisor Dr. V. Renganathan for his constant help throughout my Ph.D. studies. His scientific enthusiasm, patience, and valuable advice enabled me to successfully complete my studies at OGI. I would like to thank Dr. Paul G. Tratnyek for helping me study QSARs, which would have been impossible without his help. I would also like to thank my thesis committee for their efforts on my behalf.

TABLE OF CONTENTS

ACKNOWLEDGEMENTS	iii
TABLE OF CONTENTS	iv
LIST OF TABLES	vii
LIST OF FIGURES	viii
ABSTRACT	xi
CHAPTER 1. INTRODUCTION	1
1.1 A Perspective of Azo Dyes	1
1.1.1 Introduction to azo dyes	1
1.1.2 Pollution created by azo dyes	4
1.1.3 Carcinogenicity and toxicity of azo dyes	4
1.1.4 Processes for eliminating dyes from effluent	5
1.2 Biological Reduction and Oxidation	8
1.2.1 Biological reduction	8
1.2.2 Biological oxidation	10
1.3 New Technologies for Azo Dye Waste Treatment	18
1.3.1 Advanced oxidation processes	18
1.3.2 Photochemical oxidation	19
1.3.3 Chemical oxidation	19
1.3.4 Degradation of organic pollutants by AOPs	20
1.4 Thesis Outline	21
CHAPTER 2: A QSAR STUDY OF AZO DYE OXIDATION BY PEROXIDASES	25
2.1 Introduction	25

2.2	Materials and Methods	29
2.2.1	Chemicals	29
2.2.2	Synthesis of azo dyes	29
2.2.3	Preparations of lignin and manganese peroxidases	30
2.2.4	Azo dye reaction by peroxidases	30
2.2.5	Comparing Mn ^{III} -malonate reaction with MnP reaction	31
2.2.6	Correlation analysis	31
2.3	Results	32
2.3.1	Substrate specificity of HRP	32
2.3.2	Substrate specificity of MnP	32
2.3.3	Substrate specificity of LiP	35
2.4	Discussion	37
 CHAPTER 3: OXIDATION OF AZO DYES BY THE Fe^{III}/H₂O₂ SYSTEM		48
3.1	Introduction	48
3.2	Materials and Methods	51
3.2.1	Chemicals	51
3.2.2	Syntheses of azo dyes	51
3.2.3	¹⁴ C-radiolabeled azo dye synthesis	51
3.2.4	Experimental procedures	53
3.3	Results and Discussion	55
3.3.1	Effects of azo dye structures	55
3.3.2	Product analysis and probable mechanism	57
3.3.3	Effect of H ₂ O ₂ concentrations on azo dye oxidation	63
3.3.4	Estimations of ·OH generation and H ₂ O ₂ decomposition	63
3.3.5	Effect of additives on azo dye oxidation	63
 CHAPTER 4: NON-ENZYMATIC REDUCTION OF AZO DYES BY NADH		74
4.1	Introduction	74
4.2	Materials and Methods	76
4.2.1	Chemicals	76

4.2.2	Syntheses of azo dyes	76
4.2.3	Reduction of azo dye with NADH	76
4.2.4	Effect of pH on azo dye reduction	76
4.2.5	Effect of NADH levels on azo dye reduction	76
4.2.6	Kinetics of azo dye reduction	78
4.2.7	Analytical methods	78
4.3	Results and Discussion	78
4.3.1	pH effect on azo dye reduction	79
4.3.2	Effect of NADH levels on azo dye reduction	79
4.3.3	Product analysis	79
4.3.4	Kinetics of azo dye reduction	84
4.3.5	Proposed mechanism for azo dye reduction by NADH	84
4.3.6	Effect of dye structures on azo dye reduction	88

CHAPTER 5: KINETICS OF AZO DYE REDUCTION BY ZERO-VALENT

	IRON	92
5.1	Introduction	92
5.2	Materials and Methods	93
5.2.1	Chemicals	93
5.2.2	Batch system	96
5.2.3	Analytical methods	96
5.3	Results and Discussion	96
5.3.1	Characterization of reduction products	96
5.3.2	Kinetics	98
5.3.3	Effects of azo dye structure on k_{obs} values	105
5.4	Conclusions	106

CHAPTER 6. FINAL COMMENTS 109

LITERATURE CITED 112

BIOGRAPHICAL SKETCH 129

LIST OF TABLES

1.1	Azo dye degradation by AOPs	21
2.1	Oxidation of substituted phenolic azo dyes by HRP, MnP, and LiP	33
2.2	Comparison of specific activities of HRP and LiP for phenolic compounds	34
2.3	Comparison of azo dye oxidation by MnP and Mn ^{III} -malonate complex . . .	36
2.4	Representative descriptor variables related to the correlation analysis of azo dye oxidation by peroxidases	41
2.5	Comparison of log activity of peroxidase versus $\Sigma\sigma$, $\Sigma\sigma$, $\Sigma\sigma^0$, and $\Sigma\sigma^+$. .	43
2.6	Descriptors used in the correlation analysis of azo dye oxidation by peroxidases	45
3.1A	Oxidation of 4-(4'-sulfophenylazo)-phenol dyes	52
3.1B	Oxidation of 2-(4'-sulfophenylazo)-phenol dyes	52
3.1C	Oxidation of commercial azo dyes	52
3.2	Descriptors used in the correlation analysis of azo dye oxidation by Fe ^{III} /H ₂ O ₂	59
3.3	Effect of additives on Orange II decolorization by Fenton reagent	68
4.1A	Reduction of 4-(4'-sulfophenylazo)-phenol dyes by NADH	77
4.1B	Reduction of 2-(4'-sulfophenylazo)-phenol dyes by NADH	77
4.1C	Reduction of commercial azo dyes by NADH	77
5.1	Dyes used and their physical properties	94
5.2	Summary of kinetic data	101
5.3	LUMO energy of azo dyes	107

LIST OF FIGURES

1.1	Classification of dyes by chemical structure	2
1.2	Scheme of azo dye synthesis	3
1.3	Carcinogenic azo dyes	6
1.4	Proposed pathway for the degradation of Mordant Yellow 3 by mixed bacteria	9
1.5	Catalytic cycles for LiP and MnP	14
1.6	Proposed mechanism for the desulfonation of 3,5-dimethyl-4- hydroxy- and 3,4-dimethyl-6-aminobenzenesulfonic acids	16
1.7	Proposed mechanism of 1-(4-acetamidophenylazo)-2-naphthol by peroxidases	17
1.8	Probable mechanism for benzene generation from the degradation of azo dyes with phenylazo substitution by $\cdot\text{OH}$: $\text{R} = \text{NH}_2, \text{OH}$	23
2.1	The mechanism for the oxidation of 4-(4'-sulfophenylazo)-2,6- dimethylphenol by LiP	26
2.2	Structures of synthetic azo dyes tested	28
2.3	A, B, C, and D. Plots of log activity of HRP, MnP, and LiP versus the sum of substituent constants ($\Sigma\sigma$, $\Sigma\sigma^-$, $\Sigma\sigma^0$, and $\Sigma\sigma^+$) for data shown in Table 2.4	40
2.4	A, B, C. A plot of log activity of HRP, MnP, and LiP versus the sum of substituent constants for data shown in Table 2.6	44
3.1	Structures of azo dyes	56
3.2	A plot of amount of dye decolorized versus charge density on the protonated and deprotonated forms of azo dyes	58
3.3	HPLC analysis of products from $\text{Fe}^{\text{III}}/\text{H}_2\text{O}_2$ oxidation of Orange II	60
3.4	Mass spectrum of 4-hydroxyazobenzene oxidation product acetylated	

	with pyridine and acetic anhydride (1:2)	61
3.5	A proposed mechanism for the degradation of Orange II by Fe ^{III} /H ₂ O ₂ . . .	62
3.6	Oxidation of Orange II at various [H ₂ O ₂]	64
3.7	Estimation of hydroxyl radical concentrations	65
3.8	H ₂ O ₂ consumption in Fenton's reaction	66
3.9	Effect of KNO ₃ on Orange II decolorization	69
3.10	Effect of nitrate levels on Orange II oxidation	70
3.11	Effect of KNO ₃ on oxidation of 4-(4'-sulfophenylazo)-2,6- dimethylphenol	71
3.12	Effect of nitrate on the mineralization of ¹⁴ C-labeled 4-(4'- sulfophenylazo)-2,6-dimethylphenol	72
4.1	Effect of pH on the reduction of Orange I by NADH	80
4.2	Effect of different NADH concentrations on the reduction of Orange I	81
4.3	HPLC analysis of Orange I reduction products by NADH	82
4.4	The mass spectrum of 4-hydroxyazobenzene reduction product acetylated with pyridine and acetic anhydride (1:2)	83
4.5	The reduction of Orange I by NADH	85
4.6	Linear regression of log C/C ₀ versus time for the same data shown in Figure 4.5	86
4.7	A probable mechanism for azo dye reduction by NADH	87
4.8	Structures of azo dyes	89
5.1	Dye structures	95
5.2	Time course of decolorization of Orange II by Fe ⁰ and formation of 4-aminobenzenesulfonic acid	97
5.3	C ₀ and C are the Orange II concentrations at time 0 and time t, respectively	99
5.4A	Effect of mixing rate on the pseudo first-order rate constant for Crocein Orange G reduction	103
5.4B	A plot of rate of Crocein Orange G reduction versus square root of rpm for the data shown in Figure 5.4A	103

5.5A	Effect of initial dye concentration on the pseudo first-order rate constant for Crocein Orange G reduction a 100 rpm on an orbital-shaker	104
5.5B	A plot of rate of Crocein Orange G reduction versus initial dye concentration for the data shown in Figure 5.5A	104
5.6	Correlation between k_{obs} and E_{LUMO} for data shown in Table 5.3	108

ABSTRACT

Azo Dye Transformation by Enzymatic and Chemical Systems

Sangkil Nam

Supervising Professor: V. Renganathan

Almost all dyes used in industrial applications are synthetic, and of these, approximately 50% are azo dyes. Azo dyes are recalcitrant to biodegradation; yet they are released into the environment with little or no treatment. This dissertation describes an investigation of azo dye decolorization by peroxidases, hydroxyl radicals, zero-valent iron, and NADH. Since azo dyes have widely differing substituent patterns, the effect of substituents on the reaction was examined using quantitative structure–activity relationships (QSARs). Two different groups of azo dyes were used: 4-(4'-sulfophenylazo)-phenol and 2-(4'-sulfophenylazo)-phenol. Substituent changes were made only in the phenolic ring of the azo dyes.

Horseradish peroxidase (HRP), manganese peroxidase (MnP), and lignin peroxidase (LiP) oxidized a variety of substituted 4-(4'-sulfophenylazo)-phenol dyes. None of the peroxidases oxidized the 2-(4'-sulfophenylazo)-phenol dyes. HRP was the most active in dye oxidation, and LiP was the least active.

Enzyme reactions can be controlled by electronic factors, steric factors, or both. In the Hammett correlation analysis, HRP and MnP oxidation of azo dyes exhibited a negative correlation with σ constants, suggesting that HRP and MnP prefer substrates with electron-donating substituents ($-\sigma$) in the phenolic ring. MnP showed a stronger correlation compared to HRP, suggesting that MnP reactions are primarily controlled by electronic factors. HRP showed only a weak correlation, suggesting that its reaction could be controlled by electronic and steric factors.

Hydroxyl radicals generated using Fe^{III}-EDTA and H₂O₂ at pH 7.0 readily decolorized all dyes tested. Substitution of an electron-withdrawing substituent increased the rate of dye oxidation. A correlation was observed between the rate of decolorization and the charge density of deprotonated azo dyes, suggesting that the initial attack of ·OH is on the phenolate species of azo dyes whose formation is favored when the phenolic ring is substituted with electron-withdrawing substituents.

All azo dyes tested were reduced by NADH under aerobic conditions to produce two aromatic amines. Reduction was favored at low pH. The substituent effect was dependent upon the location in the phenolic ring. For example, substitution of a chlorine at the 2-position decreased the azo linkage reduction, whereas its introduction into the 3-position (ortho to azo linkage) enhanced reduction. A 2-chlorine substitution decreases the *pKa* of phenol and favors phenoxide formation. The phenoxide donates electron density to the phenolic ring and the azo linkage. The increased electron density of the azo linkage might resist reduction by NADH. Alternatively, a 3-chlorine substitution might not substantially decrease the dye *pKa*; nevertheless, it can strongly deplete the electron density from azo linkage via inductive mechanisms and this could favor reduction of azo linkage. However, NADH reduction did not exhibit a strong correlation with parameters such as *pKa* and substituent constants.

Zero-valent iron readily reduced azo dyes at neutral pH under anaerobic conditions. Reduction rates were apparently influenced by mass transport of the dye to the iron metal surface. A weak correlation was observed between *k*_{obs}, the first-order rate constant, and energy of the lowest unoccupied molecular orbital, suggesting that reduction might also be influenced by the reduction potential of the dyes.

CHAPTER 1

INTRODUCTION

1.1 A Perspective of Azo Dyes

1.1.1 Introduction to azo dyes

Dye stuffs are classified based on chemical structure, usage, or application method (Zollinger, 1987; Gregory, 1990). Based on chemical structure, they can be classified as azo dyes, anthraquinone dyes, triarylmethane dyes, indigoid dyes, and polycyclic aromatic carbonyl dyes (Figure 1.1). Azo dyes constitute more than 50% of all dyes produced in the world (Betowski et al., 1987; Zollinger, 1987), and their structure is characterized by the presence of an azo linkage ($-N=N-$).

Azo dyes are produced by coupling a diazonium salt of an aromatic amine with either a phenol under alkaline conditions or an aromatic amine under acidic conditions (Figure 1.2) (Zollinger, 1987; Gregory, 1990). Since the diazonium salts are unstable, the reaction temperature is maintained at 0–4°C. Azo dyes became popular because they can be easily synthesized (Glover, 1992). Depending on the substituents, azo dyes can be either water-soluble or -insoluble. Azo dyes such as food dyes and reactive dyes contain one or more sulfonate ($-SO_3^-$) or carboxylate ($-COO^-$) groups, which enhance dye solubility in water. These groups also help to bind dye molecules to fiber surfaces (polar surfaces) such as wool and cotton (Wade, 1991). However, water-insoluble dyes such as disperse dyes are hydrophobic and contain nitro- and chloro-substituents (Gregory, 1990). Disperse dyes are used for dyeing synthetic fibers such as nylon and polyester.

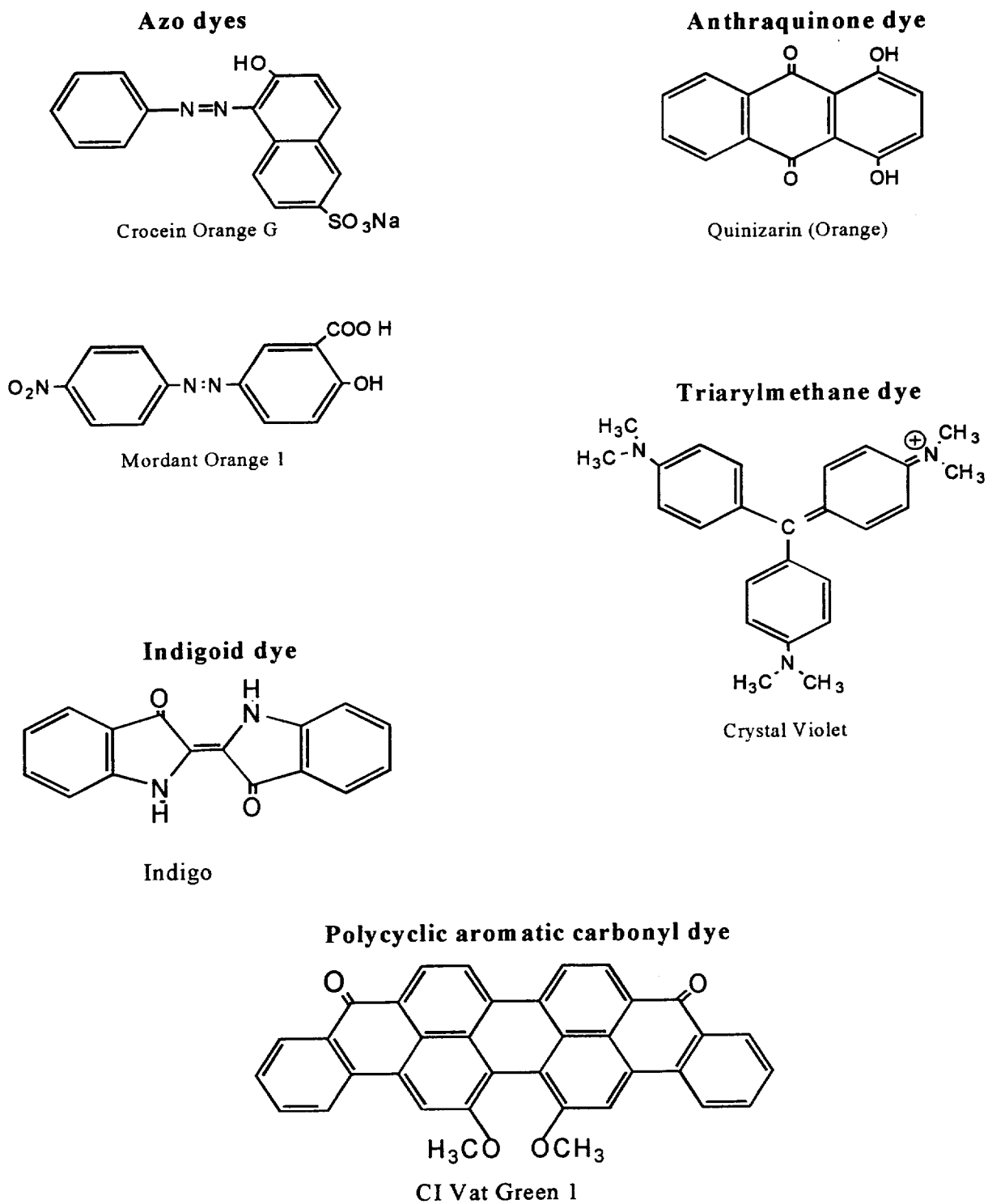


Figure 1.1 Classification of dyes by chemical structure.

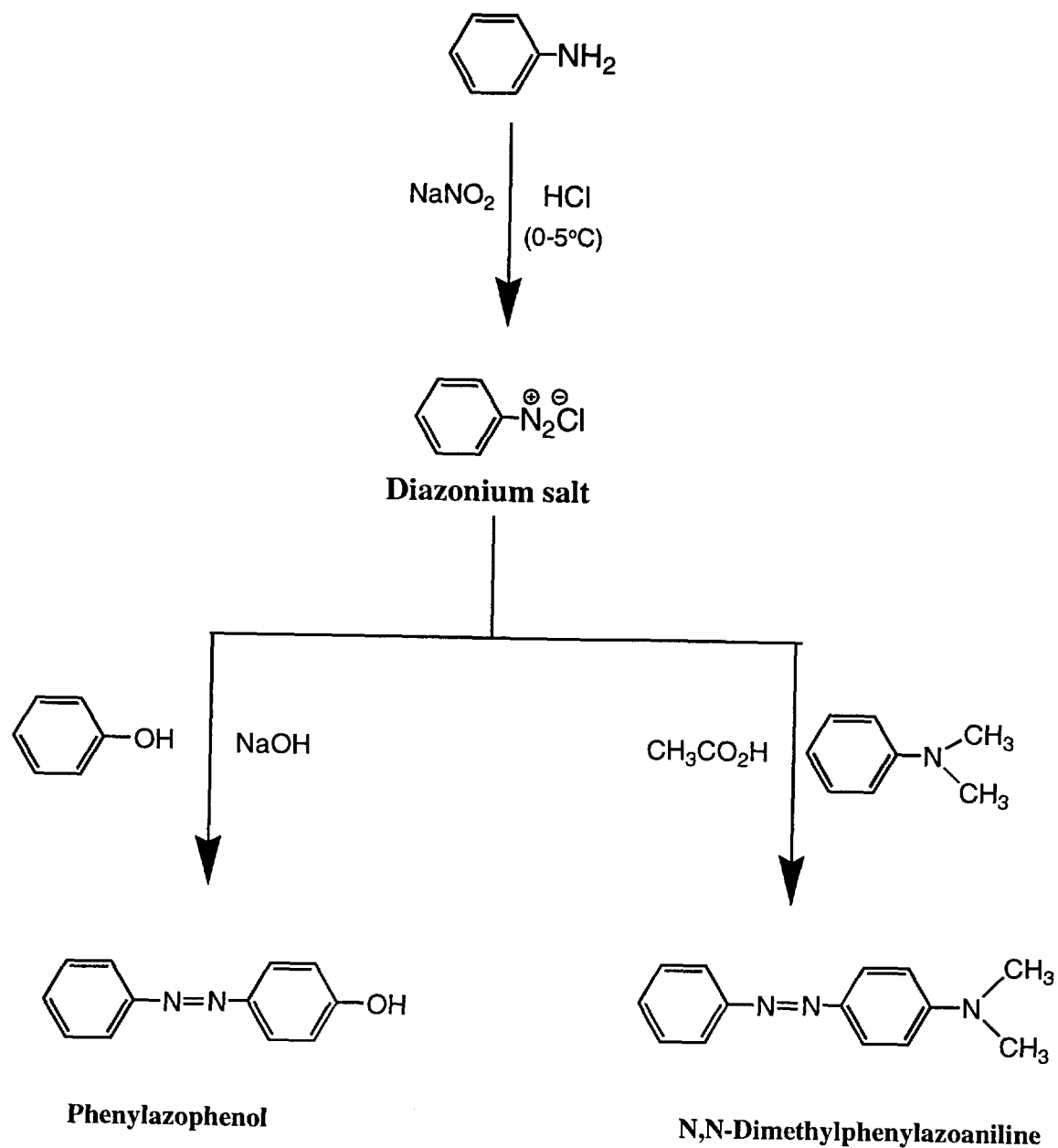


Figure 1.2 Scheme of azo dye synthesis.

[Reprinted with permission of the American Society for Microbiology; originally published as Fig. 1 in: Spadaro, J. T., Gold, M. H., and Renganathan, V. (1992) Degradation of azo dyes by the lignin-degrading fungus *Phanerochaete chrysosporium*. *Appl. Environ. Microbiol.* **58**, 2397-2401.]

1.1.2 Pollution created by azo dyes

Approximately 3,000 different azo dyes are used in industry (Chudgar, 1992). In 1994, over 219,000 tons of synthetic organic colorants were produced in the United States alone (U.S. International Trade Commission, 1995). The textile industry consumes the largest volume of dyes, and it is also one of the largest water-consuming industries in the world (Vaidya & Datye, 1982). It is estimated that approximately 10–15% of textile dyes used are discharged in the waste stream during the manufacturing processes (Brown et al., 1981). About 20% of dye waste ends up in the environment (Clarke & Anliker, 1980). For example, it has been reported that at least seven disperse and seven acid dyes, which originated from a carpet mill, were found in the Coosa River Basin in Georgia (Tincher & Robertson, 1982). Disperse dyes which were released from a textile mill were also found in river water and sediments in the Yamaska River in Quebec, Canada (Maguire & Tkacz, 1991).

In general, synthetic azo dyes have substitutions (such as sulfonic acid, bromo, fluoro, nitro, or chloro groups) as part of their structure. Consequently, these azo dyes are highly resistant to degradation (Clarke & Anliker, 1980; Kulla et al., 1983). Several azo dyes and their reductive metabolism products are toxic (Jungclaus et al., 1976; Nelson & Hites, 1980; Cartwright, 1983; Matthews et al., 1993). In addition, dye industry effluent also contains other environmental contaminants, such as heavy metals, detergents, metal complexing agents, dye carriers (e.g., phenols, chlorinated benzenes, and phthalates), and inorganic anions (e.g., chloride, sulfate, and carbonate) (Park & Shore, 1984). Some of these are additives used in the dyeing process. Thus, dye industry effluent is a significant source of environmental pollution.

1.1.3 Carcinogenicity and toxicity of azo dyes

Several synthetic azo dyes have been classified as carcinogens as well as mutagens (McCann & Ames, 1975; Krishna et al., 1986; Sandhu & Chipman, 1990; Chung & Cerniglia, 1992). For example, azo dyes such as 4-aminoazobenzene, *o*-aminoazotoluene, and 4-methylamino- and 4-dimethylamino-azobenzene are carcinogenic as well as mutagenic (McCann et al., 1975). The carcinogenicity of an

azo dye may be due either to the dye itself or to the aryl amines derived via the reduction transformation of azo dyes. Such reduction can be brought about by biological, chemical, or photochemical systems (Riefe, 1992). In mammals, aryl amines are oxidized to the corresponding aryl-hydroxylamines, which are further transformed to aryl-nitrosoamines by enzymes such as cytochrome P-450, flavin monooxygenases, and peroxidases in liver (Kadlubar, 1987). Aryl-hydroxylamines and aryl-nitrosamines are reactive electrophiles and are capable of forming covalent bonds with DNA (Kadlubar, 1987). Azo dyes are reduced to aryl amines by a flavin-dependent reductase in liver, an extracellular flavin-dependent reductase produced by anaerobic bacteria in the intestine, and even by hepatic cytochrome P-450 under anaerobic conditions (Huang et al., 1979; Rafii et al., 1990). For example, azo dyes such as Evans Blue, Trypan Blue, Direct Black 38, and Direct Blue 6 (Figure 1.3) include a biphenyl diazo linkage. These dyes are transformed to benzidine (4,4'-diaminobiphenyl), a potent carcinogen, via the reductive cleavage of the azo linkage (Brown & DeVito, 1993). Other aryl amines that may be generated via hepatic reduction of azo dyes are 4-aminobiphenyl, α - and β -naphthylamines, dichloro and dimethyl analogs of benzidine and *o*-toluidine (McCann et al., 1975).

1.1.4 Processes for eliminating dyes from effluent

Currently the wastewater from dye industries is treated by physical, chemical, and biological methods (Park & Shore, 1984). Physical methods include adsorption, chemical precipitation, and reverse osmosis (Riefe, 1992). The adsorption process uses activated carbon, and organic pollutants including dyes bind to carbon through hydrophobic interaction (Arvanitoyannis et al., 1987; Yang et al., 1988). In the chemical precipitation process, salts of ferric iron, calcium, magnesium, ferrous iron, and aluminum are used (Fytianos et al., 1985). These inorganic salts form insoluble hydroxides at neutral pH. These precipitated hydroxides remove dyes by adsorbing dye molecules onto them. In the reverse osmosis process, a semipermeable membrane such as cellulose acetate is used. This membrane selectively retains dyes and permits only water to pass through (Park & Shore, 1984).

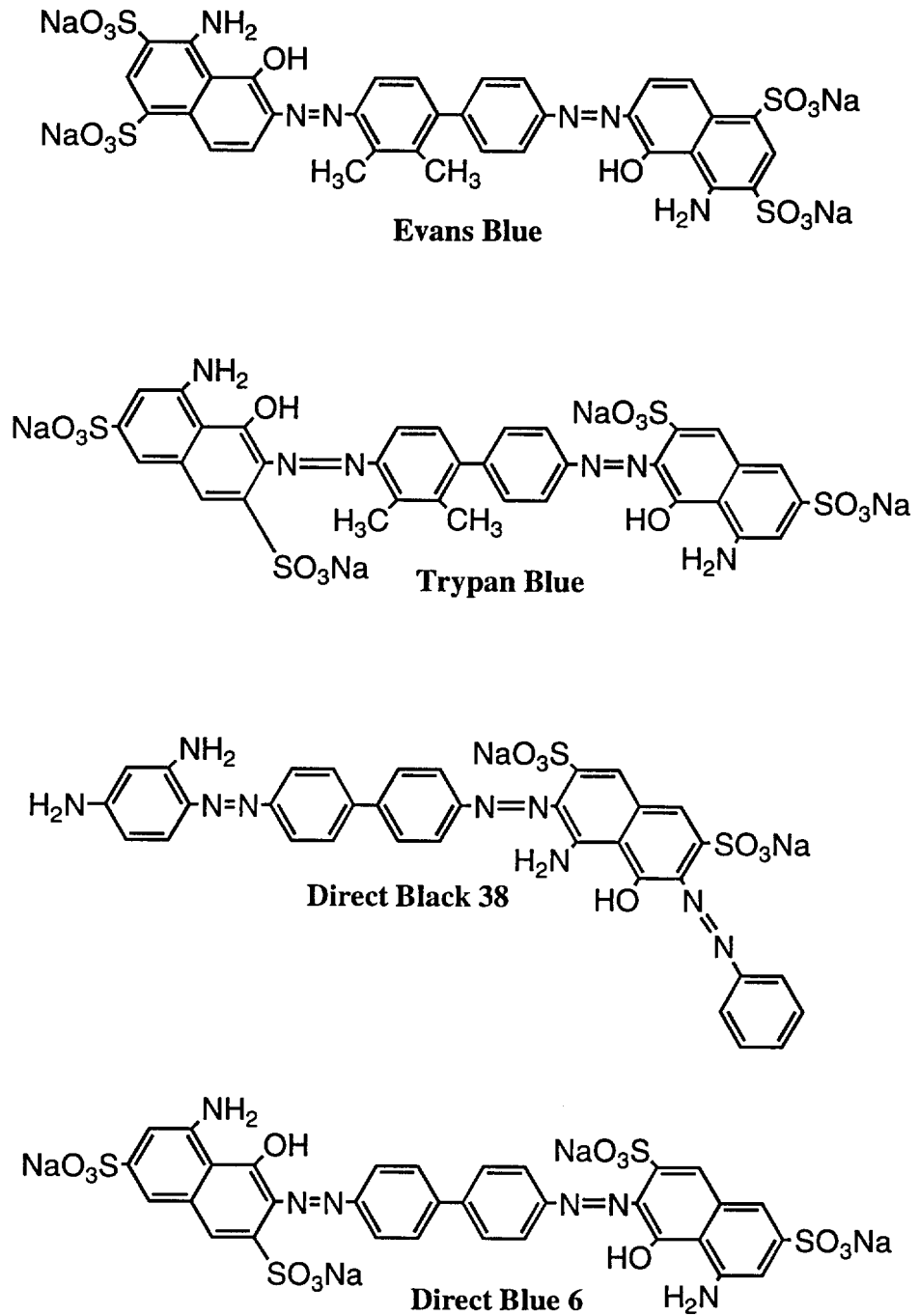


Figure 1.3 Carcinogenic azo dyes.

Chemical processes include reduction and oxidation. In chemical reduction, removal of azo dye color is mainly achieved by the cleavage of the azo linkage using reducing agents such as sodium borohydride, zinc sulfoxylate, sodium hydrosulfite, and thiourea dioxide (Riefe, 1992). Sodium hydrosulfite under alkaline conditions is a powerful reducing agent (Riefe, 1992). Azo dyes also can be treated with oxidizing agents such as chlorine, bleach, ozone, hydrogen peroxide, Fenton reagent, and permanganate (Riefe, 1992).

Synthetic azo dyes often contain azo, nitro, and sulfo groups. These substituents might be responsible for the resistance of azo dyes to biodegradation (Zimmerman et al., 1982). It has been demonstrated that bacterial degradation of dye wastes is difficult (Kulla et al., 1983). Dye degradation systems such as activated sludge treatments are dependent on soil microorganisms in sediments. These organisms do not significantly degrade textile dyes (Pagga & Brown, 1986; Shaul et al., 1991). The color removal by these systems primarily results from the dye adsorption to biomass (Pagga & Brown, 1986). The lignin-degrading white-rot fungus *Phanerochaete chrysosporium* is the only organism that can mineralize both sulfonated and non-sulfonated azo dyes to CO₂ (Paszczynski et al., 1992; Spadaro et al., 1992). However, the white-rot fungi are not yet ready for industrial application.

Industrial dye waste treatments are performed in four stages: preliminary, primary, secondary, and tertiary stages (Riefe, 1992; Atlas & Bartha, 1993). In the preliminary stage, dye wastes are treated by mixing, disinfection, and neutralization. In the primary stage, solid dye wastes are removed by physical methods using screening, sedimentation, and flotation processes. In the secondary stage treatment, pollutants are removed by biological oxidation, biological reduction, chemical separation, and physical separation. In tertiary treatment, non-biodegradable dye wastes are mainly removed by electrochemical, chemical, or ion exchange methods.

Among these treatment processes, flocculation with lime, activated charcoal adsorption, and biotreatment appear to be popular for removing color from effluents (Park & Shore, 1984). Lime treatment and charcoal adsorption generate solid wastes which require costly disposal methods. Biotreatment processes rely on indigenous soil

microorganisms to degrade dye compounds. Since the synthetic dyes are resistant to biodegradation, this process is likely to be inefficient (Brown & Laboureur, 1983; Shaul et al., 1991). Thus, there is a need for the development of treatment technologies that are more effective in eliminating dyes from waste streams at their source.

1.2 Biological Reduction and Oxidation

1.2.1 Biological reduction

1.2.1.1 Bacterial metabolism of azo dyes. A few azo dyes can be degraded by bacteria under both aerobic and anaerobic conditions (Brown & Laboureur, 1983; Haug et al., 1991). Both types of degradation are apparently initiated by the cleavage of the azo linkage (Walker, 1970; Brown & Laboureur, 1983). Azo reductases involved in the reductive process require cofactors such as NADH and NADPH for maximum activity (Chung & Stevens, 1992).

In aerobic bacterial degradation, azo dye is intracellularly reduced to primary aromatic amines, and the amines are then further metabolized via degradative pathways that involve hydroxylations and ring opening reactions (Idaka et al., 1987; Chung & Stevens, 1992; Brown & DeVito, 1993). The azo reductases are apparently inhibited by oxygen (Mason et al., 1978; Brown & Laboureur, 1983). Bacterial dye degradation under aerobic conditions generally requires long adaptation (Yatome et al., 1993). Research in the past two decades has suggested that it is difficult to isolate bacteria which use azo dye as a sole source of carbon.

Many azo dyes are readily reduced to the corresponding aromatic amines by bacteria under anaerobic conditions (Walker, 1970; Mallett et al., 1982). This reduction is non-specific. Since anaerobic bacteria cannot metabolize aromatic amines well, most aromatic amines can be further degraded by aerobic bacteria (Berry et al., 1987; Brown & Hamburger, 1987). For example, Haug et al. (1991) also demonstrated that mixed bacterial cultures (*Pseudomonas* sp. BN9 and BN6), which pass through successive anaerobic and aerobic conditions, can mineralize azo dyes to CO₂ (Figure 1.4). This degradation is initiated by the anaerobic cleavage of the azo

bond, and the amines generated from that process are further degraded under aerobic conditions. Donlon et al. (1997) also demonstrated the partial anaerobic mineralization of Mordant Orange 1 (Figure 1.1) in methanogenic consortia under anaerobic conditions. However, mineralization was very limited. In their study, 4-nitroaniline, a reductive product, was not further mineralized. Zimmerman et al. (1982) reported that bacteria isolated from *Pseudomonas* sp. strains (KF22 and KF46) completely degraded Carboxyorange I and II, but their corresponding sulfo analogs (Orange I and II) were only reduced to the corresponding aromatic amines, which were not further degraded.

1.2.1.2 Azo dye reduction in mammals. In mammals, reductive cleavage of azo linkage might occur in the liver (Walker et al., 1971) or in the intestinal microflora (Scheline et al., 1970; Zimmermann et al., 1982; Idaka et al., 1987). Azo reductases in liver can reduce many azo dyes to their corresponding aromatic amines, showing a broad substrate specificity for water-soluble and water-insoluble azo dyes (Fujita & Peisach, 1977; De Long et al., 1986; Brown & DeVito, 1993). They require cofactors such as NADPH, and have variable oxygen sensitivities, which depend upon dye substrates. It has been reported that hepatic reductase systems in rat liver did not reduce amaranth and tartrazine in the presence of oxygen, but they partially reduced Orange II and Orange G (Brown & DeVito, 1993).

Azo reductases in intestinal bacteria mainly reduce water-soluble azo dyes to their corresponding aromatic amines. The aromatic amines generated are mostly excreted from the body (Brown & DeVito, 1993). It is possible that less soluble amine products are absorbed via the intestinal lining. These reductases are inhibited by oxygen.

1.2.2 Biological oxidation

1.2.2.1 Degradation of organic pollutants by *Phanerochaete chrysosporium*. The plant cell wall consists of cellulose, lignin, and hemicellulose (Eriksson et al., 1990). Lignin is the most abundant aromatic polymer in the biosphere. It is an optically inactive, heterogeneous, and aromatic biopolymer.

Lignin is highly resistant to biodegradation; only white-rot basidiomycetous fungi can completely degrade lignin to CO₂ and H₂O (Kirk & Farrell, 1987; Gold et al., 1989; Higson, 1991). The lignin-degrading system of white-rot fungi is nonspecific in that it can also degrade other aromatic compounds (Bumpus et al., 1985; Tien, 1987; Hammel, 1989; Chung & Aust, 1995).

Phanerochaete chrysosporium is the best studied white-rot fungus. White-rot fungi degrade cellulose under primary metabolic conditions and lignin under secondary metabolic conditions (Kirk et al., 1978). Lignin degradation is regulated by nutrient nitrogen and carbon (Kirk et al., 1978). Lignin-degrading cultures of *P. chrysosporium* produce two extracellular peroxidases—lignin peroxidase (LiP) and manganese peroxidase (MnP)—and glyoxal oxidase, an extracellular H₂O₂-generating system (Gold et al., 1984; Kersten & Kirk, 1987; Hammel & Moen, 1991). The peroxidases are presumed to depolymerize lignin to the corresponding monomers and dimers which are further oxidized by the intracellular enzymes (Hammel & Moen, 1991).

In 1980, Eaton et al. reported that *P. chrysosporium* can degrade chlorinated organic compounds. Later, it was reported that lignin-degrading cultures of *P. chrysosporium* are capable of mineralizing polychlorinated biphenyls (Eaton, 1985). Priority organic pollutants such as DDT, benzo[a]pyrene, and dioxin were degraded by lignin-degrading cultures of *P. chrysosporium* (Bumpus et al., 1985). These studies led to immense interest in the bioremediation capabilities of white-rot fungi. Since then, numerous studies have demonstrated that lignin-degrading cultures of *P. chrysosporium* can degrade a number of aromatic pollutants, including nitrotoluenes (Fernando et al., 1990; Valli et al., 1992a), polycyclic aromatic hydrocarbons (Bumpus et al., 1985; Sanglard et al., 1986; Hammel et al., 1991), 2,4,5-trichlorophenoxyacetic acid (Ryan & Bumpus, 1989; Yadav & Reddy, 1992), polychlorobiphenyls (Dietrich et al., 1995), and alachlor (Ferrey et al., 1994). The probable degradation pathways of 2,4-dichlorophenols (Valli & Gold, 1991), 2,7-dichlorodibenzo-*p*-dioxin (Valli et al., 1992b), 2,4,5-trichlorophenol (Joshi & Gold, 1993), 2,4-dinitrotoluene (Valli et al., 1992a), phenanthrene (Hammel et al., 1992), and anthracene (Hammel et al., 1991) by *P. chrysosporium* have been proposed.

1.2.2.2 Degradation of synthetic dyes by *P. chrysosporium*. Glenn and Gold (1983) first demonstrated that the lignin-degrading system of *P. chrysosporium* is capable of decolorizing sulfonated polymeric dyes such as Poly B-411, Poly R-418, and Poly Y-606. Cripps et al. (1990) demonstrated that *P. chrysosporium* under ligninolytic conditions can decolorize azo dyes such as Orange II, Tropeolin O, and Congo Red. Bumpus and Brock (1988) reported that *P. chrysosporium* can also decolorize triphenylmethane dyes such as Crystal violet, Basic green 4, Brilliant green, and Cresol red. Since decolorization does not demonstrate complete dye degradation but only transformation of the chromophoric group of dyes, Spadaro et al. (1992) examined complete degradation of azo dyes using ¹⁴C-labeled compounds. They demonstrated that *P. chrysosporium* under low nitrogen conditions can mineralize non-sulfonated hydrophobic azo dyes such as Disperse Yellow 3, *N,N*-dimethylphenylazoaniline, Disperse Orange 3, and Solvent Yellow 14 to CO₂. In that study, the azo dyes containing aromatic substituents such as amino, acetamido, hydroxyl, or nitro groups were found to be mineralized to a greater extent than the unsubstituted dyes. Paszczynski et al. (1992) demonstrated that *P. chrysosporium* can also mineralize several water-soluble sulfonated azo dyes.

1.2.2.3 Degradation of synthetic dyes by other white-rot fungi. A common characteristic of white-rot fungi is their ability to degrade lignin under nitrogen-limiting conditions. Among these fungi, *Phlebia tremellosa*, *Phlebia radiata*, *Dichomitus squalens*, and *Trametes versicolor* mineralize lignin efficiently (Hatakka, 1994). Recently, azo dyes such as Reactive Blue 38 and Reactive Violet 5 were shown to be decolorized by *T. versicolor* and *Bjerkandera adusta* (Heinfling et al., 1997; Young & Yu, 1997). Remazol Brilliant Blue R was demonstrated to be decolorized by an extracellular H₂O₂-requiring enzyme extracted from the white-rot fungus *Pleurotus ostreatus* (Shin et al., 1997). Remazol Brilliant Blue R was also decolorized by another white-rot fungus, *Pycnoporus cinnabarinus* (Schliephake & Lonergan, 1997).

1.2.2.4 Oxidation of azo dyes by peroxidases.

1.2.2.4.1 Peroxidases. In the early 1980s it was first observed that ligninolytic cultures of *P. chrysosporium* produce two extracellular peroxidases,

LiP and MnP (Glenn et al., 1983; Tien & Kirk, 1983; Gold et al., 1984). These peroxidases were induced under nutrient nitrogen-limiting conditions (Kirk & Farrell, 1987; Gold et al., 1989). LiP and MnP oxidize several phenol- and aniline-type compounds (Glenn et al., 1986; Kirk et al., 1986; Renganathan & Gold, 1986; Wariishi et al., 1989b).

The catalytic cycles of horseradish peroxidase (HRP), LiP, and MnP are similar (Figure 1.5) (Chance, 1952; Renganathan & Gold, 1986; Wariishi et al., 1988). In this cycle, the native enzyme, which is in the ferric (Fe^{III}) form, is first oxidized by H_2O_2 to produce compound I, a two-electron oxidized intermediate. Compound I is then reduced by the one-electron oxidation of substrate, forming compound II, a ferryl-oxo intermediate. Reduction of compound II by a second electron of substrate brings the enzyme back to the native enzyme and completes the catalytic cycle. The catalytic cycle of MnP is different from those of other peroxidases, because MnP requires Mn^{II} as an electron donor (Figure 1.5) (Wariishi et al., 1988). In the catalytic cycle, Mn^{II} is oxidized to Mn^{III} (Wariishi et al., 1989a). In the absence of substrate and in the presence of excess H_2O_2 , compound II is converted to compound III, a ferrous-oxo or ferric superoxide species. In this process, H_2O_2 reduces compound II by one electron to produce a ferric enzyme and a superoxide radical. The latter readily combines with the ferric peroxidase to produce compound III.

Veratryl alcohol (VA) (3,4-dimethoxybenzyl alcohol) is a fungal secondary metabolite produced in ligninolytic cultures of *P. chrysosporium* (Eriksson et al., 1990; Valli et al., 1990). LiP can oxidize a poor substrate efficiently in the presence of VA. However, in the absence of VA, LiP is inactivated because it is readily converted to compound III. VA can help LiP oxidation of poor substrates by two different mechanisms (Valli et al., 1990; Wariishi & Gold, 1990). Since it is a good substrate, it could readily reduce compound II and thus avoid formation of compound III. Alternatively, LiP can also revert compound III to the native enzyme by releasing a superoxide from compound III. The exact mechanism by which VA releases superoxide from compound III is not known.

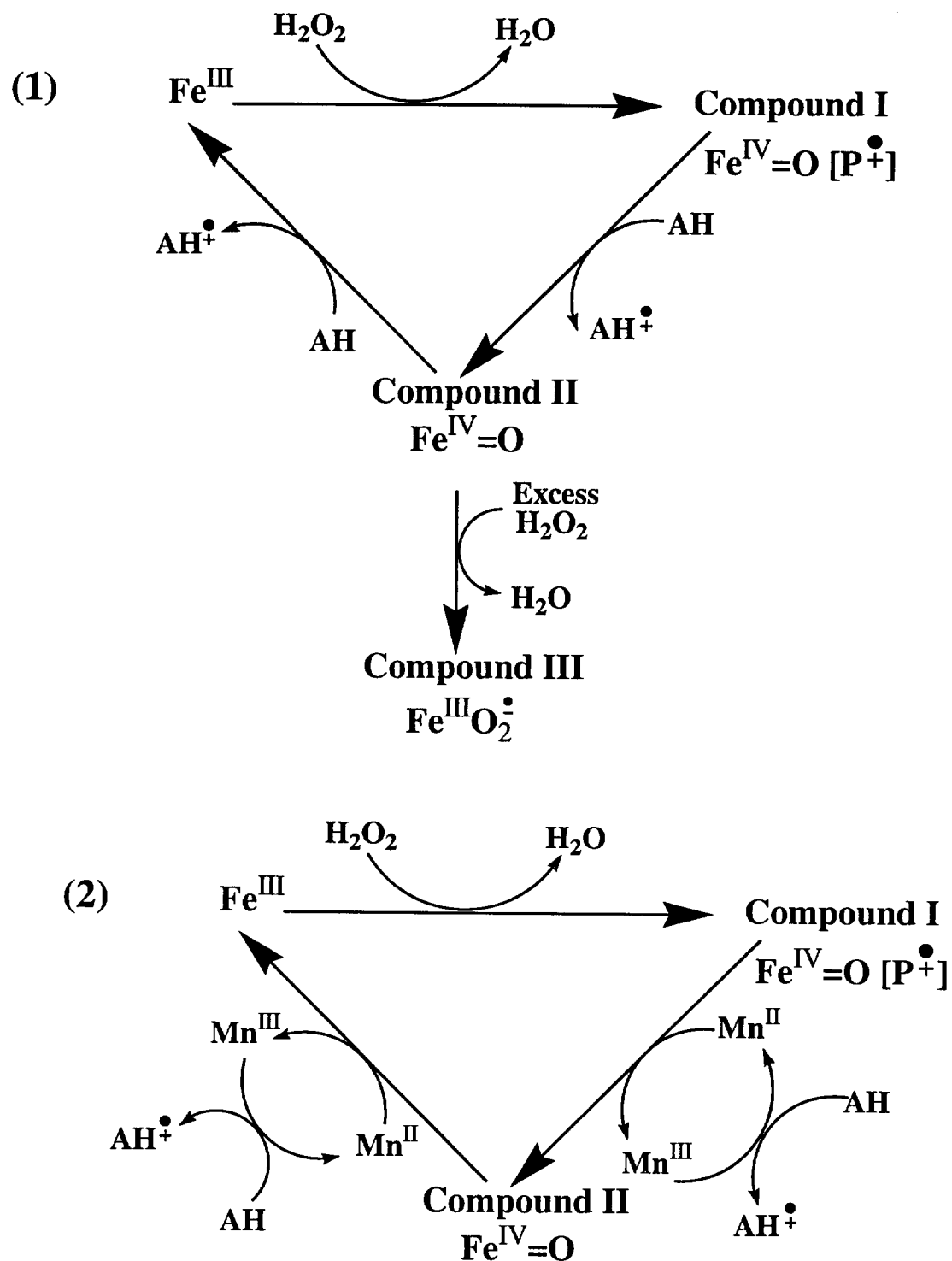


Figure 1.5 Catalytic cycles for LiP (1) and MnP (2).

[Reprinted with permission of the American Chemical Society; originally published as Fig. 3 in: Gold, M. H., Wariishi, H., and Valli, K. (1989) Extracellular peroxidases involved in lignin degradation by the white-rot basidiomycete *Phanerochaete chrysosporium*. *ACS Symp. Ser.* 389, 127-140.]

1.2.2.1.2 Mechanism for the oxidation of azo dyes by

peroxidases. Substrates of LiP, MnP, and HRP include various substituted phenols and anilines. Peroxidases are known to dehalogenate, denitrate, and desulfonate these aromatic substrates (Figure 1.6) (Valli & Gold, 1991; Valli et al., 1992; Muralikrishna & Renganathan, 1993). Thus peroxidases readily oxidize azo dyes that are substituted with either a hydroxyl or amine group. Recently our laboratory proposed the mechanism of oxidation of Orange II (a water-soluble azo dye) and an analog of Disperse Yellow 3 (a hydrophobic azo dye) by peroxidases (Spadaro & Renganathan, 1994; Chivukula et al., 1995). Goszycznski et al. (1994) also reported the possible mechanism of azo dye oxidation by LiP. However, the initial steps of dye oxidation mechanisms proposed in the two reports are similar.

1-(4'-Acetamidophenylazo)-2-naphthol (NDY3) is an analog of Disperse Yellow 3 (DY3). In the oxidation of NDY3, peroxidases successively oxidize the naphthol ring of NDY3 by two one-electron steps to produce a carbonium ion on the C-1 carbon of the naphthol ring (Figure 1.7). Then, an unstable tetrahedral intermediate is produced by nucleophilic attack of H₂O. This intermediate breaks down to generate 1,2-naphthoquinone and 4-acetamidophenyldiazine. One-electron oxidation of phenyldiazene by O₂ generates a phenyldiazene radical. The latter radical loses the azo linkage as nitrogen via homolytic bond cleavage to yield an acetamidophenyl radical, which abstracts a hydrogen radical from the organic impurities in the medium to yield acetanilide.

Oxidation of Orange II by LiP generated 1,2-naphthoquinone and a novel 4-sulfophenyl hydroperoxide (Chivukula et al., 1995). The mechanism for oxidation of Orange II is similar to the NDY3 mechanism. Orange II oxidation by peroxidases generate 1,2-naphthoquinone and 4-sulfophenyl diazene. The latter is non-enzymatically oxidized first to sulfophenyl diazene radical and then to sulfophenyl radical. The phenyl radical is then scavenged by oxygen to produce a stable 4-sulfophenyl hydroperoxide (SPH). SPH is novel because it is the first phenyl hydroperoxide known in organic chemistry (Chivukula et al., 1995). It is also unusual in that it is stable in the presence of transition metals, and hydroperoxide can be displaced with azide and iodide by nucleophilic substitution reaction. Formation of

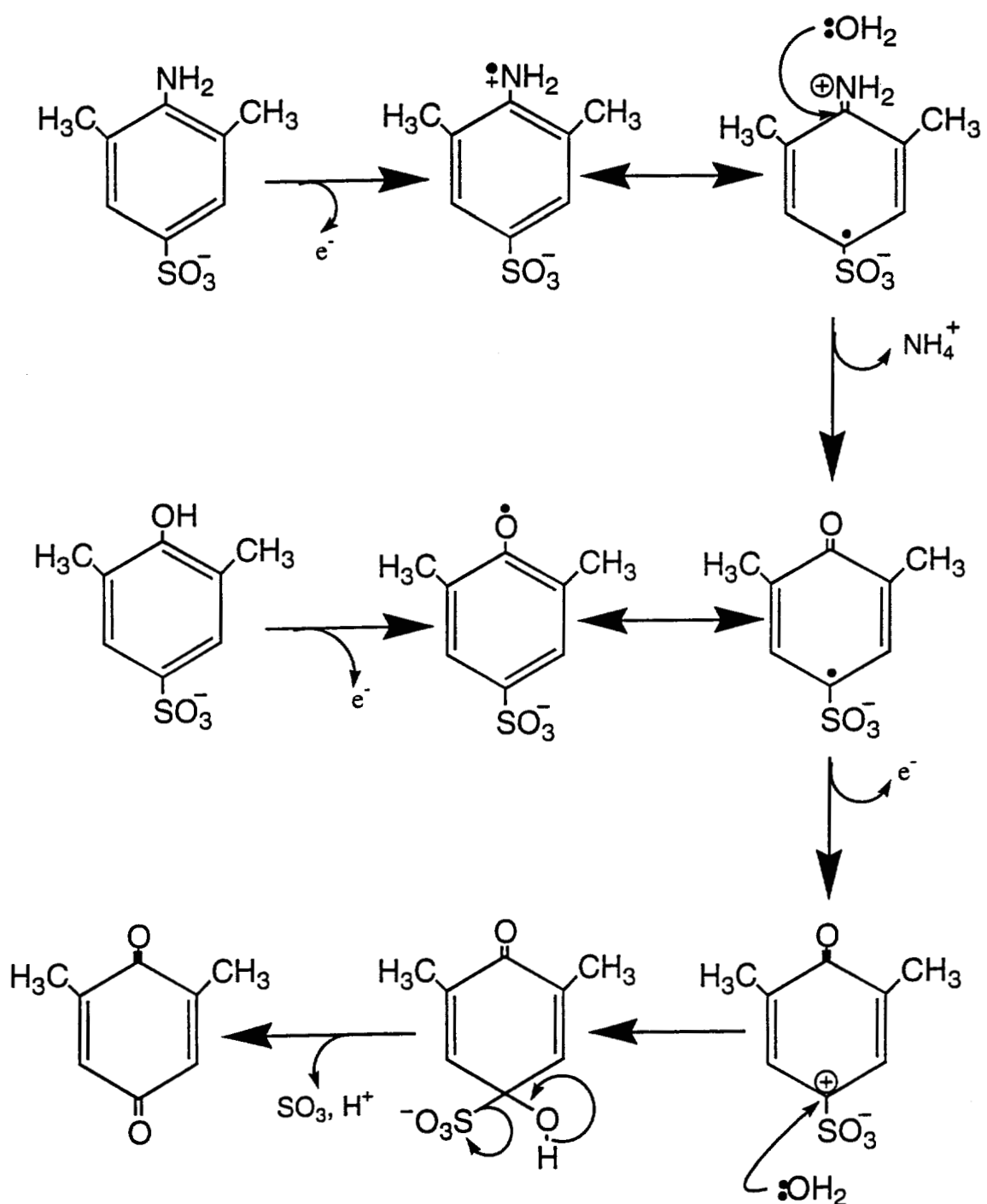


Figure 1.6 Proposed mechanism for the desulfonation of 3,5-dimethyl-4-hydroxy- and 3,4-dimethyl-6-aminobenzenesulfonic acid.

[Reprinted with permission of Academic Press; originally published as Fig. 3 in: Muralikrishna, C., and Renganathan, V. (1993) Peroxidase-catalyzed desulfonation of 3,5-dimethyl-4-hydroxy and 3,5-dimethyl-4-aminobenzenesulfonic acids. *Biochem. Biophys. Res. Commun.* 197, 798-804.]

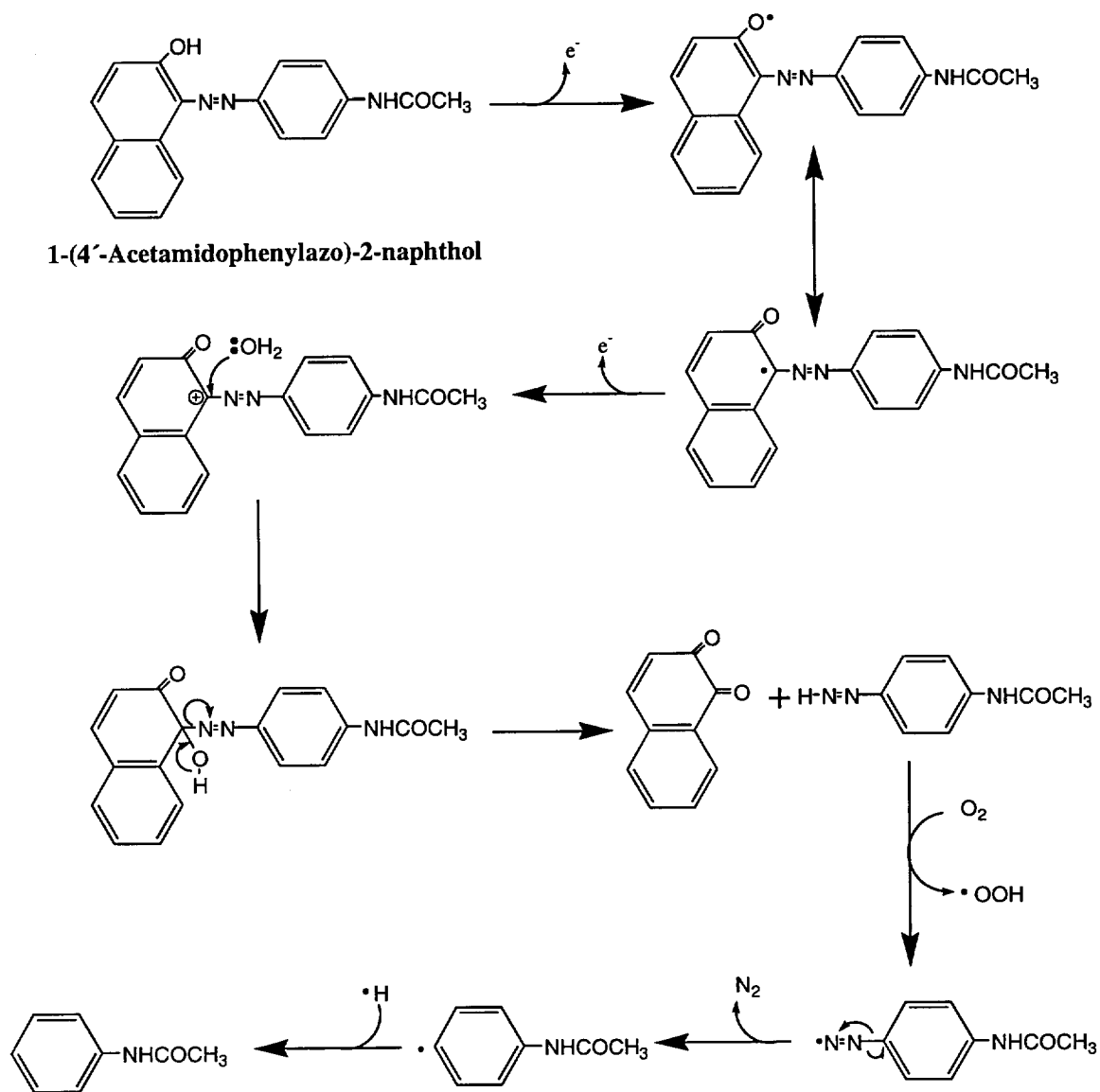


Figure 1.7 Proposed mechanism of 1-(4'-acetamidophenylazo)-2-naphthol by peroxidases.

[Reprinted with permission of Academic Press; originally published as Fig. 4 in: Spadaro, J. T., and Renganathan, V. (1994) Peroxidase-catalyzed oxidation of azo dyes: mechanism of Disperse Yellow 3 degradation. *Arch. Biochem. Biophys.* 312, 301-307.]

SPH is also interesting, because phenyl radicals are not supposed to react with oxygen; they are only known to abstract a hydrogen radical from suitable organic compounds. For example, the acetamidophenyl radical formed from NDY3 does not react with O₂; instead it abstracts a hydrogen radical from dioxane, which is added to the reaction mixture (Spadaro & Renganathan, 1994).

1.2.2.5 Oxidation of azo dyes by laccases. Laccases (EC 1.10.3.2) are extracellular copper-dependent phenol oxidases produced by plants and white-rot fungi (Bollag, 1992; De Jong et al., 1992; Givaudan et al., 1993; Thurston, 1994). Laccase can oxidize aromatic organic pollutants such as phenolic compounds and aromatic amines in the presence of oxygen (Hoff et al., 1985; Bollag et al., 1988). Laccase oxidizes substrates to the corresponding phenoxy radicals by one-electron processes. The resulting phenoxy radicals are either polymerized to a phenolic polymer or further oxidized to a quinone. Electrons that the laccase receives in the process are transferred to oxygen, which is reduced to water (Bollag, 1992).

Chivukula and Renganathan (1995) demonstrated oxidation of phenolic azo dyes by laccase from *Pyricularia oryzae*. Their study showed that the proposed mechanism for phenolic azo dye oxidation is very similar to that of peroxidase. However, the laccase from *P. oryzae* appeared to be less efficient than peroxidases, oxidizing only a selected number of dyes.

1.3 New Technologies For Azo Dye Waste Treatment

1.3.1 Advanced oxidation processes

Hydroxyl radicals ($\cdot\text{OH}$) are the most potent oxidants known. They generally can degrade any organic compound to CO₂ (Kunai et al., 1986; Cha et al., 1996; Bahorsky, 1997). Advanced oxidation processes (AOPs) make use of this high oxidation potential of $\cdot\text{OH}$. These technologies generate $\cdot\text{OH}$ using UV/H₂O₂, UV/O₃, and TiO₂ (Watts et al., 1990; Masten & Davies, 1994; Shu et al., 1994; Hong et al., 1996). AOPs are particularly useful alternatives for eliminating organic pollutants which are resistant to biodegradation (Kuo, 1992; Leung et al., 1992; Legrini et al., 1993; Masten & Davis, 1994; Shu et al., 1994). Applications of AOPs

to the treatment of industrial wastewater and groundwater have been demonstrated (Baozhen & Jun, 1986; Ruppert et al., 1994; Gunten & Olivers, 1997).

1.3.2 Photochemical oxidation

The common oxidizing agents used for the photochemical degradation of azo dyes are hydrogen peroxide (H_2O_2), chlorine (Cl_2), fluorine (F_2), and ozone (O_3) (Langlais et al., 1991; Riefe, 1992; Hong et al., 1996; Gunten & Olivers, 1997).

Practically, ozone treatment removes dye wastes, but ozonation is expensive and has limited efficiency (Matsui et al., 1981; Park & Shore, 1984; Masten & Davies, 1994). The UV/ O_3 system produces $\cdot\text{OH}$ as shown in equations 1.1 and 1.2 (Ruppert et al., 1994; Hong et al., 1996):



UV/ TiO_2 and UV/ H_2O_2 systems have been used for removal of organic contaminants (Ruppert et al., 1994; Vinodgopal & Kamat, 1995; Gunten & Olivers, 1997). These systems have some advantages such as high stability at wide range of pH, non-toxicity, and cost effectiveness (Matthews, 1991).

In UV/ TiO_2 and UV/ H_2O_2 systems, $\cdot\text{OH}$ is generated as shown in equations 1.3–1.5 (Kormann et al., 1988; Laat et al., 1994; Ruppert et al., 1994; Vinodgopal & Kamat, 1995):



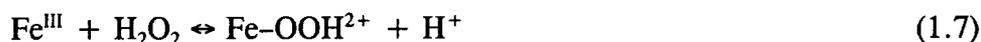
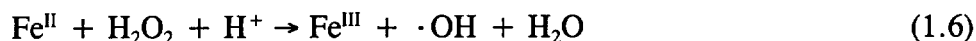
Where $h\nu$ = photon, h_{vb}^+ = valence band holes, and e_{cb}^- = conduction band electrons.

1.3.3 Chemical oxidation

Fenton (1894) reported that a mixture of ferrous ion (Fe^{II}) and hydrogen peroxide (H_2O_2) oxidizes tartaric acid to dihydroxy maleic acid. Later it was proved that a combination of ferrous salts and H_2O_2 (Fenton's reagent) is an effective oxidant of various organic substrates (Walling, 1975). In 1934, Haber and Weiss proposed

that hydroxyl radicals ($\cdot\text{OH}$) are the actual oxidant generated by the decomposition of H_2O_2 by iron.

In Fenton's system, a ferrous (Fe^{II}) or ferric (Fe^{III}) salt (Fenton's reagent) reacts with H_2O_2 to generate $\cdot\text{OH}$ as shown in equations 1.6–1.12 (Walling, 1975; Pignatello, 1992):



Various transition metal ions in lower oxidation states, such as Cu^{I} , Ti^{III} , Co^{II} , and Cr^{II} , can be used as substitutes for iron in the Fenton reaction (Czapski et al., 1971; Heckman & Espenson, 1979). The general reaction of a transition metal with H_2O_2 is shown in equation 1.13 (Goldstein et al., 1993):



1.3.4 Degradation of organic pollutants by AOPs

The hydroxyl radical reacts with aromatic compounds very rapidly and has very high oxidation potential ($E_0 = 2.02$) (Anbar et al., 1966; Walling, 1975; Hoigne et al., 1989; Leung et al., 1992). In addition, $\cdot\text{OH}$ reacts nonspecifically with most organic compounds (Walling, 1975; Masten & Davies, 1994). Kunai et al. (1986) studied the mechanism of benzene degradation by Fenton's reagent. Organic pollutants such as chlorophenoxy herbicides (Pignatello, 1992) and formaldehyde (Murphy et al., 1989) were mineralized by the $\text{Fe}^{\text{III}}/\text{H}_2\text{O}_2$ system. Some azo dyes were also degraded by the $\text{Fe}^{\text{II}}/\text{H}_2\text{O}_2$ system (Kuo, 1992; Solozhenko et al., 1995). Removal of textile dyes in wastewater was examined using the $\text{UV}/\text{H}_2\text{O}_2$ system (Prat et al., 1988; Ince & Goenenc, 1997). Other examples are summarized in Table 1.1. However, the utility of AOPs in eliminating azo dyes from waste streams remains to be proven.

Table 1.1 Azo Dye Degradation by AOPs.

System	Dye	Reference
UV/O ₃ , UV/H ₂ O ₂ , UV/TiO ₂ , and UV/H ₂ O ₂ /Fe ^{II}	Reactive Red 218 and Reactive Orange 16	Ruppert et al., 1994
UV/H ₂ O ₂	Acid Red 1 and Acid Yellow 23	Shu et al., 1994
Iron power/H ₂ O ₂	Reactive Red 120, Direct Blue 160, and Acid Blue 40	Tang & Chen, 1996
UV/TiO ₂	4-Hydroxyazobenzene, Solvent Red 1, Acid Orange 7, and Orange G	Hustert & Zepp, 1992
UV/SnO ₂ /TiO ₂	Acid Orange 7	Vinodgopal & Kamat, 1995
UV/O ₃	Direct Yellow 4, Acid Black 1, Acid Red 1, and Acid Yellow 17	Shu & Huang, 1995
Fe ^{III} H ₂ O ₂	Textile wastewater	Lin & Chen, 1997
UV/TiO ₂	Wastewater dyes	Davis & Gainer, 1994
UV/TiO ₂	4-Hydroxyazobenzene and Solvent Red 1	Dieckmann et al., 1994
UV/TiO ₂	Methyl Orange	Chen & Chu, 1993
Fe ^{III} /H ₂ O ₂	4-Hydroxyazobenzene, Disperse Yellow 3, Solvent Yellow 14, Disperse Orange 3, 4-Phenylazoaniline, and N,N-Dimethyl-4-phenylazoaniline	Spadaro et al., 1994

Among the dye waste treatment methods, the $\text{Fe}^{\text{II}}/\text{H}_2\text{O}_2$ system has been suggested as an alternative for removing color from dye-containing industrial effluents (Kuo, 1992). However, a detailed study of this process has not been published. Most reports have been based on monitoring only the loss of color as an indication of dye degradation. Decolorization generally demonstrates only the transformation of the chromophoric group of dyes; it does not demonstrate total dye degradation (Bigda & Elizardo, 1992). Spadaro et al. (1994) examined the mineralization of ^{14}C -labeled azo dyes to CO_2 using the $\text{Fe}^{\text{III}}/\text{H}_2\text{O}_2$ system. In addition, they suggested the mechanism for benzene generation from phenyl azo substituted dyes (Figure 1.8). The proposed mechanism involves initial addition of $\cdot\text{OH}$ to the C-4 carbon of the phenyl ring. The resulting $\cdot\text{OH}$ adduct then breaks down to generate phenyldiazene and a phenoxy radical. Phenyldiazene is very unstable, so $\cdot\text{OH}$ or O_2 were proposed to oxidize this intermediate to a phenyldiazene radical. This latter radical is also unstable, and is homolytically cleaved to produce a phenyl radical and N_2 . Subsequently, the phenyl radical was suggested to abstract a hydrogen radical from $\cdot\text{O}_2\text{H}$, dye-degradation products, or Tween-80 (a detergent added to the reaction) to generate benzene. The phenoxy radical was proposed to be further degraded to CO_2 by $\cdot\text{OH}$ and oxygen (Spadaro et al., 1994).

1.4 Thesis Outline

In order to gain a detailed insight into azo dye degradation, the oxidation and reduction of azo dyes by enzymatic and chemical systems under aerobic and anaerobic conditions were investigated. Peroxidases such as HRP, MnP, and LiP and hydroxyl radicals ($\cdot\text{OH}$) were used for dye oxidation; zero-valent iron (Fe^0) and NADH were used for dye reduction. Only the study of dye reduction by Fe^0 was performed under anaerobic conditions. Other studies were done under aerobic conditions.

In Chapter 2, substrate specificity of peroxidases such as HRP, MnP, and LiP for azo dyes is investigated. In total, 35 azo dyes were tested. Substituents were introduced into the 2- and 3-position of 4-(4'-sulfophenylazo) phenol. In the case of HRP, the oxidation rates for 2-substituted dyes were 116–486 $\text{mmol min}^{-1} \text{mg}^{-1}$

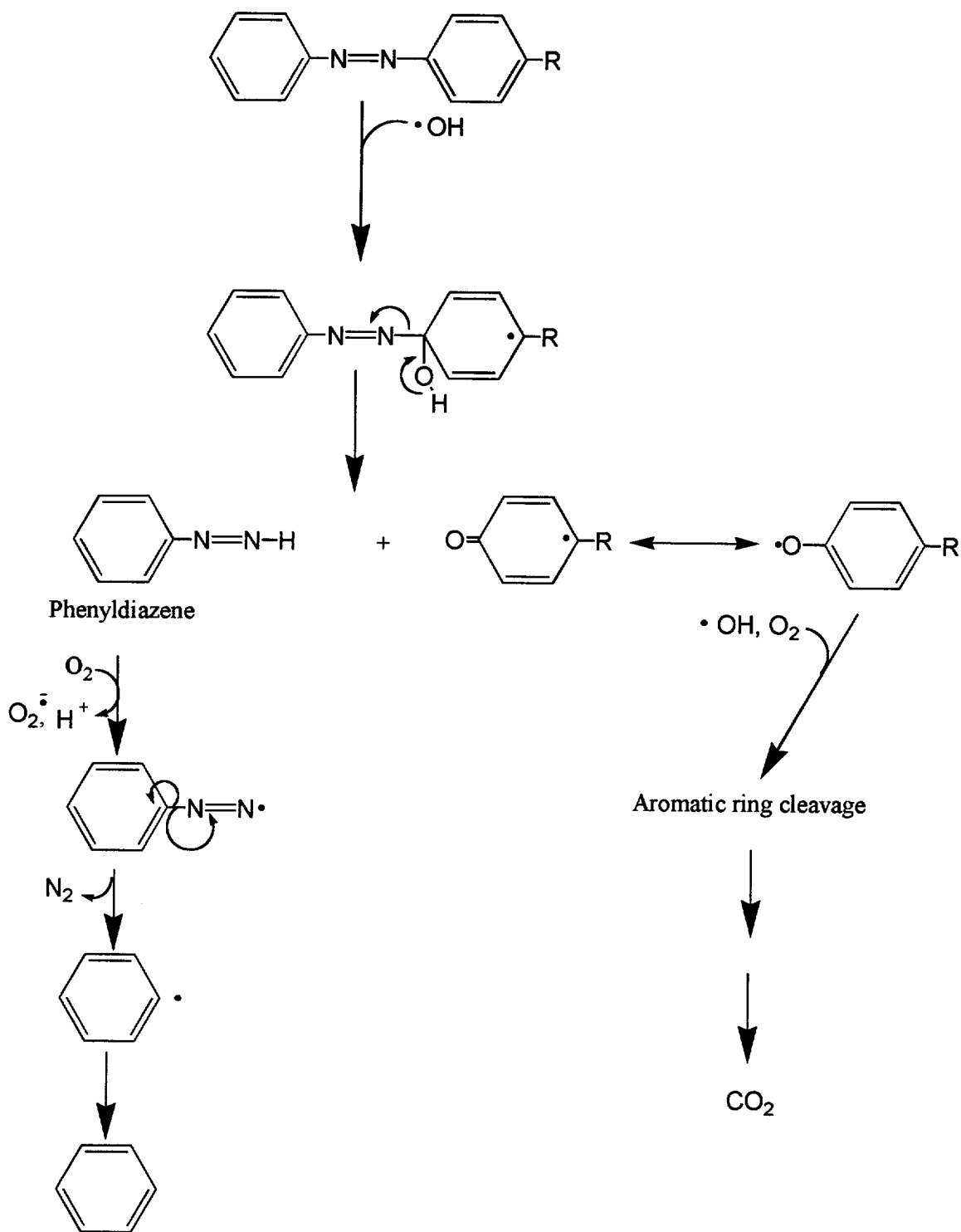


Figure 1.8 Probable mechanism for benzene generation from the degradation of azo dyes with phenylazo substitution by $\cdot\text{OH}$: $\text{R} = \text{NH}_2, \text{OH}$.

[Reprinted with permission of the American Chemical Society; originally published as Scheme I in: Spadaro, J. T., Isabelle, L., and Renganathan, V. (1994) Hydroxyl radical mediated degradation of azo dyes: evidence for benzene degradation. *Environ. Sci. Technol.* **28**, 1389–1393.]

greater than those for 3-substituted dyes. The preferred substitution pattern for di-substituted dyes is shown to be dependent upon the nature of the substituents. In the case of MnP, only the 2-methoxy substituted dye among mono-substituted dyes is oxidized, but others are either poor substrates or non-substrates. All MnP reactions appear to be mediated by a Mn^{III} -malonate complex. In the case of LiP, all of the azo dyes examined serve as poor substrates. In QSAR studies, the Hammett correlations for azo dye oxidation by HRP and MnP are weak and strong, respectively, and LiP oxidation does not indicate any correlation.

In Chapter 3, all of the azo dyes tested are oxidized by $\cdot OH$ generated by the Fe^{III}/H_2O_2 system. In QSAR studies for the dye oxidation by $\cdot OH$, the charge density of the phenolate anion is the best correlated. This result suggests that the dye oxidation by $\cdot OH$ might be controlled by the charge density of phenolate. Based on a QSAR study and product analyses, the probable mechanism is proposed. Azo dye oxidation is influenced by the nature and position of substituents. Most additives, except sodium sulfate and potassium nitrate, decrease the dye oxidation by $\cdot OH$. In particular, potassium nitrate greatly enhances the dye oxidation.

In Chapter 4, azo dyes including food and pharmaceutical dyes are non-enzymatically reduced by NADH. The HPLC and GC-MS analyses indicate that the cleavage of azo linkage by NADH readily generates corresponding aromatic amines. Dye reduction is a strong pH-dependent reaction, showing that dye reduction increases with decreasing pH values. The probable mechanism for azo dye reduction by NADH is proposed. NADH is selective in dye reduction, and azo dye reduction is strongly affected by its substituents.

In Chapter 5, all of the azo dyes examined are reduced by the Fe^0/H_2O system under anaerobic conditions. Dye reduction appears to be the first-order reaction. The correlation between k_{obs} and the mixing rate demonstrates that the observed reduction rates are controlled by mass transport of dye to the iron metal surface. However, the correlation between k_{obs} and the energy of their lowest unoccupied molecular orbital (E_{LUMO}) suggests that dye reduction is also influenced by reduction potentials of dyes.

CHAPTER 2

A QSAR STUDY OF AZO DYE OXIDATION BY PEROXIDASES

2.1 Introduction

Only white-rot basidiomycete fungi can degrade recalcitrant lignin, an aromatic biopolymer, to CO₂ and H₂O (Kirk & Farrell, 1987; Gold et al., 1989). This lignin-degrading system is nonspecific and nonstereoselective; consequently, it is also effective in degrading recalcitrant organic pollutants (Tien, 1987; Chung & Aust, 1995). The white-rot basidiomycete fungus *Phanerochaete chrysosporium*, the best-studied of the white-rot basidiomycete fungi, produces two extracellular heme peroxidases—lignin peroxidase (LiP) and manganese peroxidase (MnP)—under nitrogen-limiting culture conditions. These two enzymes, along with an extracellular H₂O₂-generating system (glyoxal oxidase), are the major components of the lignin degradative system (Gold et al., 1984; Tien & Kirk, 1984; Glenn & Gold, 1985; Kersten & Kirk, 1987).

Glenn and Gold (1983) first demonstrated that *P. chrysosporium* cultures can decolorize some polymeric dyes. Subsequently, several laboratories also demonstrated the decolorization of azo dyes such as Congo Red, Acid Red 88, Orange II [1-(4'-sulfophenylazo)-2-naphthol], Acid Red 114, Tropeolin O, Direct blue 15, Biebrich Scarlet, Tartrazine, Yellow 9, and Chrysophenine with lignin-degrading cultures of *P. chrysosporium* (Cripps et al., 1990; Paszczynski & Crawford, 1991; Paszczynski et al., 1991). Spadaro et al. (1992) and Paszczynski et al. (1992) showed that *P. chrysosporium* cultures are able to completely mineralize sulfonated and nonsulfonated azo dyes to CO₂. LiP and MnP produced under nitrogen-limiting culture conditions were proposed to initiate the mineralization of azo dyes (Figure 2.1).

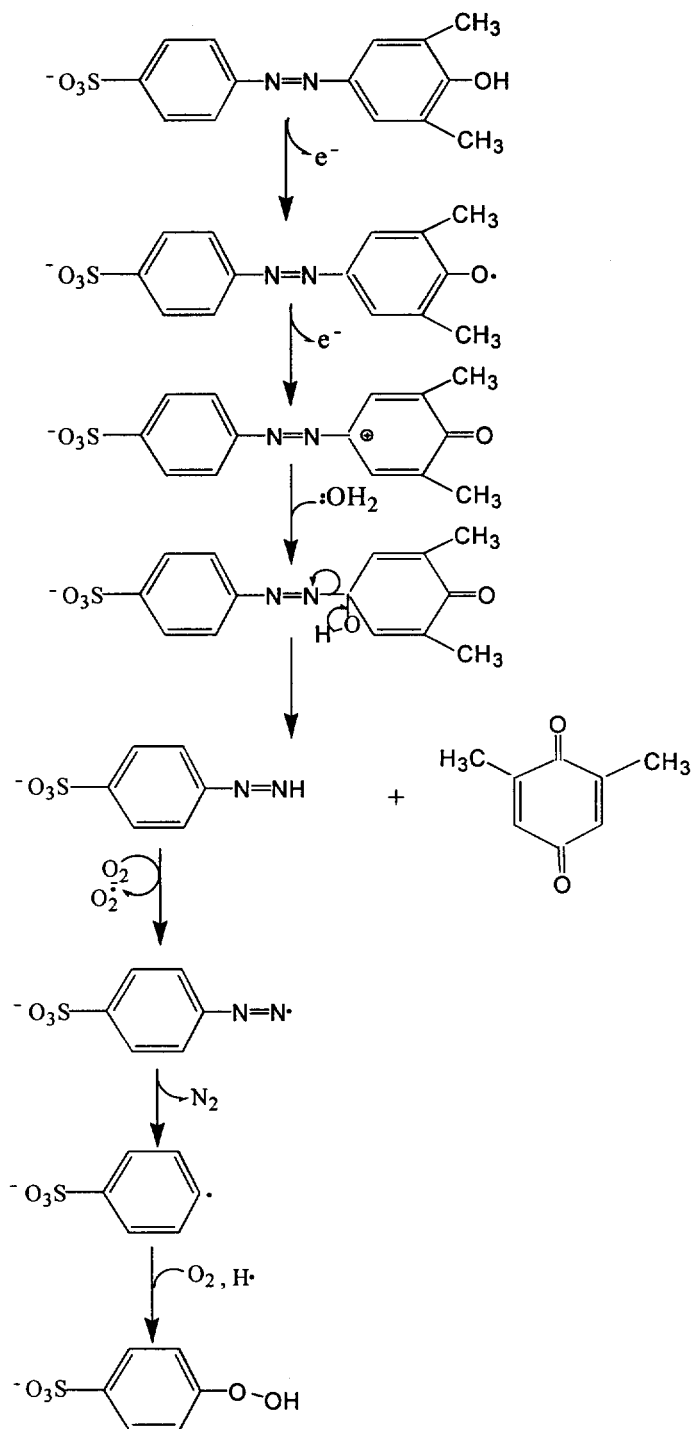


Figure 2.1 Mechanism for the oxidation of 4-(4'-sulfophenylazo)-2,6-dimethylphenol by LiP.

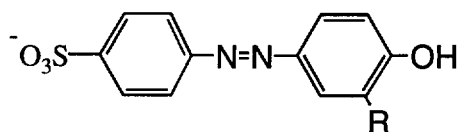
[Reprinted with permission of the American Chemical Society; originally published as Fig. 6 in: Chivukula, M., Spadaro, J. T., and Renganathan, V. (1995) Lignin peroxidase-oxidation of sulfonated azo dyes generates novel sulfophenyl hydroperoxidases. *Biochemistry* **34**, 7765-7772.]

Our laboratory studied the oxidation of two commercial azo dyes, Disperse Yellow 3 and Orange II, by horseradish peroxidase (HRP), LiP, and MnP (Spadaro & Renganathan, 1994; Chivukula et al., 1995). Disperse Yellow 3 [2-(4'-acetamidophenylazo)-4-methylphenol] was oxidized to 4-methyl-1,2-benzoquinone, acetanilide, and a dimer of Disperse Yellow 3. Orange II was oxidized to 1,2-naphthoquinone and 4-sulfophenyl hydroperoxide. In these reactions, the H₂O₂-oxidized form of a peroxidase initiates the oxidation of the phenolic ring of Disperse Yellow 3 or Orange II by two electrons to produce a carbonium ion. A nucleophilic attack by H₂O on the carbon bearing the azo linkage generates a quinone and a phenyl diazene. The phenyl diazene is oxidized either by O₂ or by the H₂O₂-oxidized form of peroxidase to yield the corresponding phenyl diazene radical, which readily eliminates the azo linkage as nitrogen to yield a phenyl radical. In the oxidation of Disperse Yellow 3, this phenyl radical yields acetanilide by the abstraction of a hydrogen radical from the organic impurities in the medium. However, in the oxidation of Orange II, this phenyl radical is scavenged by oxygen to produce a novel 4-sulfophenyl hydroperoxide in the medium (Figure 2.1).

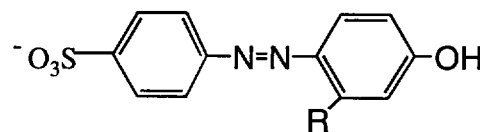
In this study, substrate specificity of HRP, LiP, and MnP for azo dyes is examined to understand the effect of substituents on peroxidase-dependent oxidation of azo dyes. Substituents of azo dyes tested included methyl, methoxy, chloro, bromo, iodo, fluoro, and nitro groups. Only the substituents on the phenolic rings of azo dyes were altered (Figure 2.2).

In biological systems, quantitative structure-activity relationships (QSARs) help in understanding the correlation between the rate of microbial degradation or enzymatic reaction and the molecular descriptors of a series of structurally similar substrates (Paris et al., 1982; Dolfing & Tiedje, 1991; Hansch & Gao, 1997; Kubinyi, 1997). Hence QSARs provide a useful means for predicting biological reactivity between similar substrates (Hsuanyu & Dunford, 1992; Ryu & Dordick, 1992; Hansch & Gao, 1997). The Hammett correlation is an empirical relationship between substituent constants and reactivity (Ritchie, 1990; Roe & Goodin, 1993; Hansch & Gao, 1997; Tratnyek, 1998). The Hammett equation and its extensions have been applied to enzymatic systems. Kobayashi et al. (1987) used the Hammett

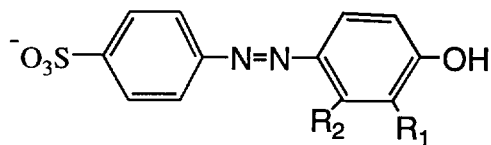
4-(4'-Sulfophenylazo)-phenol derivatives



R = CH₃, OCH₃, NO₂, or X.

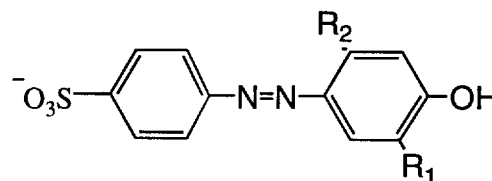


R = CH₃, OCH₃, NO₂, or X.



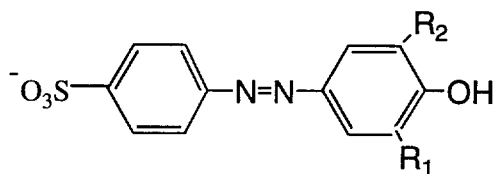
R₁ = CH₃, OCH₃, or X.

R₂ = CH₃, OCH₃, or X.



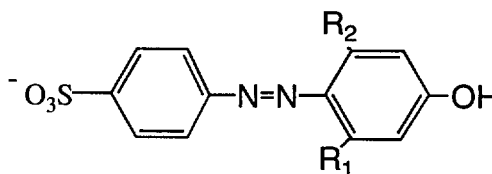
R₁ = CH₃ or X.

R₂ = CH₃ or X.



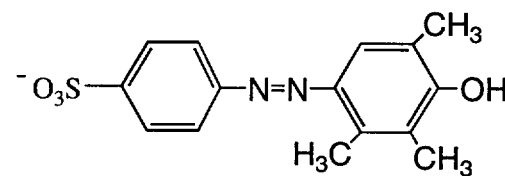
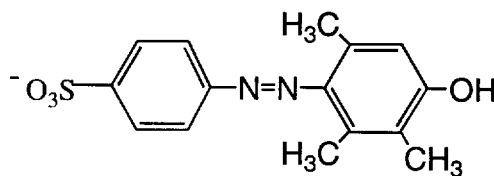
R₁ = CH₃, OCH₃, or X.

R₂ = CH₃, OCH₃, or X.

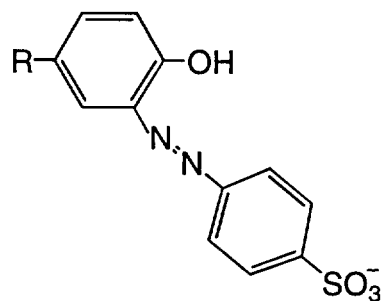


R₁ = CH₃, OCH₃, or X.

R₂ = CH₃, OCH₃, or X.



2-(4'-Sulfophenylazo)-phenol derivatives



R = CH₃, OCH₃, or X.

Figure 2.2 Structures of synthetic axo dyes tested.

correlation to elucidate the oxygen-transfer reaction from H_2O_2 to thioanisoles by HRP and chloroperoxidase. In that study, *para*-substituted thioanisoles were oxidized by HRP compound II. Blée and Schuber (1989) also found a linear Hammett correlation between the substituents and the formation of *para*-substituted thioanisole sulfoxides catalyzed by a soybean sulfoxidase. That Hammett correlation suggested that S-oxygenation involved a one-electron transfer mechanism. Ryu and Dordick (1992) examined the usefulness of the Hammett correlation for evaluating solvent effects on HRP catalysis. The Hammett correlation for phenol oxidation with compound II of prostaglandin H synthase and compound I and compound II of HRP suggested that the electronic effect of the substituent is predominant in determining the phenol oxidation rate (Job & Dunford, 1976; Dunford & Adeniran, 1986; Hsuanyu & Dunford, 1992).

In this study, the correlation between the specific activity of HRP, MnP, and LiP and substituent constants (σ , σ^- , σ^0 , and σ^+) in peroxidase-catalyzed oxidation of azo dyes was examined. This correlation might provide a useful method to understand the mechanism of azo dye oxidation by peroxidases and to predict the susceptibility of an azo dye to peroxidatic degradation.

2.2 Materials and Methods

2.2.1 Chemicals

4-Aminobenzenesulfonic acid, 2,6-dimethylphenol, 2-dianisidine, sodium nitrite, guaiacol, and all substituted phenols were purchased from Aldrich Chemical Company (Milwaukee, WI). Horseradish peroxidase (Type VIa), 2,2'-azino-bis(3-ethylthiazoline-6-sulfonate) (ABTS), and H_2O_2 were obtained from Sigma Chemical Company (St. Louis, MO) and used as received.

2.2.2 Synthesis of azo dyes

Azo dyes were prepared by coupling the diazonium salt of 4-aminobenzenesulfonic acid with substituted phenols at 0–5°C under alkaline conditions as described (Goszczyński et al., 1994). Synthesis of 4-(4'-sulfophenylazo)-phenol is described as an example (Chivukula & Renganathan, 1995):

4-aminobenzenesulfonic acid (125 mmol) was mixed with sodium nitrite (125 mmol) in 1 N NaOH (12.5 ml). The diazonium salt of 4-aminobenzenesulfonic acid was formed by the slow addition of 3 N HCl (8.5 ml). The diazonium salt, which precipitated from solution, was reacted with a cold basic solution of phenol (125 mmol) in 1 N NaOH (12.5 ml) for 10 min. The reaction temperature was maintained at 0–5°C during the coupling reaction. The precipitated product was completely dissolved by boiling on the steam bath. This dye solution was acidified with HCl, concentrated, and then crystallized.

The crude azo dye was filtered, rinsed three times with water, and dried at room temperature. All crude azo dyes synthesized were purified by silica gel column chromatography with a mixture of 5–10% methanol and ethyl acetate as an eluent. All azo dyes were analyzed by high-performance liquid chromatography using a reverse phase C-18 column with the water–methanol (1:1) solvent system. All azo dyes synthesized indicated >98% purity. The structures of all azo dyes were confirmed by fast atom bombardment–mass spectrometry using a VG Analytical 7070E mass spectrometer equipped with an Ion-Tech saddle field atom gun operated with xenon at 6 kV (Chivukula et al., 1995).

2.2.3 Preparations of lignin and manganese peroxidases

LiP and MnP were purified from the extracellular medium of lignin-degrading cultures of *P. chrysosporium* as previously described (Gold et al., 1984). The specific activity of lignin peroxidase for the oxidation of veratryl alcohol was 20.9 U/mg (Wariishi & Gold, 1990). The specific activity of manganese peroxidase, as determined by monitoring the oxidation of Mn^{II} to Mn^{III}, was 10.1 U/mg (Wariishi et al., 1992).

2.2.4 Azo dye reaction by peroxidases

Peroxidases (0.1–3 µg) were incubated with an azo dye (50 µM) and H₂O₂ (25 or 100 µM) in an appropriate buffer (1 ml) at room temperature. HRP reactions were performed in 10 mM potassium phosphate (pH 6.0). MnP reactions were performed in 50 mM malonate (pH 4.5) containing 0.5 mM MnSO₄. LiP reactions were

performed in 20 mM sodium succinate (pH 4.5). LiP reaction included veratryl alcohol (10 μ M) to enhance enzyme activity and to prevent enzyme inactivation (Wariishi & Gold, 1990). The determination for azo dye oxidation was done by monitoring the decrease of absorbance at the maximum wavelength for azo dye with a UV-visible spectrophotometer (Model UV-265, Shimadzu Corporation, Kyoto, Japan). The amount of azo dye oxidation was calculated from the corresponding extinction coefficients of azo dyes tested. HRP and LiP reactions for substrates, such as 2-dianisidine, 2,6-dimethylphenol, guaiacol, and ABTS, were performed as described above for azo dyes.

2.2.5 Comparing Mn^{III}-malonate reaction with MnP reaction

A solution of Mn^{III} acetate (10 mM) in 0.5 M malonate (pH 4.5) was prepared. Azo dye (50 μ M) was added to 50 mM malonate buffer (pH 4.5). Then, 100 μ l of Mn^{III}-malonate (1 μ mol) complex was added to this mixture in 10 aliquots over 1 h at room temperature. The reaction volume was 1 ml. The amount of azo dye oxidation was determined by monitoring the decrease in absorbance due to color loss at maximum wavelength of each azo dye tested.

MnP reaction was performed in 50 mM malonate (pH 4.5) containing 50 μ M azo dye, 0.5 mM MnSO₄, and 100 μ M H₂O₂, as described previously. The reaction time was 1 h at room temperature, and then the color loss was compared with the Mn^{III}-malonate reaction.

2.2.6 Correlation analysis

Substituent constants (σ , σ^- , σ^0 , and σ^+) have been previously calculated (Exner, 1978). σ values of *ortho*-substituents were substituted with those of the corresponding *para*-substituents. The σ value for a multi-substituted substrate was determined by adding substituent constants for each position.

Other parameters, such as energy of the highest occupied molecular orbital (E_{HOMO}), half-wave potential ($E_{1/2}$), and ionization constants (pKa), were calculated by using CAChe computer program of Oxford Molecular (Beaverton, OR).

2.3 Results

In this study, the effect of substituent introduction into the 2- and 3-position of 4-(4'-sulfophenylazo)-phenol on its oxidation by HRP, MnP, and LiP was examined. These substituent changes were made only in the phenolic ring of azo dyes (Figure 2.2). In total, 35 substituted azo dyes were investigated (Table 2.1).

2.3.1 Substrate specificity of HRP

HRP oxidized all the mono-substituted 4-(4'-sulfophenylazo)-phenol dyes, except nitro-substituted dye (Table 2.1). High oxidation rates were observed with 2-methyl, 2-methoxy, 2-fluoro, 2-chloro, and 2-iodo substituents. In general, the oxidation rates for 2-substituted dyes were higher than those of 3-substituted dyes. HRP also oxidized several di-substituted dyes, and the preferred substitution pattern was dependent on the nature of the substituent. Thus, the 2,5-disubstitution was preferred for the methyl group, 2,3-disubstitutions were preferred for methoxy and chloro groups, and 2,6-disubstitution was preferred for the fluoro group. The 3,5-disubstitution pattern appears to be the least preferred for any substituent. The 2,3-, 2,5-, and 2,6-disubstituted dyes were oxidized at lower rates compared to the corresponding 2-substituted dyes. The only exception to this observation was the 2,5-dimethyl-substituted dye which was oxidized at a faster rate compared to the 2-methyl dye. HRP oxidation rates for 2,3,5- and 2,3,6-trimethyl-substituted dyes were 1109 and 751 $\mu\text{mol min}^{-1} \text{mg}^{-1}$, respectively. The specific activity of the 2,3,5-trimethyl dye was comparable to that of other standard peroxidase substrates such as 2-dianisidine, guaicol, and 2,2'-azino-bis(3-ethylthiazoline-6-sulfonate) (ABTS) (Table 2.2). This suggests that the 2,3,5-trimethyl dye could be routinely used for assaying HRP and other peroxidases.

2.3.2 Substrate specificity of MnP

MnP is unique because its preferred substrate is Mn^{II} . MnP oxidizes Mn^{II} to Mn^{III} , which is complexed by chelators such as oxalate, malonate, or lactate (Glenn et al., 1986; Wariishi et al., 1992; Kuan et al., 1993). The Mn^{III} complex functions as

Table 2.1 Oxidation of substituted phenolic azo dyes by HRP, MnP, and LiP

<i>4-(4'-Sulfophenylazo)-phenol dyes</i>				Activity ($\mu\text{mol min}^{-1} \text{mg}^{-1}$)		
Monosubstituted derivatives		λ_{max} (nm)	Sum of σ^-	HRP	MnP	LiP
	Substituents					
1	2-Methyl	358	-0.15	550.9	6.3	1.2
2	3-Methyl	362	-0.07	434.4	1.9	0.9
3	2-Methoxy	369	-0.16	492.9	85.5	1.1
4	3-Methoxy	382	0.10	239.8	3.2	0.9
5	2-Fluoro	356	0.05	564.6	0.9	1.8
6	3-Fluoro	352	0.34	78.7	0.0	1.0
7	2-Chloro	354	0.27	427.8	0.2	1.2
8	3-Chloro	359	0.37	80.8	0.0	1.3
9	2-Bromo	362	0.28	328.7	1.9	1.6
10	2-Iodo	361	0.30	341.4	3.8	1.4
11	3-Iodo	368	0.35	108.0	0.0	1.3
12	2-Nitro			ND*	ND	ND
13	3-Nitro	349	0.71	0.6	0.0	0.5
Disubstituted derivatives						
	Substituents					
14	2,3-Dimethyl	362	-0.22	564.7	32.2	1.5
15	2,5-Dimethyl	366	-0.22	852.5	25.8	1.1
16	2,6-Dimethyl	359	-0.30	574.0	118.5	2.5
17	3,5-Dimethyl	359	-0.14	360.4	1.7	1.2
18	2,3-Dimethoxy	362	-0.06	288.3	7.9	1.0
19	2,6-Dimethoxy	377	-0.32	5.4	129.2	0.5
20	3,5-Dimethoxy	421	0.20	0.8	0.0	1.5
21	2,3-Difluoro	374	0.39	103.8	0.0	1.6
22	2,5-Difluoro	419	0.39	209.7	0.0	0.8
23	2,6-Difluoro	416	0.10	449.0	2.7	3.6
24	3,5-Difluoro	350	0.68	5.4	0.0	0.9
25	2,3-Dichloro	420	0.64	405.1	0.0	0.9
26	2,5-Dichloro	420	0.64	122.2	0.0	1.1
27	2,6-Dichloro	342	0.54	0.0	5.3	2.7
28	3,5-Dichloro	430	0.74	6.0	0.0	1.6
Trisubstituted derivatives						
	Substituents					
29	2,3,5-Trimethyl	351	-0.29	1109.0	0.3	2.5
30	2,3,6-Trimethyl	366	-0.37	751.8	206.1	2.6
2-(4'-Sulfophenylazo)-phenol dyes						
Monosubstituted derivatives						
	Substituents					
31	4-Methyl	326		0.0	0.5	0.3
32	4-Methoxy	324		0.0	15.1	0.2
33	4-Fluoro	318		0.3	0.0	0.5
34	4-Chloro	318		0.2	0.0	0.3
35	4-Bromo	340		0.1	0.1	0.8

*Not determined

Table 2.2 Comparison of specific activities of HRP and LiP for phenolic compounds

Compounds	Specific activity ($\mu\text{mol min}^{-1} \text{mg}^{-1}$)		λ_{max} (nm)
	HRP	LiP	
2-Dianisidine	1100.0	5.3	420
2,6-Dimethyl phenol	4.6	10.1	420
Guaiacol	20.7	0.6	420
4-(4'-Sulfophenylazo)-2,6-dimethylphenol*	574.4	2.5	359
4-(4'-Sulfophenylazo)-2,3,5-trimethylphenol*	1109.0	2.5	351
ABTS	15.2	ND [#]	420

*Azo dyes synthesized.

[#]Not determined

a diffusible redox mediator. It diffuses away from the enzyme active site and oxidizes phenols (Glenn et al., 1986; Wariishi et al., 1992). MnP oxidized the 2-methoxy-substituted dye among all the mono-substituted 4-(4'-sulfophenylazo)-phenol derivatives (Table 2.1). Other mono-substituted dyes were either poor substrates or non-substrates for MnP. Among the di-substituted dyes, the 2,3-dimethyl-, 2,5-dimethyl-, 2,6-dimethyl-, and 2,6-dimethoxy-substituted dyes were oxidized by MnP, and the observed activity ranged from 32 to 129 $\mu\text{mol min}^{-1} \text{mg}^{-1}$. The 2,3,6-trimethyl-substituted dye was the best substrate for MnP, and it was oxidized at the rate of 206.1 $\mu\text{mol min}^{-1} \text{mg}^{-1}$. The 2,3,5-trimethyl-substituted dye (0.3 $\mu\text{mol min}^{-1} \text{mg}^{-1}$), the best substrate for HRP, was oxidized by MnP very sluggishly. Halogen-substituted dyes were either very poor substrates or non-substrates for MnP. Substrate specificity for azo dye oxidation by chemically prepared Mn^{III} -malonate complex was the same as that of MnP, suggesting that all MnP reactions were mediated by a Mn^{III} -malonate complex (Table 2.3).

2.3.3 Substrate specificity of LiP

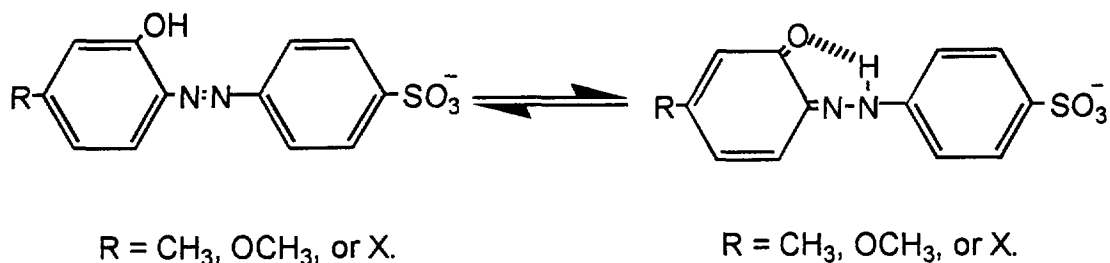
All of the azo dyes examined served as poor substrates for LiP. A possible reason is that, unlike other peroxidases, LiP does not oxidize phenols efficiently. A high level of H_2O_2 , particularly in the absence of a suitable substrate, is known to inactivate LiP. Chung and Aust (1995) demonstrated that the high concentration of H_2O_2 lowers the initial oxidation rate of phenol. Wariishi and Gold (1990) suggested that veratryl alcohol, a secondary metabolite of *P. chrysosporium*, protected LiP from enzyme inactivation. Pasti-Grigsby et al. (1992) demonstrated that the oxidation of azo dyes by LiP proceeded at a faster rate in the presence of veratryl alcohol. Hence, the oxidation of azo dyes was examined in the absence and in the presence of 10 μM veratryl alcohol. Inclusion of veratryl alcohol increased the azo dye oxidation rate two-fold, but rates were not comparable to those of HRP and MnP.

All of the 2-(4'-sulfophenylazo)-phenol dyes tested were poor substrates or non-substrates for HRP, MnP, and LiP. Probably lower oxidation rates of 2-(4'-sulfophenylazo)-phenol dyes than those of 4-(4'-sulfophenylazo)-phenol dyes result from the steric hindrance between the OH substituent and azo linkage (Figure 2.2).

Table 2.3 Comparison of azo dye oxidation by MnP and Mn^{III}-malonate complex

<i>Compounds</i>	Conc. of azo dye (μM)	
	<i>MnP</i>	<i>Mn^{III}-malonate</i>
4-(4'-Sulfophenylazo)-2,6-dimethylphenol	7.4	8.4
4-(4'-Sulfophenylazo)-2-methylphenol	22.4	18.4
4-(4'-Sulfophenylazo)-2,3-dimethylphenol	12.2	13.3
4-(4'-Sulfophenylazo)-2-chlorophenol	35.5	29.3
4-(4'-Sulfophenylazo)-2-methoxyphenol	13.8	15.5
4-(4'-Sulfophenylazo)-2,6-dichlorophenol	21.9	20.6
4-(4'-Sulfophenylazo)-2,6-dimethoxyphenol	15.7	11.5
4-(4'-Sulfophenylazo)-3-methoxyphenol	30.4	31.7
4-(4'-Sulfophenylazo)-2-fluorophenol	30.9	27.0
2-(4'-Sulfophenylazo)-4-methylphenol	42.8	39.6
4-(4'-Sulfophenylazo)-2,6-dibromophenol	5.6	12.0
4-(4'-Sulfophenylazo)-2,3,6-trimethylphenol	11.0	11.7

2-(4'-Sulfophenylazo)-phenol dyes can exist in the phenolic form or in its alternate tautomeric structure hydrazo form. The latter form is likely to be either a non-substrate or poor substrate because it is not a phenol. Thus, possibly the concentration of individual tautomeric forms could affect its oxidation.



4. Discussion

Biological QSARs are useful for studying relationships between microbial or enzyme activities and physical properties of closely related substrates (Dorn & Knackmuss, 1978; Paris et al., 1982; Dolfig & Tiedje, 1991; Hansch & Gao, 1997). The Hammett correlation, which assesses the electronic effect of substituents on organic reactions, has been successfully applied to enzyme reactions also (Reineke & Knackmuss, 1978; Hsuanyu & Dunford, 1992; Kubinyi, 1997). The Hammett equation is described as shown in equation 1:

$$\log k_x - \log k_H = \rho\sigma_x \quad (2.1)$$

where k_x is the reaction rate constant of the substituted (with electronic effects of substituents) substrate, and k_H is the reaction rate constant of unsubstituted (without electronic effects of substituents) substrate. σ_x is a substituent constant, which reflects the ability of a substituent to change the electron density at a reaction site. A positive σ indicates that the substituent tends to withdraw electron density from the aromatic ring, whereas a negative σ indicates that the substituent tends to donate electron density to the ring (Blée & Schuber, 1989; Ritchie, 1990; Hansch & Gao, 1997; Tratnyek, 1998). This depends on the nature of the substituent and the position

of the substituent on the aromatic ring. ρ , a reaction constant, is a measure of the reaction sensitivity to substituent effects. This equation was originally applied only to aromatic compounds with either *meta*- or *para*-substituents (Job & Dunford, 1976; Dolfing & Tiedje, 1991). However, later extensions of the Hammett equation included *ortho*-substituents, and their correlations used *para*-substituent constants for *ortho*-substituents also (Fujita and Nishioka, 1976; Hoigné and Bader, 1993; Elovitz & Fish, 1994; Tratnyek, 1998).

σ was originally determined using the dissociation of benzoic acids in water at 25°C (Blake & Coon, 1981; Ritchie, 1990). However, recently variations of σ values such as σ^- , σ^0 , and σ^+ have been used for assessing the effects of resonance interactions between the substituents and the reaction sites (Shorter, 1982; Brezonik, 1990; Ritchie, 1990; Hansch & Gao, 1997). σ^- values, derived from the ionization of phenols or anilines in water, are used for dealing direct resonance interactions between negatively charged reaction sites and substituents. σ^0 values are based on ionization of substituted phenylacetic acids, and in this case the substituent does not have resonance interaction with the reaction site (Ritchie, 1990). σ^+ values, derived from *t*-cumyl chloride solvolysis studies, correlate aromatic electrophilic substitution reactions with aromatic substituents (Ritchie, 1990; Hansch & Gao, 1997).

The Hammett correlation has been applied to the oxidation of substituted phenols by peroxidases. Dunford and coworkers correlated the oxidation of *meta*- and *para*-substituted phenols by HRP compound I, HRP compound II, and prostaglandin H synthase compound II with the Hammett equation (Job & Dunford, 1976; Dunford & Adeniran, 1986; Hsuanyu & Dunford, 1992). Phenol derivatives examined in that study included substituents such as $-\text{NH}_2$, $-\text{OCH}_3$, $-\text{CH}_3$, $-\text{OH}$, $-\text{SO}_3^-$, $-\text{Cl}$, $-\text{CHO}$, $-\text{C}_2\text{H}_5$, $-\text{OC}_2\text{H}_5$, and COO^- . They observed that electron-donating substituents such as $-\text{NH}_2$, $-\text{OCH}_3$, and $-\text{CH}_3$ enhanced the oxidation of phenols, whereas electron-withdrawing substituents such as $-\text{SO}_3^-$ and $-\text{Cl}$ decreased the oxidation of phenols. The ρ values for the oxidation of phenols by HRP compound I, HRP compound II, and prostaglandin H synthase were -6.9 , -4.6 ± 0.5 , and -2.0 ± 0.1 , respectively. These ρ values indicate that HRP compound I is

more sensitive to the electronic effects of substituents than HRP compound II and prostaglandin H synthase compound II.

In this study, the Hammett correlation was applied to peroxidase-catalyzed azo dye oxidation. The correlation with σ , σ^- , σ^0 , and σ^+ values was examined (Figure 2.3A, B, C, and D and Table 2.4). The Hammett correlation with σ^- provided very similar fit to the correlation with σ . The ρ value of correlation with σ^- for MnP oxidation was the largest (Table 2.5).

Plotting log activity versus the sum of σ^- substituent constants for oxidation of phenolic azo dyes by HRP is shown in Figure 2.4A and Table 2.6; regression on these data yielded:

$$\log \text{ activity} = -0.79(\pm 0.16)\sigma^- + 2.57(\pm 0.58) \quad (2.2)$$

where $n = 23$, $s = 0.38$, $r = 0.74$. The rate of azo dye oxidation by HRP decreased as a function of σ^- . A negative slope ($-\rho$) indicates that electron-donating substituents ($-\sigma$) enhance the oxidation of dye, and electron-withdrawing substituents ($+\sigma$) decrease oxidation rates. However, the low ρ and r values ($\rho = -0.79$ and $r = 0.74$) indicate that this correlation is relatively poor. This finding suggests that the reaction might be controlled by other factors such as steric hindrance. For example, the σ^- substituent constants for 3-methyl- and 2-chloro-substituted dyes are -0.07 and 0.27 , respectively, but both of these dyes essentially exhibited the same level of activity (Table 2.1). Similarly, 2,3-dichloro-substituted dye with a σ^- value of 0.64 exhibited higher activity ($405 \mu\text{mol min}^{-1} \text{mg}^{-1}$) than 2,6-dimethyl-substituted dye ($5.4 \mu\text{mol min}^{-1} \text{mg}^{-1}$) with a σ^- value of -0.32 .

Plotting log activity versus the sum of σ^- substituent constants for oxidation of phenolic azo dyes by MnP is shown in Figure 2.4B and Table 2.6; regression on these data yielded:

$$\log \text{ activity} = -5.04(\pm 0.55)\sigma^- + 0.36(\pm 1.19) \quad (2.3)$$

where $n = 17$, $s = 0.48$, $r = 0.92$. As was observed in the HRP correlation, a negative slope ($-\rho$) between the rate of dye oxidation by MnP and σ^- was observed. The ρ and r values ($\rho = -5.04$ and $r = 0.92$), which are comparable to results reported by Dunford and coworkers for HRP (Job & Dunford, 1976; Dunford & Adeniran, 1986; Hsuanyu & Dunford, 1992), indicate that the correlation is relatively

Figure 2.3A

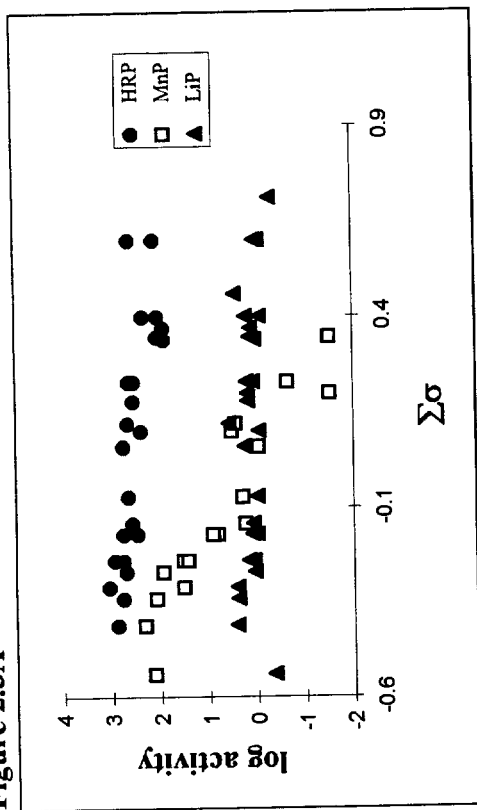


Figure 2.3B

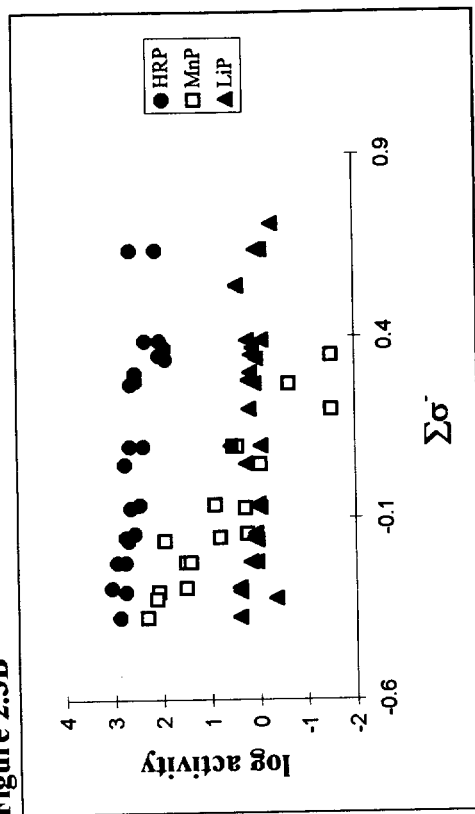


Figure 2.3C

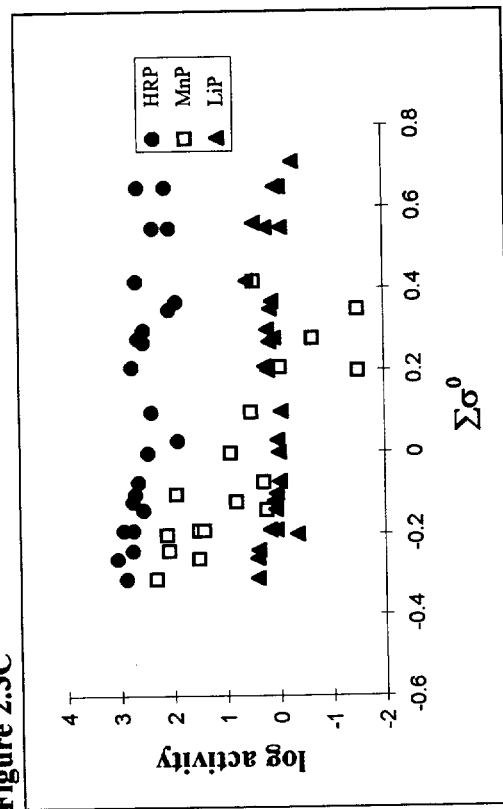


Figure 2.3D

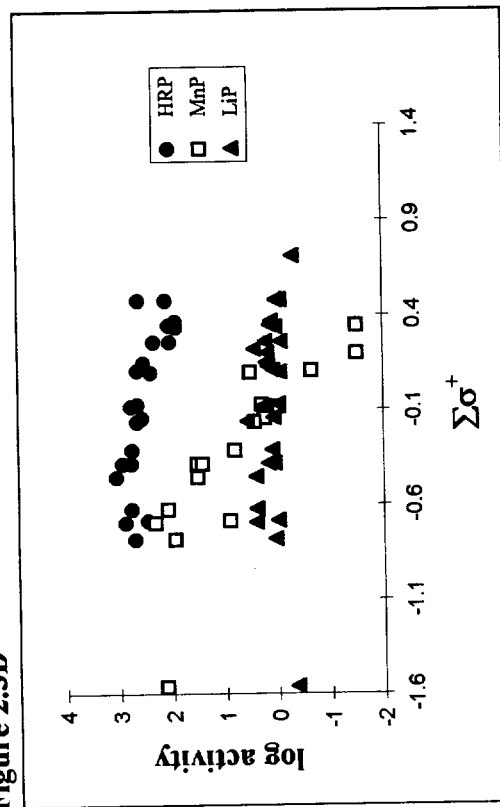


Figure 2.3A, B, C, and D. Plots of log activity of HRP, MnP, and LiP versus the sum of substituent constants (σ , σ' , σ^0 , and σ^+) for data shown in Table 2.5.

Table 2.4 Representative descriptor variables related to the correlation analysis of azo dye oxidation by peroxidases

No.	Sum of σ	Sum of σ^0	Sum of σ^+	<i>log activity</i>		
				HRP	MnP	LiP
1	-0.17	-0.12	-0.31	2.741	0.799	0.086
2	-0.07	-0.07	-0.07	2.638	0.279	-0.027
4	0.10	0.10	0.10	2.380	0.505	-0.056
6	0.34	0.03	0.34	1.896	NA	0.017
8	0.37	0.37	0.37	1.907	NA	0.097
10	0.18	0.27	0.13	2.533	NA	0.158
12	0.78	0.81	0.79	NA	NA	NA
14	-0.24	-0.19	-0.38	2.752	1.508	0.167
16	-0.34	-0.24	-0.62	2.759	2.074	0.389
18	-0.17	0.00	-0.68	2.460	0.898	-0.009
19	-0.54	-0.20	-1.56	NA	2.111	-0.347
20	0.20	0.20	0.20	NA	-1.523	0.176
21	0.40	0.55	0.26	2.016	NA	0.204
22	0.40	0.55	0.26	2.322	NA	-0.086
23	0.12	0.42	-0.16	2.652	0.431	0.561
24	0.68	0.68	0.68	0.732	NA	-0.027
25	0.60	0.65	0.48	2.608	NA	-0.066
26	0.60	0.65	0.48	2.087	NA	0.021
27	0.46	0.56	0.22	NA	NA	0.423
28	0.74	0.74	0.74	0.777	NA	NA
29	-0.31	-0.26	-0.45	3.045	1.505	0.405
30	-0.41	-0.31	-0.69	2.876	2.314	0.407

Table 2.4 Representative descriptor variables related to the correlation analysis of azo dye oxidation by peroxidases (continued)

No.	E_{HOMO}^*	Charge density of phenol	Charge density of phenolate	$E_{1/2}^\#$
1	-2.7358	-0.2495	-0.6250	0.556
2	-2.7124	-0.2497	-0.6284	0.607
3	-2.6633	-0.2336	-0.5987	0.456
4	-2.9352	-0.2441	-0.6144	0.619
5	-2.9661	-0.2375	-0.5986	0.000
6	-3.0872	-0.2463	-0.6125	0.733
7	-3.0481	-0.2365	-0.5908	0.625
8	-3.1310	-0.2473	-0.6128	0.734
9	NA	NA	NA	NA
10	NA	NA	NA	NA
11	NA	NA	NA	NA
12	-3.9954	-0.2434	-0.4970	0.846
13	-3.6637	-0.2397	-0.5918	0.855
14	-2.8423	-0.2470	-0.6185	0.530
15	-2.7760	-0.2484	-0.6230	0.530
16	-2.8385	-0.2514	-0.6186	0.427
17	-2.7525	-0.2487	-0.6264	0.587
18	NA	NA	NA	0.442
19	NA	NA	NA	0.317
20	NA	NA	NA	0.605
21	NA	NA	NA	NA
22	NA	NA	NA	NA
23	NA	NA	NA	NA
24	NA	NA	NA	NA
25	-3.4495	-0.2319	-0.5699	0.726
26	-3.4110	-0.2318	-0.5739	0.695
27	-3.3778	-0.2287	-0.5511	0.617
28	-3.4480	-0.2426	-0.5959	0.835
29	-2.8770	-0.2471	-0.6168	0.504
30	NA	NA	NA	0.453

*Energy of the highest occupied molecular orbital.

#Polarographic half-wave potential.

Table 2.5 Comparison of log activity of peroxidase vs. $\Sigma\sigma$, $\Sigma\sigma^-$, $\Sigma\sigma^0$, and $\Sigma\sigma^+$

Correlation	HRP	MnP	LiP
ρ	-0.79 ± 0.12	-4.45 ± 0.24	-0.1 ± 0.11
ρ^-	-0.79 ± 0.16	-5.04 ± 0.55	-0.12 ± 0.11
ρ^0	-0.65 ± 0.16	-4.16 ± 0.45	-0.08 ± 0.12
ρ^+	-0.59 ± 0.09	-2.16 ± 0.76	-0.02 ± 0.07
Correlation coefficient	HRP	MnP	LiP
r	0.74	0.92	0.16
r^-	0.74	0.92	0.21
r^0	0.61	0.81	0.13
r^+	0.72	0.83	0.05

Figure 2.4A

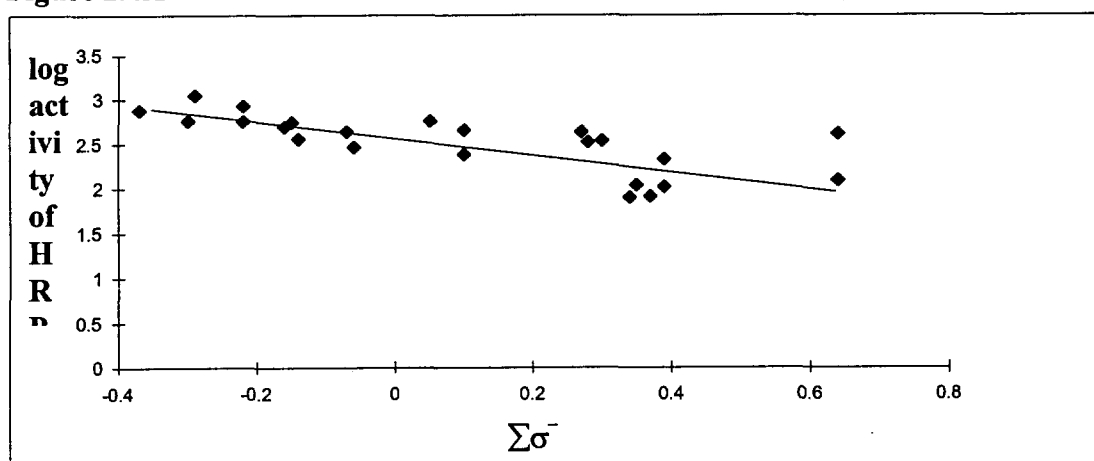


Figure 2.4B

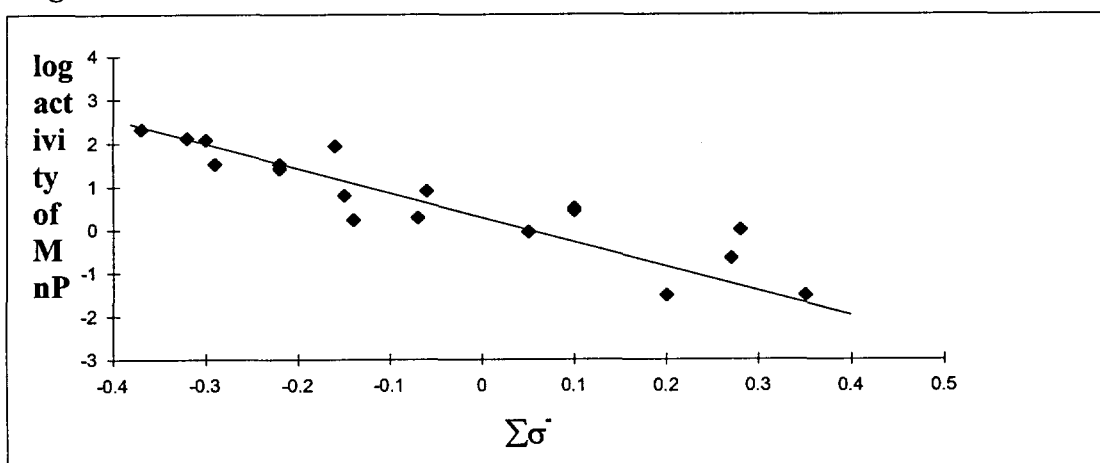


Figure 2.4C

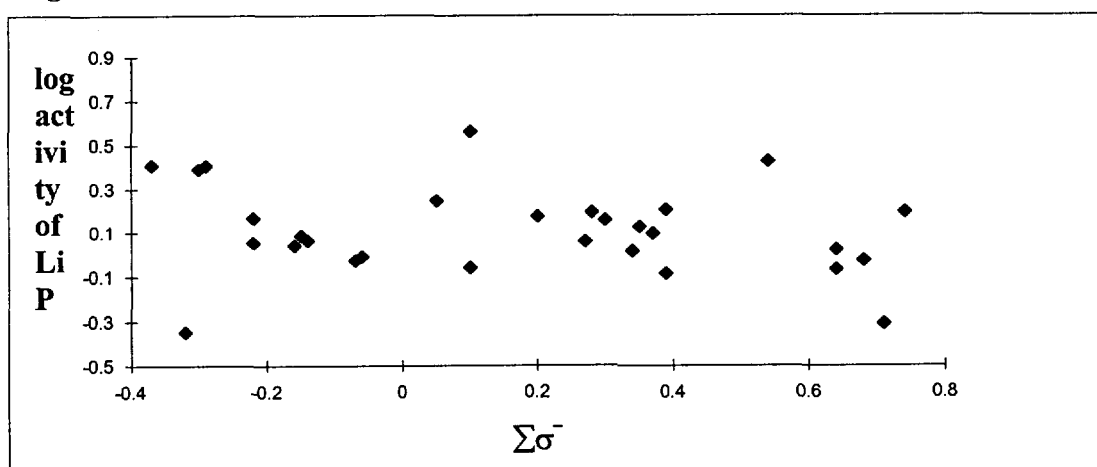


Figure 2.4A, B, and C. A plot of log activity of HRP, MnP, and LiP versus the sum of substituent constants for data shown in Table 2.5.

Table 2.6 Descriptors used in the correlation analysis
of azo dye oxidation by peroxidases

No.	Substituents	p <i>K</i> a	Sum of σ^-	<i>log activity</i>		
				HRP	MnP	LiP
1	2-Methyl	10.33	-0.15	2.741	0.799	0.086
2	3-Methyl	10.09	-0.07	2.638	0.279	-0.027
3	2-Methoxy	9.88	-0.16	2.693	1.932	0.041
4	3-Methoxy	9.65	0.10	2.380	0.505	-0.056
5	2-Fluoro	8.81	0.05	2.752	-0.046	0.246
6	3-Fluoro	9.28	0.34	1.896	NA	0.017
7	2-Chloro	8.56	0.27	2.631	-0.658	0.061
8	3-Chloro	9.12	0.37	1.907	NA	0.097
9	2-Bromo	8.45	0.28	2.517	NA	0.193
10	2-Iodo	8.51	0.30	2.533	NA	0.158
11	3-Iodo	9.03	0.35	2.033	-1.523	0.127
12	2-Nitro	7.23	1.24	NA	NA	NA
13	3-Nitro	8.35	0.71	NA	NA	-0.31
14	2,3-Dimethyl	10.54	-0.22	2.752	1.508	0.167
15	2,5-Dimethyl	10.40	-0.22	2.931	1.412	0.053
16	2,6-Dimethyl	10.62	-0.30	2.759	2.074	0.389
17	3,5-Dimethyl	10.20	-0.14	2.557	0.23	0.064
18	2,3-Dimethoxy	NA	-0.06	2.46	0.898	-0.009
19	2,6-Dimethoxy	7.68	-0.32	NA	2.111	-0.347
20	3,5-Dimethoxy	9.35	0.20	NA	-1.523	0.176
21	2,3-Difluoro	NA	0.39	2.016	NA	0.204
22	2,5-Difluoro	NA	0.39	2.322	NA	-0.086
23	2,6-Difluoro	NA	0.1	2.652	0.431	0.561
24	3,5-Difluoro	NA	0.68	0.732	NA	-0.027
25	2,3-Dichloro	7.70	0.64	2.608	NA	-0.066
26	2,5-Dichloro	7.51	0.64	2.087	NA	0.021
27	2,6-Dichloro	6.79	0.54	NA	NA	0.423
28	3,5-Dichloro	8.19	0.74	0.777	NA	NA
29	2,3,5-Trimethyl	10.67	-0.29	3.045	1.505	0.405
30	2,3,6-Trimethyl	NA	-0.37	2.876	2.314	0.407

strong, and, therefore, the reaction is predominantly controlled by electronic factors. A low σ value appears to be a necessary but not a sufficient condition for a dye to function as a good substrate for MnP. For example, 2,6-dimethyl- and 2,3,5-trimethyl-substituted dyes have very similar σ values (Table 2.1), but their MnP oxidation rates were $118 \mu\text{mol min}^{-1} \text{mg}^{-1}$ and $0.3 \mu\text{mol min}^{-1} \text{mg}^{-1}$, respectively.

Plotting log activity versus the sum of σ substituent constants for oxidation of phenolic azo dyes by LiP is shown in Figure 2.4C and Table 2.6; regression on these data yielded:

$$\log \text{ activity} = -0.12(\pm 0.11)\sigma + 0.13(\pm 0.20) \quad (2.4)$$

where $n = 29$, $s = 0.20$, $r = 0.21$. LiP activity does not indicate any correlation with σ substituent constants, possibly because, unlike HRP and MnP, LiP is extremely weak in azo dye oxidation.

Based on these correlation results, electronic effects appear to strongly influence azo dyes oxidation by MnP and weakly influence HRP oxidation. These effects might be related to two successive one-electron transfers from azo dye to the oxidized heme iron of the enzyme. In the peroxidase catalytic cycle, the native enzyme is transformed into two intermediates, compound I and compound II. These intermediates are electron acceptors. Azo dyes serve as electron donors. In azo dye oxidation (Figure 2.1), compound I initially oxidizes the hydroxyl group of the phenolic ring to a phenoxy radical by a one-electron process and is converted to compound II. In the next step, the phenoxy radical is oxidized by compound II to produce a carbonium ion, and this electron transfer completes the catalytic cycle. Electron-donating groups (negative σ values) on the benzene ring may increase the electron density on oxygen atoms of active sites, whereas electron-withdrawing groups (positive σ values) decrease the electron density. Consequently, the rate of reduction for compound I and compound II could be increased by electron-donating groups on the phenolic ring and decreased by electron-withdrawing groups. These results are in agreement with the correlation for phenol oxidation by peroxidases as shown in other studies (Job & Dunford, 1976; Dunford & Adeniran, 1986; Hsuanyu & Dunford, 1992). The current findings also suggest that, in addition to electronic effects, steric

effects might be important in peroxidase oxidation of azo dyes. The importance of the steric effect is dependent on the peroxidase.

Other molecular descriptors which can affect the electronic charge density at the reaction site were used for QSARs (Table 2.4). These molecular descriptors are the energy of the highest occupied molecular orbital (E_{HOMO}), half-wave potential ($E_{1/2}$), and ionization constants ($\text{p}K_a$). Generally, these descriptor variables reflect properties of substrate molecules in the reaction system. Plots of E_{HOMO} , $E_{1/2}$ and $\text{p}K_a$ versus peroxidase activities did not show any correlation (data not shown).

CHAPTER 3

OXIDATION OF AZO DYES BY THE $\text{Fe}^{\text{III}}/\text{H}_2\text{O}_2$ SYSTEM

3.1 Introduction

Azo dyes form the largest class of synthetic dyes used in industrial applications, constituting more than 50% of all dyes (Zollinger, 1987). It is estimated that approximately 10% of the dyes used in dyeing applications are ultimately released in waste water (Vaidya & Datye, 1982). Effluents discharged into the environment could contain up to 20% of unutilized dyes (Brown et al., 1981).

Currently dye waste is treated by several physical, chemical, and biological processes (Park & Shore, 1984). In physical processes, traditional methods such as adsorption and coagulation are widely used (Riefe, 1992). In the adsorption process, dyes bind to activated charcoal through hydrophobic interaction. In the coagulation process, calcium or ferric salts are added to the effluent; these metal salts are transformed to the corresponding insoluble hydroxides which adsorb the dyes. Drawbacks of these methods are that they do not degrade dyes and that it is expensive to dispose of the dyes that are absorbed by metal hydroxides and charcoal (Davis et al., 1994).

Chemical processes include chlorination, ozonation, and reduction (Park & Shore, 1984; Riefe, 1992; Cha et al., 1996). Chlorination is likely to produce toxic chlorinated dyes and their byproducts, which are difficult to biodegrade (Riefe, 1992; Davis et al., 1994). Ozone decolorizes dyes by an oxidative mechanism, but is limited by its efficiency and cost (Matsui et al., 1981; Park & Shore, 1984). Azo dyes can be decolorized using reducing agents such as alkaline dithionate or sodium borohydride (Riefe, 1992; Laszlo, 1997). However, a potential problem of this method is that the aromatic amines generated are potentially toxic or carcinogenic.

Azo dyes can be degraded by biological systems such as bacteria and white-rot fungi (Haug et al., 1991; Spadaro et al., 1992). In bacterial systems, azo dye degradation is generally initiated by the reductive cleavage of azo linkage under aerobic or anaerobic conditions (Walker, 1970; Brown & Laboureur, 1983; Haug et al., 1991). Bacterial degradation has been predicted to be economical, but very few bacteria which utilize dye as a sole source of carbon have been isolated. In addition, bacteria are not known to degrade dyes in a non-specific manner. Pagga and Brown (1986) observed that many azo dyes are highly resistant to aerobic bacterial degradation. Spadaro et al. (1992) demonstrated that under low nitrogen conditions the white-rot basidiomycete *Phanerochaete chrysosporium* can mineralize non-sulfonated azo dyes such as Disperse Orange 3, Disperse Yellow 3, *N,N*-dimethylphenylazoaniline, and Solvent Yellow 14 to CO₂. Paszczyński et al. (1992) demonstrated the mineralization of several sulfonated azo dyes. These oxidative systems are not yet suitable for remediating dye effluent.

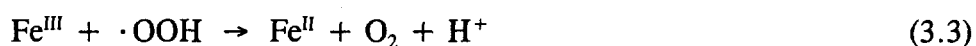
Since the biodegradation processes appear to be ineffective, there is a need for effective alternative technologies for eliminating dye from effluents. Advanced oxidation processes (AOPs), which use hydroxyl radicals ($\cdot\text{OH}$), might provide useful alternatives (Cha et al., 1996; Bahorsky, 1997). In AOP systems, $\cdot\text{OH}$ is produced using Fe^{III}/H₂O₂, UV/O₃, UV/H₂O₂, or TiO₂ systems (Walling, 1975; Goldstein et al., 1993; Ruppert et al., 1994; Gunten & Olivers, 1997). In particular, AOPs could be useful for eliminating non-biodegradable azo dyes (Leung et al., 1992; Legrini et al., 1993; Tang & An, 1995).

AOPs have been demonstrated to remove many hazardous organic pollutants (Masten & Davies, 1994; Shu et al., 1994; Hong et al., 1996). The reaction of $\cdot\text{OH}$ with aromatic compounds is very fast and approaches the diffusion-controlled rate (Walling, 1975). Kunai et al. (1986) studied the mechanism for benzene degradation by Fenton's reagent. The reaction of benzene with $\cdot\text{OH}$ resulted in mono- and di-hydroxylation of the ring. Several reports also demonstrated similar hydroxylations with chlorobenzene (Sedlak & Andren, 1991), dinitrotoluene (Ho, 1986), and nitrobenzene (Lipczynska-Kochany, 1991). Continued reaction with $\cdot\text{OH}$ results in further hydroxylation of phenols and then cleavage of the aromatic ring. Ring

cleavage products are further degraded to carboxylic acids and then oxidized to CO₂. Pignatello (1992) reported that the Fe^{III}/H₂O₂ system can mineralize chlorophenoxy herbicides to CO₂.

Many research groups attempted to decolorize azo dyes by AOPs. Dye effluents were decolorized by Fenton reagents (Bigda & Elizardo, 1992; Kuo, 1992; Solozhenko et al., 1995). Azo dyes were also decolorized by photochemical ·OH-generating systems (Hustert & Zepp, 1992; Dieckmann & Gray, 1994; Ruppert et al., 1994; Shu et al., 1994; Tang and An, 1995). However, those studies monitored only the loss of color as an indication of dye degradation. Decolorization generally demonstrates only the transformation of the chromophoric group of dyes; it does not indicate total degradation of the dye (Bigda & Elizardo, 1992). Spadaro et al. (1994) demonstrated that azo dyes can be mineralized by Fe^{III}/H₂O₂ system and proposed a probable mechanism for azo dye oxidation using ¹⁴C-labeled compounds. They further demonstrated the formation of benzene from phenylazo-substituted azo dye oxidation by ·OH.

In the Fenton system, one-electron reduction of hydrogen peroxide by Fe^{II} splits H₂O₂ homolytically to generate ·OH. Fe^{II} needed for the subsequent ·OH generation is produced by the reduction of Fe^{III} by H₂O₂. Fe^{II} can also be generated by the one-electron reduction by the hydroperoxy radical.



This study focuses on the optimization of the Fe^{III}/H₂O₂ system for azo dye oxidation and the effect of azo dye structures on its degradation by ·OH. Because the textile mill effluents contain various additives such as detergents, inorganic ions, and other solvents (Park & Shore, 1984), the effect of such additives on azo dye oxidation by the Fe^{III}/H₂O₂ system was also studied. Quantitative structure-activity relationships (QSARs) between phenolic azo dyes and ·OH reactivity were examined. These QSAR studies might help in predicting the dye substituents preferred in ·OH degradation and might suggest a probable mechanism.

3.2 Material and Methods

3.2.1 Chemicals

Mordant Orange I, Methyl Red, Orange II, benzalkonium chloride, sodium sulfate (Na_2SO_4), sodium iodide (NaI), and all substituted phenols were purchased from Aldrich (Milwaukee, WI) Orange I was obtained from TCI America (Portland, OR). All azo dyes were purchased in high purity and used without any further purification. Ferric nitrate ($\text{Fe}(\text{NO}_3)_3 \cdot 9\text{H}_2\text{O}$), D-(+)-glucose, [$U\text{-}^{14}\text{C}$]aniline, hydrogen peroxide (H_2O_2), and HPLC sorbent were obtained from Sigma Chemical Company (St. Louis, MO).

3.2.2 Syntheses of azo dyes

All azo dyes examined (Table 3.1A and B) contained two benzene rings and were synthesized by coupling the diazonium salt of 4-aminobenzenesulfonic acid with substituted phenols at 0–5°C under alkaline conditions. All azo dyes were purified and their structures were confirmed by fast atom bombardment–mass spectrometry as previously described (Chivukula et al., 1995).

3.2.3 ^{14}C -radiolabeled azo dye synthesis

Initially, ^{14}C -radiolabeled sulfanilic acid was synthesized by reacting 4 μl of ^{14}C -labeled aniline (2 μCi) in 200 μl H_2O containing 1 mg of unlabeled aniline with 50 μl of sulfuric acid (H_2SO_4) for 5 h at 180–190°C. The crude product was then purified by HPLC using a C-18 reverse phase column (0.46 \times 25 cm; Separations Group, Hesperia, CA). The eluent used in HPLC purification was a mixture of 100 mM phosphate (pH 7.0) and MeOH– H_2O (1:1). Product elution was monitored at 254 nm. To synthesize ^{14}C -labeled 4-(4'-sulfophenylazo)-2,6-dimethyl-phenol, 1 mg of ^{14}C -labeled sulfanilic acid and 3 mg of unlabeled sulfanilic acid were reacted with 3.2 mg of 2,6-dimethyl phenol, as described above. The crude product was purified using the HPLC sorbent for reverse phase chromatography (particle size 40–63 μm). A slurry of the HPLC sorbent (1 g) in methanol (5 ml) was loaded onto a small glass tube, and the methanol was allowed to drain. The sorbent was then equilibrated with

Table 3.1A Oxidation of 4-(4'-sulfophenylazo)-phenol dyes

No.	Substituent	Reaction time (min)	Amount of loss of color (%)	λ_{\max} (nm)
1	2-Methyl	10	30	358
2	3-Methyl	10	25	362
3	2-Methoxy	10	66	369
4	3-Methoxy	10	30	382
5	3-Fluoro	10	53	352
6	2-Chloro	10	95	354
7	3-Chloro	10	63	359
8	2-Bromo	10	49	362
9	3-Iodo	10	30	368
10	2,3-Dimethyl	10	42	362
11	2,5-Dimethyl	10	37	366
12	2,6-Dimethyl	10	51	359
13	3,5-Dimethyl	10	28	359
14	2,3-Dimethoxy	10	60	362
15	2,6-Dimethoxy	10	46	377
16	3,5-Dimethoxy	10	74	421
17	2,3-Difluoro	10	69	374
18	2,5-Difluoro	10	94	419
19	2,6-Difluoro	10	93	416
20	3,5-Difluoro	10	48	350
21	2,3-Dichloro	10	91	420
22	2,5-Dichloro	10	94	420
23	2,3,5-Trimethyl	10	23	351
24	2,3,6-Trimethyl	10	48	366

Table 3.1B Oxidation of 2-(4'-sulfophenylazo)-phenol dyes

No.	Substituent	Reaction time (min)	Amount of loss of color (%)	λ_{\max} (nm)
1	4-Methoxy	10	5	324
2	4-Chloro	10	24	318
3	4-Fluoro	10	21	318

Table 3.1C Oxidation of commercial azo dyes

No.	Substituent	Reaction time (min)	Amount of loss of color (%)	λ_{\max} (nm)
1	Orange II	10	90	484
2	Orange I	2	98	476
3	Methyl Red	10	71	524
4	Mordant-Orange I	10	67	385

water, and the crude product was applied to it. Dye was eluted using methanol, and the solvent was removed using nitrogen gas. If needed, the product was further purified by HPLC using the same column as described above. The purity of ^{14}C -labeled 4-(4'-sulfophenylazo)-2,6-dimethylphenol was confirmed by HPLC analysis to be approximately 99%.

3.2.4 Experimental procedures

All solutions used in this study, including stock solutions of 200 mM ferric nitrate salts, were prepared with water from a Milli-Q purification system (Millipore Corp., Bedford, MA). All experiments were performed at 25°C.

3.2.4.1 Estimation of hydroxyl radicals ($\cdot\text{OH}$). Estimation of $\cdot\text{OH}$ was performed using the deoxyribose assay (Halliwell & Gutteridge, 1981). Deoxyribose (3 mM) was reacted with 2 mM $\text{Fe}(\text{NO}_3)_3 \cdot 9\text{H}_2\text{O}$ and H_2O_2 (10–100 mM) in 2 mM EDTA (pH 7.0) for 10 min. Reaction volume was 1 ml. To that reaction mixture were added 1 ml of 1% (w/v) solution of thiobarbituric acid in 50 mM NaOH and 1 ml of 2.8% (w/v) aqueous trichloroacetic acid. This mixture was heated in a boiling water bath for 10 min. The absorbance was spectrophotometrically measured at 532 nm using a UV-visible spectrophotometer (Model UV-265, Shimadzu Corporation, Kyoto, Japan). The concentration of $\cdot\text{OH}$ was calculated using an extinction coefficient of $153 \text{ mM}^{-1} \text{ cm}^{-1}$ (Halliwell & Gutteridge, 1981).

3.2.4.2 Estimation of hydrogen peroxide (H_2O_2). H_2O_2 was estimated using horseradish peroxidase and iodide as its substrate (Cotton & Dunford, 1973). A solution of 2 mM $\text{Fe}(\text{NO}_3)_3 \cdot 9\text{H}_2\text{O}$ was reacted with H_2O_2 (10–100 mM) for 10 min in the presence of 2 mM EDTA (pH 7.0). Reaction volume was 1 ml. An aliquot of this mixture was diluted 100 times with 10 mM phosphate (pH 6.0). An aliquot (100 μl) of diluted reaction mixture was reacted with 10 μg of horseradish peroxidase and 10 mM NaI for 5 min in the presence of 10 mM phosphate (pH 6.0) in the dark. Total reaction volume was 1 ml. Triiodide formation was spectrophotometrically measured at 355 nm (Cotton & Dunford, 1973). An extinction coefficient of $255 \text{ mM}^{-1} \text{ cm}^{-1}$ was used for calculation of the H_2O_2 concentration.

3.2.4.3 Decolorization of azo dyes by the Fe^{III}/H_2O_2 system. The Fe^{III} solution (2 mM) was mixed with 2 mM EDTA (pH 7.0). Two minutes after the addition of EDTA, azo dye (200 μ M) and H_2O_2 were added. Except for 4-hydroxyazobenzene, reaction time for other reactions was 10 min. The amount of dye decolorized in that time was monitored by following the decrease in absorbance at the λ_{max} for each dye.

The effect of additives on azo dye oxidation was studied by following the oxidation of Orange II, as described above, in the presence of NaBr (20 mM), phosphate (20 mM), NaCl (20 mM), Na_2SO_4 (20 mM), glucose (1 mM), Tween 80 (0.1%), MeOH (10 μ l), chloroform (10 μ l), or benzalkonium chloride (1 mg). The effect of KNO_3 at various levels on Orange II oxidation was performed at pH 7.0 and pH 2.5 in the presence or absence of EDTA.

Products of Orange II oxidation were analyzed by HPLC and gas chromatography-mass spectrometry (GC-MS). The column and eluent used for HPLC analysis are described in Section 2.3. In GC-MS analysis, the reaction mixture of 4-hydroxyazobenzene was reduced with sodium dithionite. The reduction product was extracted with ethyl acetate, purified using HPLC, acetylated with pyridine and acetic anhydride (1:2), and then analyzed by GC-MS. GC-MS analyses were carried out at 70 eV on a VG Analytical 7070E mass spectrometer fitted with an HP 5790A GC and a fused capillary column (15 m, DB-5, J & W Scientific, Folsom, CA). A temperature gradient was used in the GC separation. The initial temperature was 70°C, and it was increased to 320°C at a rate of 10°C/min.

3.2.4.4 Correlation analysis. All charge densities of phenol and phenolate were calculated on AM1 optimized geometry of each dye using the CAChe computer program of Oxford Molecular (Beaverton, OR). Atomic charges on all atoms except hydrogen atoms, sulfonated benzene rings, and azo linkages were determined, and then charge densities of phenol and phenolate were calculated by multiple linear regressions using CAChe program (Grüber & Bub, 1989).

3.2.4.5 Mineralization of ^{14}C -labeled 4-(4'-sulfophenylazo)-2,6-dimethylphenol. The radiolabeled dye (60,000 cpm, 200 μ M) was mixed with Fe^{III} /EDTA (2 mM), KNO_3 (20 mM), and H_2O_2 (10 mM) (pH 7.0). The reaction

flask was sealed with a rubber cap and Parafilm. Samples were reacted for 4, 8, 12, and 24 h. At the end of the reaction times, the gas phase was purged with O₂ in order to displace any ¹⁴CO₂ generated in the reaction. ¹⁴CO₂ was collected by bubbling the displaced O₂ through a basic scintillation fluid (Kirk et al., 1978) and quantitated using a liquid scintillation spectrometer (Beckman LS-6500).

3.3 Results and Discussion

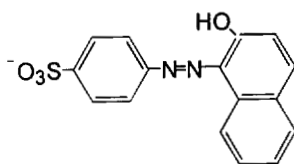
3.3.1 Effect of azo dye structures

Degradation of 32 different azo dyes by the Fe^{III}/H₂O₂ system was studied to understand the selectivity of ·OH in azo dye oxidation. QSAR studies were performed to understand the mechanism of azo dye oxidation. Except for Orange I and Orange II, all other azo dyes were phenolic dyes in which the phenolic ring was substituted with methyl, methoxy, chloro, fluoro, bromo, or iodo substituents as shown in Figure 3.1. The experimental conditions and oxidation data are summarized in Table 3.1A, B, and C.

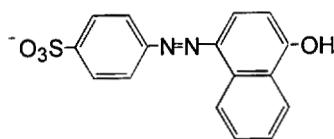
All azo dyes tested were oxidized by the Fe^{III}/H₂O₂ system. The position of mono-methyl substitution in the phenolic ring indicated only a minimal effect on dye oxidation. For example, amounts of oxidation of 2-methyl and 3-methyl substituted dyes were 30 and 25%, respectively. For the methoxy and chloro substituents, the 2-position was preferred over the 3-position. The number and position of methyl substitutions generally had only a limited effect on ·OH degradation. Introduction of one or two halogens into the phenolic ring enhanced the rate of decolorization. For example, amounts of oxidation of 2-chloro and 2,3-dichloro substituted dyes were 95 and 91%, respectively. Oxidation of Orange I was the fastest among azo dyes tested, whereas that of 4-hydroxyazobenzene (a hydrophobic dye) was the slowest. Oxidation of 2-(4'-sulfophenylazo)-phenol dyes was slower than that of 4-(4'-sulfophenylazo)-phenol dyes.

The charge density on the phenolate oxygen, protonated or deprotonated, is affected by the nature, number, and position of substituents. Since ·OH did not show any correlation with the Hammett constants, correlation with charge density on the

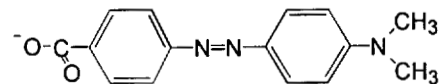
Orange II



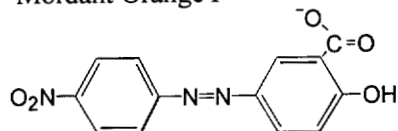
Orange I



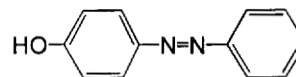
Methyl Red



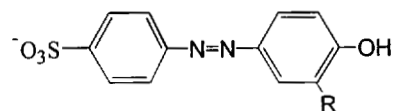
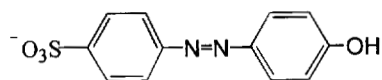
Mordant Orange I



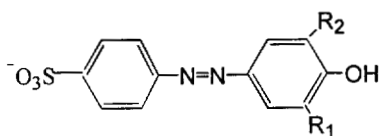
4-Hydroxyazobenzene



4-(4'-Sulfophenylazo)-phenol derivatives

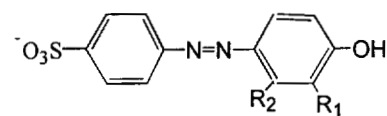


R = CH₃, OCH₃, NO₂, or X.



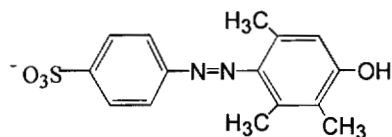
R₁ = CH₃ or OCH₃

R₂ = CH₃ or OCH₃

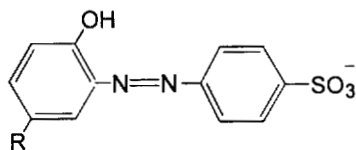


R₁ = CH₃, OCH₃, or X.

R₂ = CH₃, OCH₃, or X.



2-(4'-Sulfophenylazo)-phenol derivatives



R = CH₃, OCH₃, or X.

Figure 3.1 Structures of azo dyes.

phenolate oxygen was examined. Charge density was calculated by multiple linear regressions using the CAChe program.

A correlation was found between the amount of dye decolorized and the charge density of the phenolate anion species of the dye (Figure 3.2A and Table 3.2). A similar correlation was not observed with the charge density of the protonated form (Figure 3.2B and Table 3.2). Correction with the fraction of total phenol did not improve correlations. This correlation between the charge density on the phenolate anion and the rate of $\cdot\text{OH}$ oxidation of dyes suggested that dye oxidation is initiated by $\cdot\text{OH}$ attack on the phenolate anion.

3.3.2 Product analysis and probable mechanism

Products of Orange II and 4-hydroxyazobenzene oxidation by $\cdot\text{OH}$ were analyzed by HPLC and GC-MS. In HPLC analysis, Orange II oxidation products corresponded to 4-hydroxybenzenesulfonic acid ($t_R = 4.4$ min) and 1,2-naphthoquinone ($t_R = 22.3$ min) (Figure 3.3). Prior to GC-MS analysis, quinones were reduced and acetylated. One of the products from 4-hydroxyazobenzene was identified as the diacetoxy derivative of 1,4-benzoquinone. The mass spectrum of the 4-hydroxyazobenzene oxidation product corresponded to 1,4-benzoquinone. MS (m/z): 152 (19%); 135 (34%); 110 (85%); 93 (100%) (Figure 3.4).

Based on these analyses (Figures 3.3 and 3.4) and the QSAR study (Figure 3.2A), a possible mechanism of Orange II oxidation is proposed (Figure 3.5). The proposed mechanism resembles peroxidase oxidation of azo dyes (Spadaro & Renganathan, 1994). In this mechanism, $\cdot\text{OH}$ initially removes an electron from the phenolate anion to produce the corresponding radical. Then another $\cdot\text{OH}$ adds to the C-1 carbon of the naphthol ring, generating an unstable tetrahedral intermediate which breaks down to produce 1,2-naphthoquinone and 4-sulfophenyldiazene. One-electron oxidation of 4-sulfophenyldiazene (an unstable intermediate) by O_2 yields a 4-sulfophenyldiazene radical. Since the latter radical is an unstable intermediate, it cleaves homolytically to produce a 4-sulfophenyl radical and a nitrogen molecule. An addition of $\cdot\text{OH}$ to the 4-sulfophenyl radical might generate 4-hydroxybenzenesulfonic acid. Further degradation of 1,2-naphthoquinone and 4-hydroxybenzenesulfonic acid by $\cdot\text{OH}$ and O_2 could lead to aromatic ring degradation.

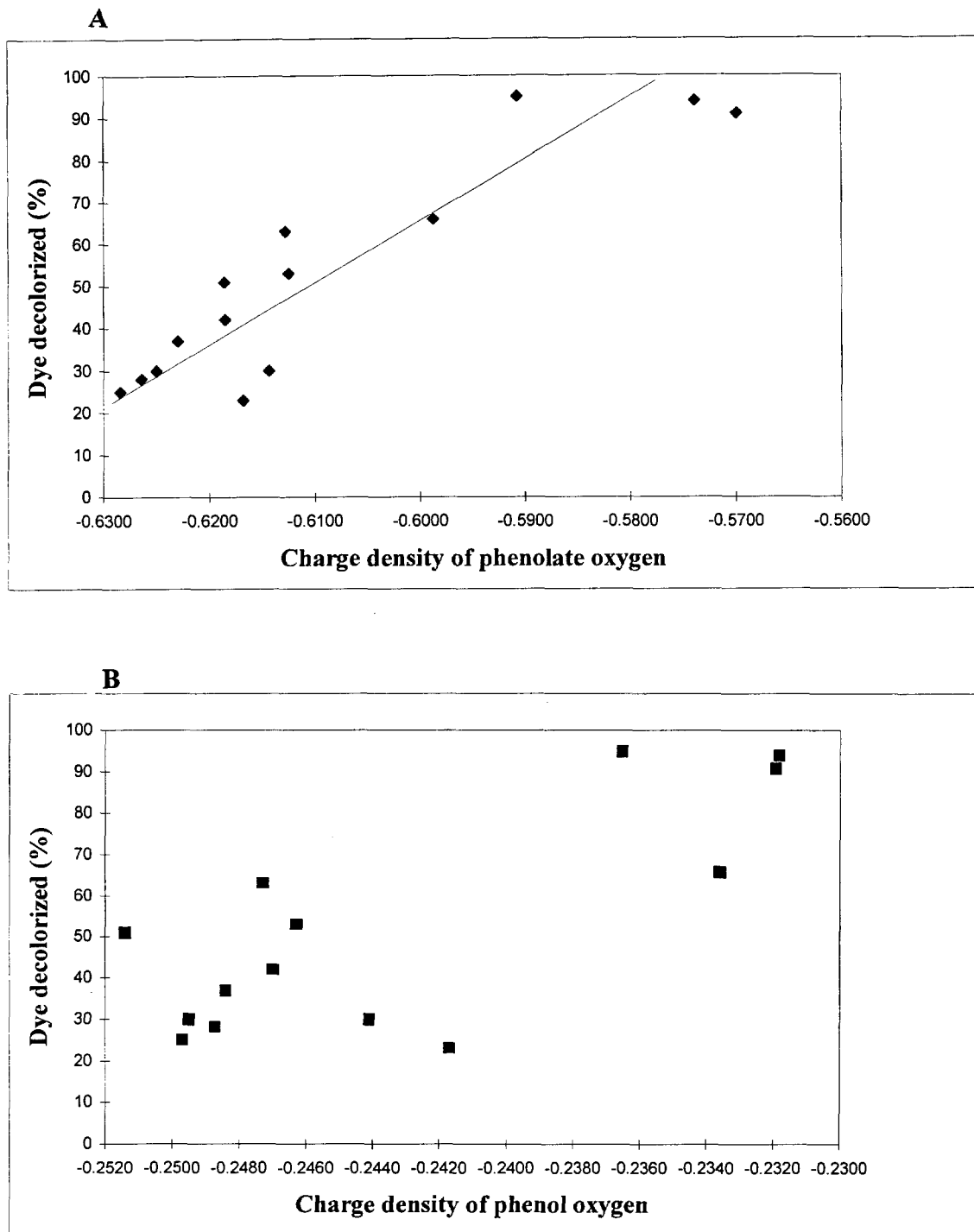


Figure 3.2 A plot of the amount of dye decolorized versus charge density on the deprotonated (A) and the protonated (B) forms of azo dyes.

Table 3.2 Descriptors used in the correlation analysis
of azo dye oxidation by $\text{Fe}^{\text{III}}/\text{H}_2\text{O}_2$

No.	Substituents	Charge density of phenol*	Charge density of phenolate*	Dye decolo- rized (%)
1	2-Methyl	-0.2495	-0.6250	30
2	3-Methyl	-0.2497	-0.6284	25
3	2-Methoxy	-0.2336	-0.5987	66
4	3-Methoxy	-0.2441	-0.6144	30
5	3-Fluoro	-0.2463	-0.6125	53
6	2-Chloro	-0.2365	-0.5908	95
7	3-Chloro	-0.2473	-0.6128	63
8	2,3-Dimethyl	-0.2470	-0.6185	42
9	2,5-Dimethyl	-0.2484	-0.6230	37
10	2,6-Dimethyl	-0.2514	-0.6186	51
11	3,5-Dimethyl	-0.2487	-0.6264	28
12	2,3-Dichloro	-0.2319	-0.5699	91
13	2,5-Dichloro	-0.2318	-0.5739	94
14	2,3,5-Trimethyl	-0.2417	-0.6168	23

*Calculated using CAChe computer program

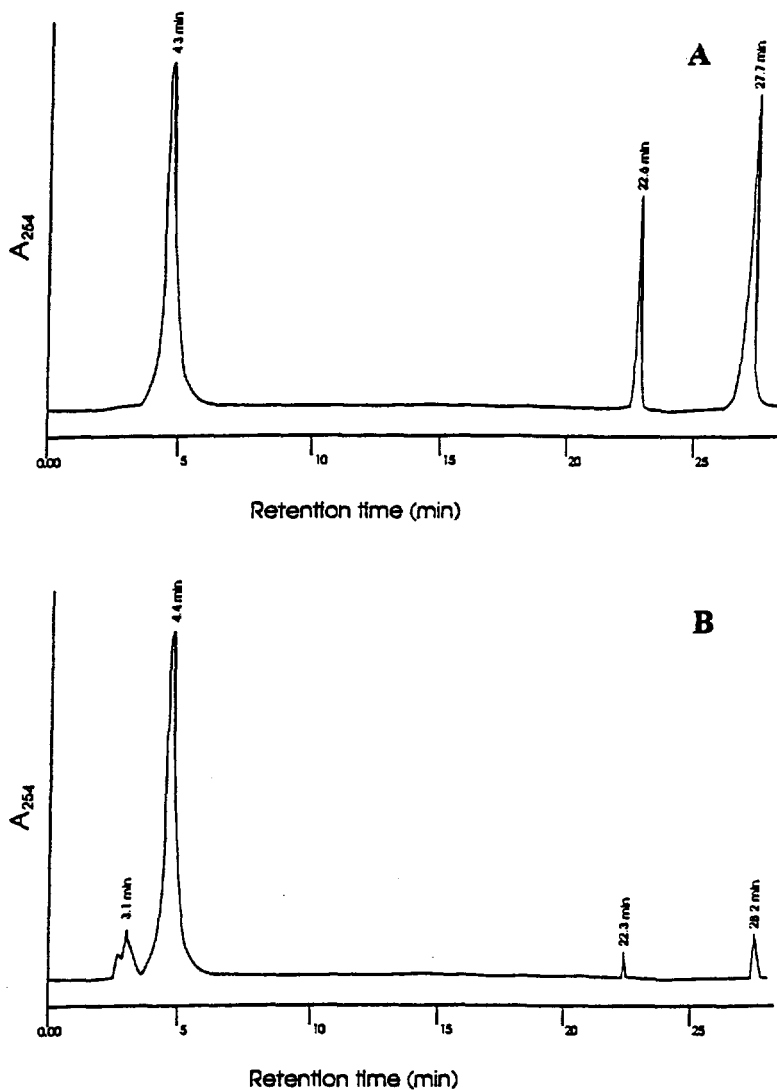


Figure 3.3 HPLC analysis of products from $\text{Fe}^{\text{III}}/\text{H}_2\text{O}_2$ oxidation of Orange II. (A) Standard of 4-hydroxybenzene sulfonic acid ($t_R = 4.3$ min), 1,2-naphthoquinone ($t_R = 22.6$ min), and Orange II ($t_R = 22.7$ min). (B) Reaction products. 4-hydroxybenzene sulfonic acid ($t_R = 4.4$ min), 1,2-naphthoquinone ($t_R = 22.3$ min), and Orange II ($t_R = 28.2$ min).

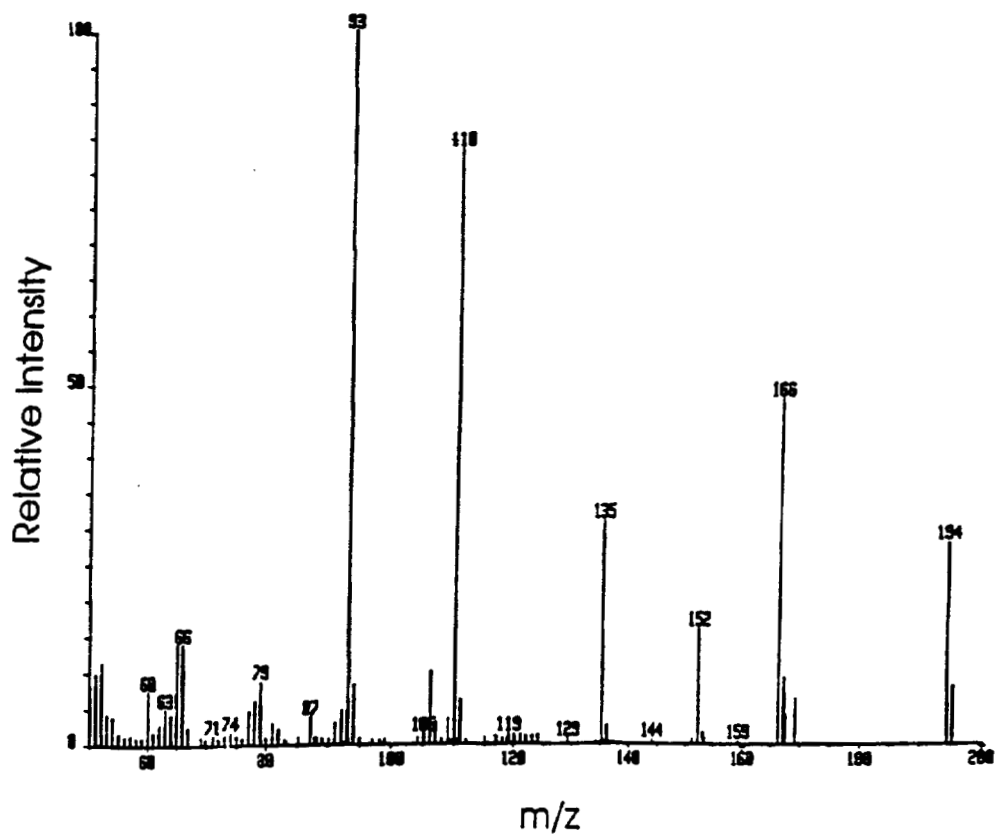


Figure 3.4 Mass spectrum of 4-hydroxyazobenzene oxidation product acetylated with pyridine and acetic anhydride (1:2). The range from 160 to 200 m/z was magnified. This product was identified as 1,4-benzoquinone.

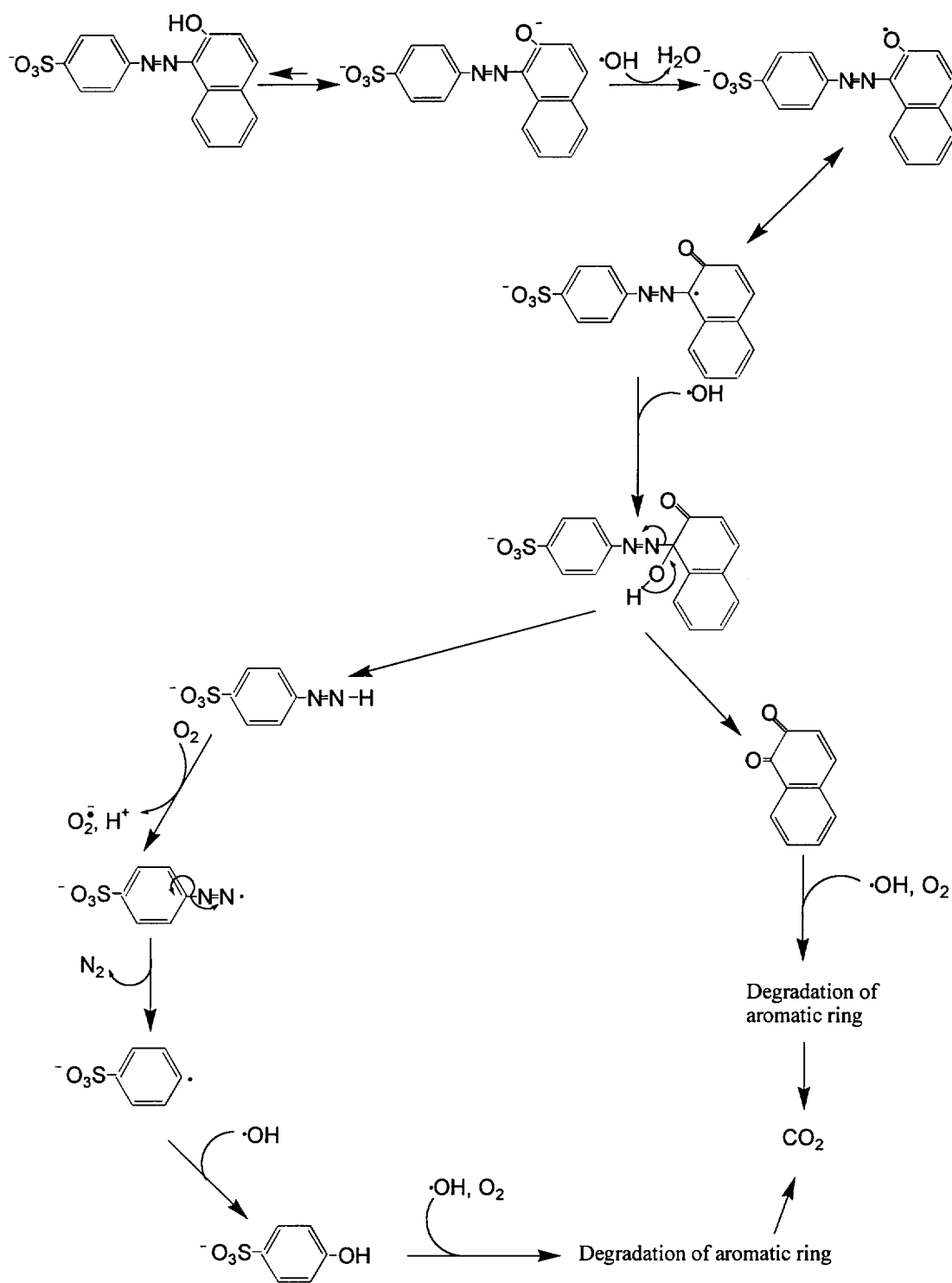


Figure 3.5 A proposed mechanism for the degradation of Orange II by $\text{Fe}^{\text{III}}/\text{H}_2\text{O}_2$.

3.3.3 Effect of H₂O₂ concentrations on azo dye oxidation

In order to investigate the relationship between azo dye oxidation and H₂O₂ concentration, oxidation of Orange II dye was carried out at various H₂O₂ concentrations. The fraction of the remaining dye ($[C]/[C_0]$) was plotted against [H₂O₂] (Figure 3.6). Dye oxidation increased with increasing H₂O₂ concentration, and its oxidation was almost complete at 50 mM H₂O₂.

3.3.4 Estimations of ·OH generation and H₂O₂ decomposition

This study was performed to determine the optimal condition between ·OH generation and H₂O₂ decomposition in the Fe^{III}/ H₂O₂ system. The amount of ·OH generated increased with the hydrogen peroxide concentration. No increase in ·OH generation was observed above 80 mM (Figure 3.7). However, H₂O₂ decomposition increased sharply above 70 mM H₂O₂ (Figure 3.8). The amount of H₂O₂ consumed ranged from 4 to 20 mM. Increased decomposition of H₂O₂ might be due to ·OH scavenging by H₂O₂. This competing reaction is described in equation 3.4 (Walling & Kato, 1971).



Such a reaction will decrease ·OH generation (40–140 μM) and increase H₂O₂ decomposition or consumption (Figure 3.7 and Figure 3.8). Thus, in the presence of high levels of H₂O₂, ·OH might be consumed by reaction with H₂O₂ rather than with the azo dyes.

3.3.5 Effect of additives on azo dye oxidation

Additives such as inorganic anions, detergents, sugar, or organic solvents are added during application of dyes. These additives are also released into the environment along with dyes. Hence, it is necessary to understand the effect of these additives on azo dye degradation by the Fenton system. Here, the effect of additives on Fenton degradation of azo dyes was tested using Orange II as the model dye. Additives tested included sodium sulfate, potassium phosphate, sodium chloride, sodium bromide, glucose, methanol, chloroform, benzalkonium chloride, and Tween 80 (Table 3.3).

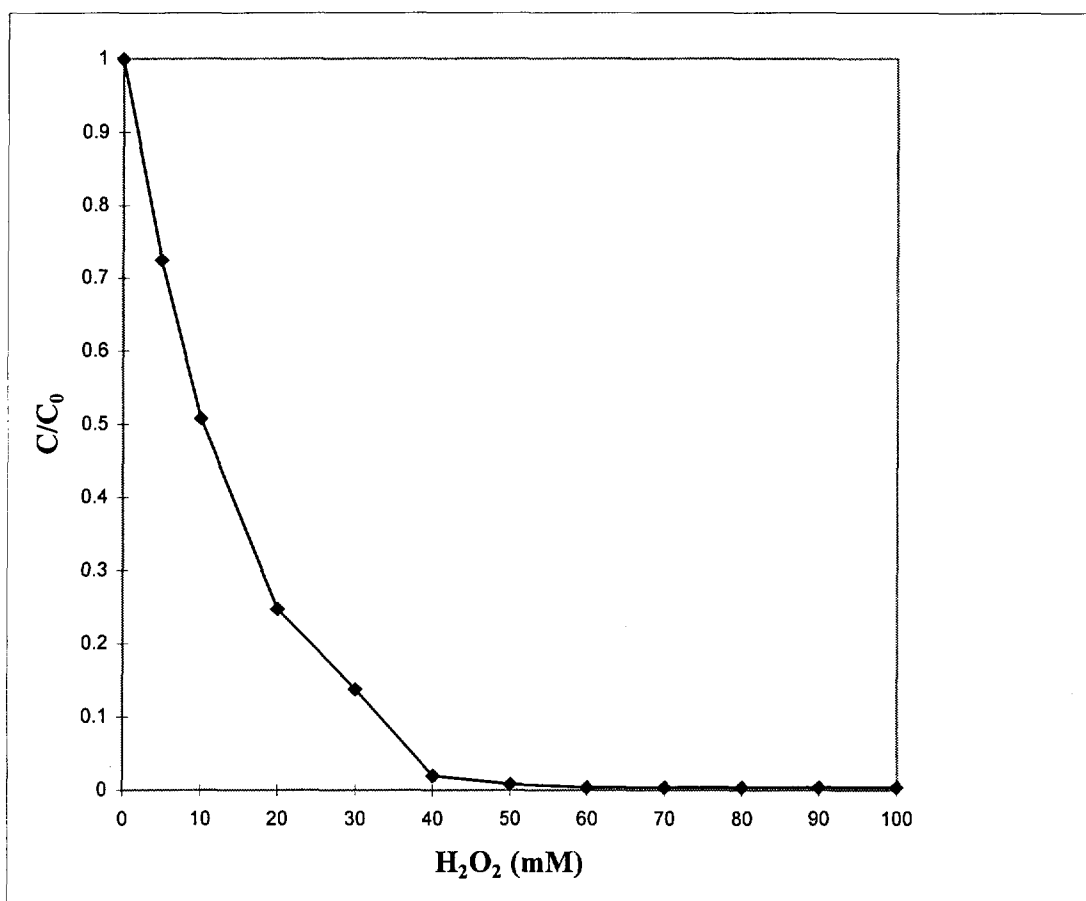


Figure 3.6 Oxidation of Orange II at various $[H_2O_2]$. Reaction conditions: $[Dye] = 200 \mu M$, $[Fe^{III}] = 2 \text{ mM}$, $[H_2O_2] = 5 \text{ mM}$, EDTA = 2 mM (pH 7.0), reaction time = 7 min at $25^\circ C$.

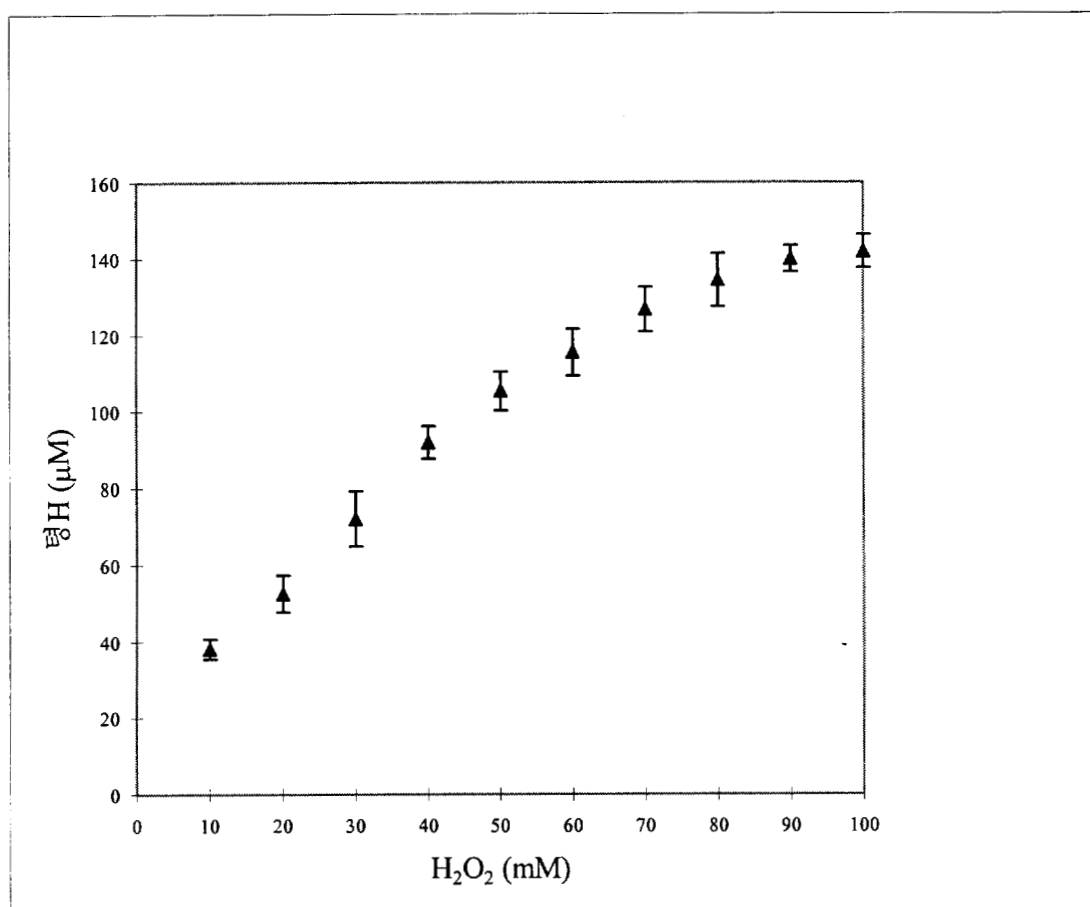


Figure 3.7 Estimation of hydroxyl radical concentrations. Reaction conditions: [Deoxyribose] = 3 mM, [Fe^{III}] = 2 mM, [H₂O₂] = 10-100 mM, EDTA = 2 mM (pH 7.0), and reaction time = 10 min at 25°C.

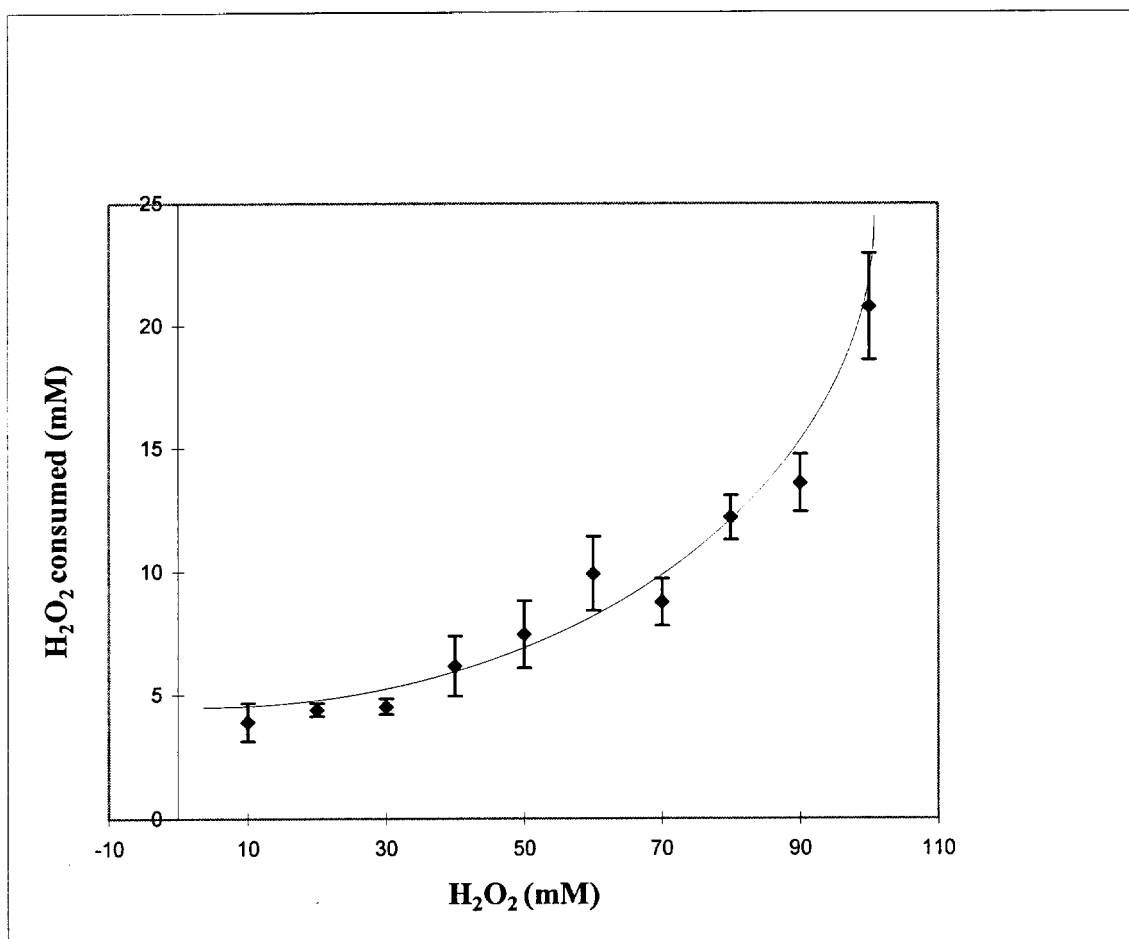


Figure 3.8 H₂O₂ consumption in Fenton's reaction. Reactions conditions: [H₂O₂] = 10–100 mM, Fe^{III} = 2 mM, EDTA = 2 mM (pH 7.0), and reaction time = 10 min at 25°C.

Chloride, bromide, and phosphate significantly affected azo dye oxidation by the $\text{Fe}^{\text{III}}/\text{H}_2\text{O}_2$ system (Table 3.3). Halides can affect dye oxidation by two different methods. They can react with $\cdot\text{OH}$ and thus make $\cdot\text{OH}$ unavailable for reaction with azo dyes. Halides react with $\cdot\text{OH}$ at the diffusion-controlled rate as described in equation 3.5 (Jayson et al., 1973). Secondly, halides can complex with iron (FeCl_2^{2+} , FeCl_2^+) and thus reduce the reactivity of iron with H_2O_2 (Pignatello, 1992).



Phosphate could affect $\cdot\text{OH}$ generation by precipitating iron from the solution which needs to be in solution for $\cdot\text{OH}$ generation. Sulfate did not affect azo dye oxidation, probably because it does not react with $\cdot\text{OH}$ and does not form a strong complex with iron.

Generally, nitrate ion (NO_3^-) is one of the common inorganic anions in textile effluents. KNO_3 (20 mM) added to the reaction mixture enhanced Orange II oxidation by 49% in 10 min in the presence of 2 mM EDTA (pH 2.5) (Figure 3.9A), and by 26% in 5 min in the absence of EDTA (pH 2.5) (Figure 3.9B). Orange II oxidation in the presence of 2 mM EDTA (pH 7.0) indicated a linear relationship, showing that Orange II disappearance is accelerated with increasing nitrate concentration (Figure 3.10). Oxidation of 4-(4'-sulfophenylazo)-2,6-dimethylphenol was also increased in the presence of nitrate anion (Figure 3.11). However, mineralization of ^{14}C -labeled 4-(4'-sulfophenylazo)-2,6-dimethylphenol by the $\text{Fe}^{\text{III}}/\text{H}_2\text{O}_2$ system was not affected by the addition of nitrate anion (Figure 3.12). GC-MS analyses of 4-hydroxyazobenzene products generated in the presence of nitrate ion showed that introduction of nitro-substitution on the aromatic benzene ring had not occurred (data not shown). The mechanism by which nitrate enhances dye decolorization is not understood.

Detergents such as benzalkonium chloride (cationic detergent) and Tween-80 (nonionic detergent) significantly decreased azo dye oxidation possibly by competing for $\cdot\text{OH}$ (Table 3.3). Other organic pollutants such as alcohol, glucose, and organic solvents might reduce dye oxidation by competing for $\cdot\text{OH}$ (Haag & Yao, 1992).

In summary, a correlation was observed between the amount of dye oxidized by the $\text{Fe}^{\text{III}}/\text{H}_2\text{O}_2$ system and the charge density on the phenolate ion. This suggests

Table 3.3 Effect of additives on Orange II decolorization by Fenton reagent

Compound	Amount of additive added	Amount of loss of color (%)
No additive	N/A	90.2
Sodium bromide	20 mM	14.5
Potassium phosphate	20 mM	0
Sodium chloride	20 mM	63.5
Sodium sulfate	20 mM	92.2
Glucose	1 mM	51.2
Methanol	10 μ l	4.9
Chloroform	10 μ l	48.8
Benzalkonium chloride	1 mg	26.8
Tween 80	0.1%	0.7

Same reaction conditions as Table 3.1.

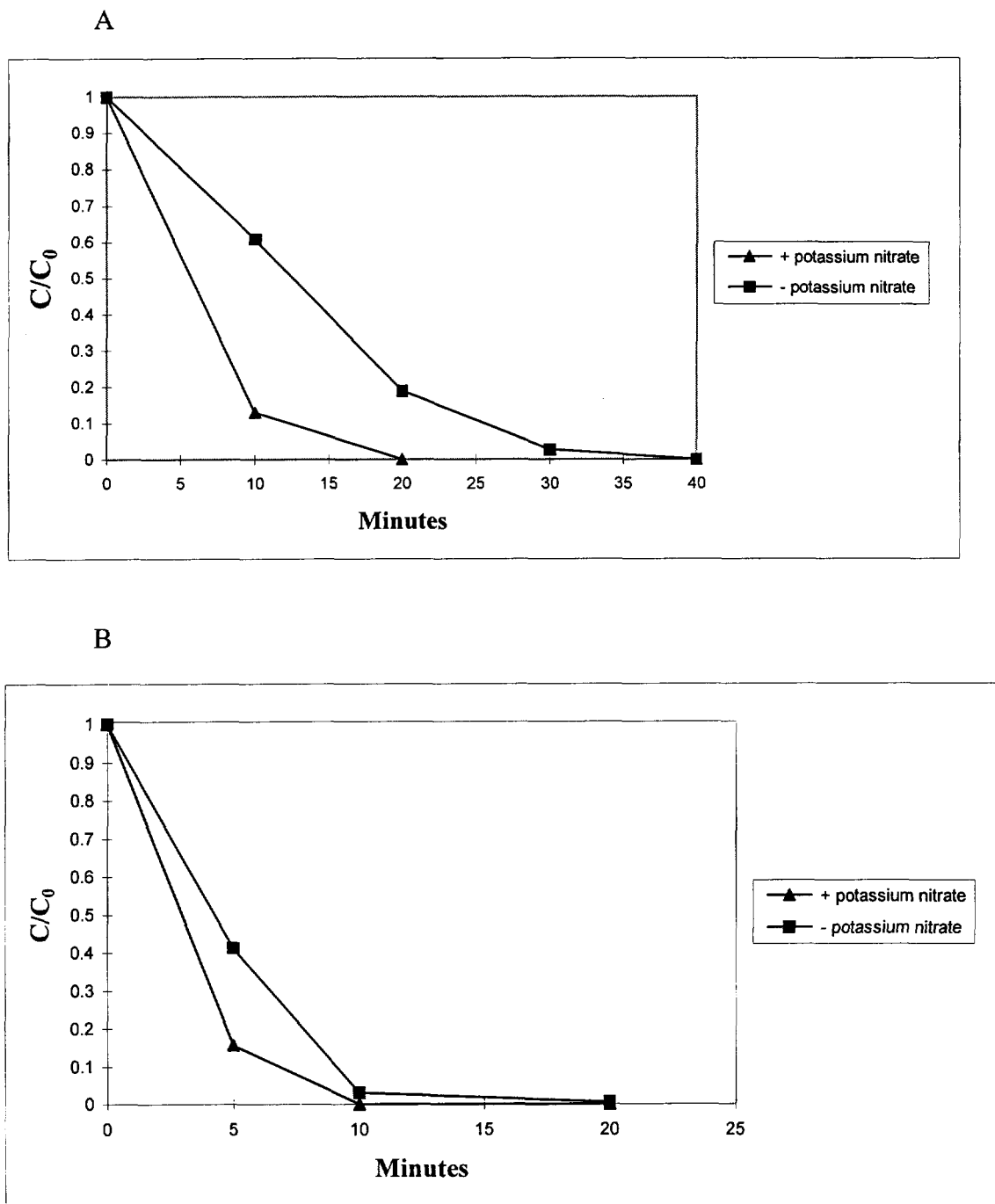


Figure 3.9 Effect of KNO_3 on Orange II decolorization. (A) Reaction conditions: $[\text{Dye}] = 200 \mu\text{M}$, $[\text{Fe}^{\text{III}}] = 2 \text{ mM}$, $[\text{H}_2\text{O}_2] = 10 \text{ mM}$, $[\text{KNO}_3] = 20 \text{ mM}$, EDTA = 2 mM (pH 2.5). (B) Reactions conditions were the same as A, except EDTA was excluded.

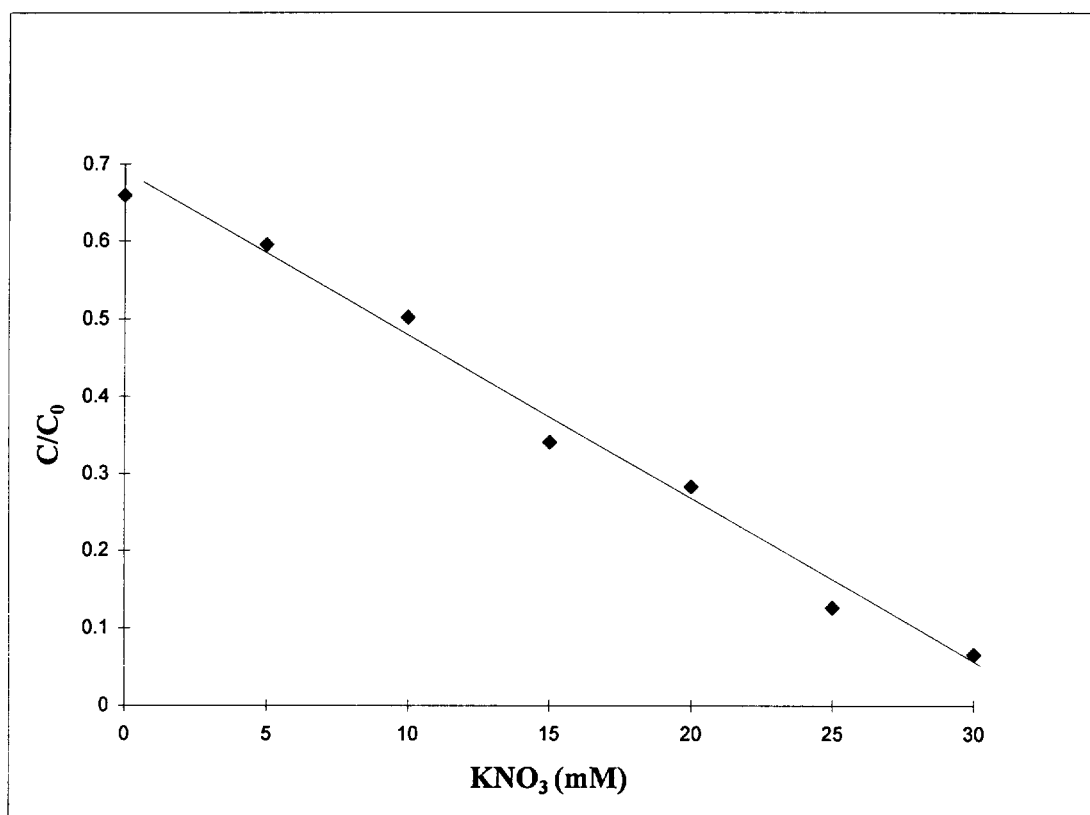


Figure 3.10 Effect of nitrate levels on Orange II oxidation. Reaction conditions: [Dye] = 200 μ M, [Fe^{III}] = 2 mM, [H₂O₂] = 10 mM, and [KNO₃] = 0–30 mM, EDTA = 2 mM (pH 7.0), and reaction time = 5 min at 25°C.

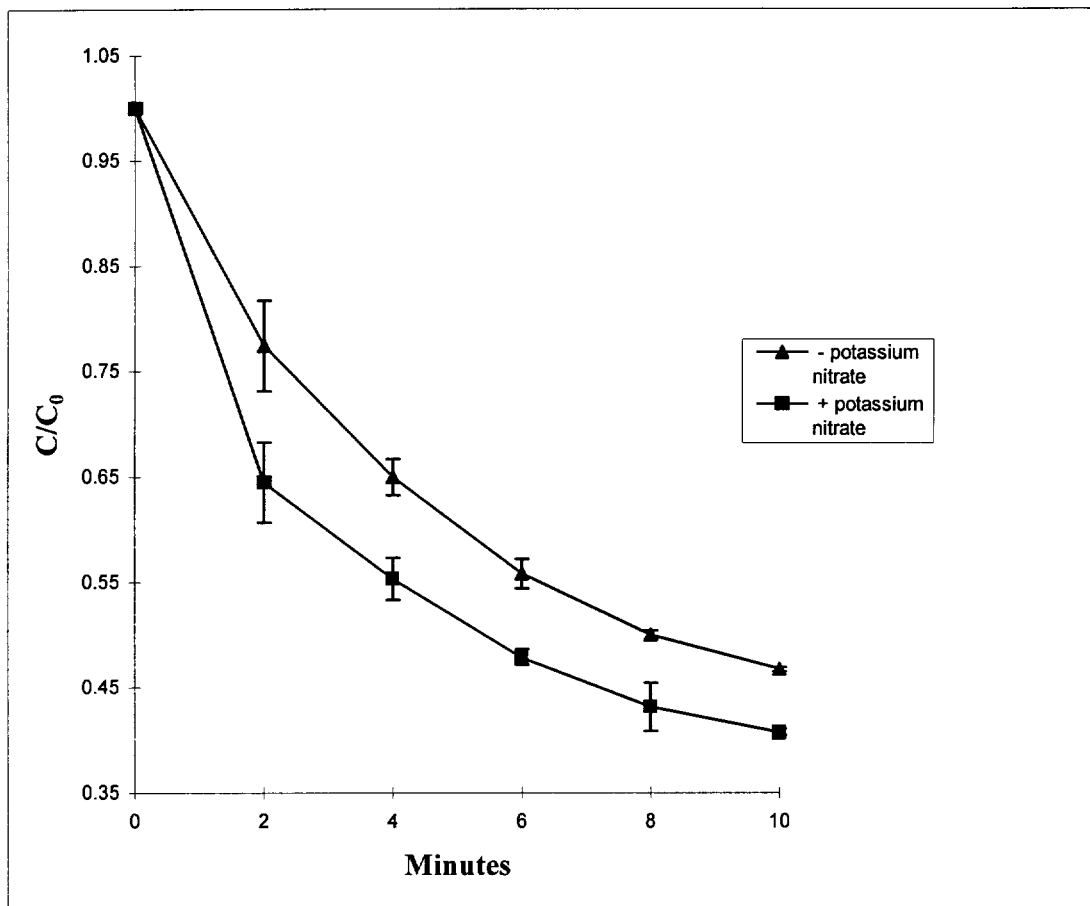


Figure 3.11 Effect of KNO_3 on oxidation of 4(4'-sulfophenylazo)-2,6-dimethylphenol. Reaction conditions: $[Dye] = 200 \mu M$, $[Fe^{III}] = 2 \text{ mM}$, $[H_2O_2] = 10 \text{ mM}$, and $[KNO_3] = 20 \text{ mM}$ in the presence of 2 mM EDTA (pH 7.0) at $25^\circ C$.

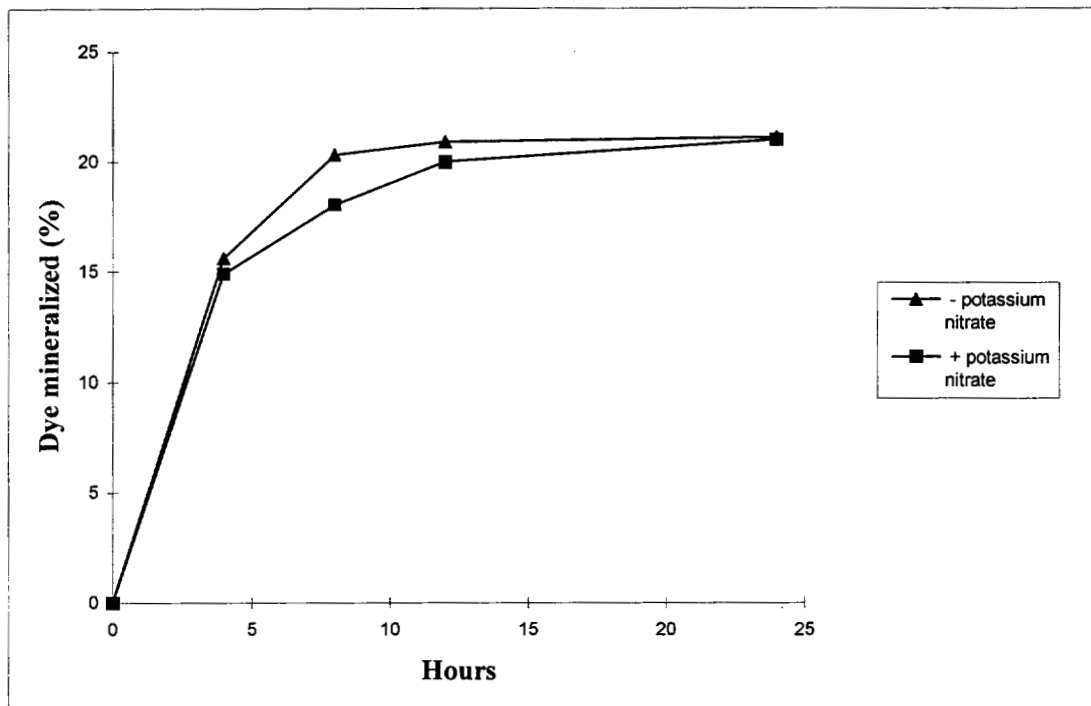


Figure 3.12 Effect of nitrate on the mineralization of ^{14}C -labeled 4-(4'-sulfophenylazo)-2,6-dimethylphenol. Reaction conditions: $[\text{Dye}] = 200 \mu\text{M}$ (60,000 cpm), $[\text{Fe}^{\text{III}}] = 2 \text{ mM}$, $[\text{H}_2\text{O}_2] = 10 \text{ mM}$, and $[\text{KNO}_3] = 20 \text{ mM}$ in the presence of 2 mM EDTA (pH 7.0) at 25°C .

that the initial reaction of $\cdot\text{OH}$ is with the deprotonated dye. The $\text{Fe}^{\text{III}}/\text{H}_2\text{O}_2$ system prefers 4-(4'-sulfophenylazo)-phenol derivatives over 2-(4'-sulfophenylazo)-phenol derivatives. Generation of $\cdot\text{OH}$ increased linearly with increasing initial H_2O_2 concentration. However, $\cdot\text{OH}$ generation at higher initial $[\text{H}_2\text{O}_2]$ is hindered, possibly due to $\cdot\text{OH}$ scavenging by H_2O_2 . Halides reduce dye decolorization perhaps by reacting with $\cdot\text{OH}$. Phosphate could retard dye decolorization by precipitating iron from solution. Surprisingly, nitrate enhances decolorization marginally, but it does not seem to have any effect on the mineralization of azo dye to CO_2 .

CHAPTER 4

NON-ENZYMATIC REDUCTION OF AZO DYES BY NADH

4.1 Introduction

Synthetic azo dyes are highly resistant to aerobic bacterial degradation (Zimmerman et al., 1982; Kulla et al., 1983; Idaka et al., 1987; Shaul et al., 1991). However, they can be reduced by chemical and biological processes. In chemical processes, azo dye reduction is primarily achieved by the cleavage of azo linkage using reducing agents such as sodium hydrosulfite, sodium dithionate, or Fe^0 (Riefe, 1992). Particularly, sodium hydrosulfite and sodium dithionate are powerful reducing agents under alkaline conditions (Riefe, 1992). Azo dyes such as Disperse Blue 79 and 4-aminoazobenzene are reduced by $\text{Fe}^{\text{II}}/\text{Fe}^{\text{III}}$ and Fe^0 redox systems (Weber & Adams, 1995; Weber, 1996). Azo linkage reduction by bacteria under aerobic as well as anaerobic conditions is known (Haug et al., 1991; Brown & DeVito, 1993). Azo dye reduction under anaerobic conditions is catalyzed by anaerobic bacteria, present in sludge, sediment, and mammalian intestines (Rafii et al., 1990; Brown & DeVito, 1993). The aromatic amines produced under anaerobic conditions could be further degraded by aerobic bacteria (Huang et al., 1979; Brown & Laboureur, 1983; Rafii et al., 1990; Haug et al., 1991; Chung & Cerniglia, 1992). Haug et al. (1991) demonstrated that a mixture of two separate aerobic and anaerobic bacterial cultures, when allowed to pass through successive anaerobic and aerobic conditions, can mineralize azo dyes to CO_2 . In that study, anaerobic cleavage of azo linkage occurred first, followed by aerobic degradation of reduction products. It was also observed that azo dye degradation by *Pseudomonas* sp. was initiated by the reductive cleavage of azo-linkage under anaerobic conditions, producing two aryl amine products (Zimmerman et al., 1982). Donlon et al. (1997) demonstrated that

methanogenic consortia can partially mineralize Mordant Orange I to CO₂ under anaerobic conditions.

In mammals, azo dye reduction by azo reductases occurs in the liver and in the intestinal microflora (Scheline et al., 1970; Walker et al., 1971; Zimmerman et al., 1982; Idaka et al., 1987). Several azo dyes are reduced to corresponding aryl amines by cytochrome P-450 and by a flavin-dependent liver cytosolic reductase (Huang et al., 1979; Rafii et al., 1990). Water-soluble azo dyes are primarily reduced to corresponding aryl amines by azo reductases in the intestinal microflora (Brown & DeVito, 1993). Partially soluble amine products might be absorbed by the intestinal lining. These enzymes require cofactors such as NADPH, FMN, or FAD (Idaka et al., 1987).

Wuhrmann et al. (1980) observed that reduced intracellular flavin nucleotides can non-enzymatically reduce azo dyes. Fujita and Peisach (1982) demonstrated that amaranth azo dye is non-enzymatically reduced by photochemically prepared FADH₂. In this process, two FADH₂ are oxidized for every one molecule of dye reduced (Fujita & Peisach, 1982). The reductive cleavage of azo linkage by reduced flavins was due to direct non-enzymatic reduction (Mallett et al., 1982). In addition, NADPH can reduce 4-aminoazobenzene non-enzymatically in the bacterial homogenate system, and the reduction increases with increasing NADPH concentration (Idaka et al., 1987).

In our search for an Orange II azo reductase from *Phanerochaete chrysosporium*, we observed that boiled intracellular extracts can reduce Orange II in the presence of NADH. This observation suggested that azo dyes can be non-enzymatically reduced by NAD(P)H (Nam & Renganathan, unpublished results). Here, NADH reduction of azo dyes is investigated in detail. The kinetics, mechanism, NADH selectivity for dyes, and products of dye reduction are examined.

4.2 Materials and Methods

4.2.1 Chemicals

Orange II, 4-aminobenzenesulfonic acid, and all substituted phenols were purchased from Aldrich, Milwaukee, WI. Reduced forms of β -nicotinamide adenine dinucleotide (NADH) and β -nicotinamide adenine dinucleotide phosphate (NADPH) were purchased from Sigma (St. Louis, MO). Sunset Yellow FCF and Allura Red were obtained from Warner Jenkinson (St. Louis, MO). 4-Hydroxyazobenzene was purchased from Fluka. Orange I was obtained from TCI America (Portland, OR). All chemicals except Orange II were purchased in high purity and used without any further purification. Orange II was purified by crystallization from hot aqueous solution.

4.2.2 Syntheses of azo dyes

All 4-(4'-sulfophenylazo)-phenol and 2-(4'-sulfophenylazo)-phenol azo dyes (Table 4.1A and B) were synthesized as described in Chapter 2.

4.2.3 Reduction of azo dye with NADH

An azo dye (50 μ M) and NADH (1 mM) were mixed in 20 mM succinate (pH 3.5), and the mixture was reacted for 40 min at 25°C. Dye reduction was monitored by following the decrease in absorbance at λ_{\max} for the dye.

4.2.4 Effect of pH on azo dye reduction

Orange I (10 μ M) and NADH (0.8 mM) were used. The pH range examined was from 3.5 to 8.0. Reaction time was 15 min at 25°C. Dye reduction was monitored by following the decrease in absorbance at 476 nm.

4.2.5 Effect of NADH levels on azo dye reduction

Orange I (100 μ M) and NADH (0.3–1.5 mM) were mixed in 20 mM succinate (pH 4.0) and the mixture was reacted for 1 h at 25°C. Dye reduction was monitored by following the decrease in absorbance at 476 nm.

Table 4.1A Reduction of 4-(4'-sulfophenylazo)-phenol dyes by NADH

No.	Substituent	λ_{\max} (nm)	Dye decolorized* (%)
1	no substitution	360	56
2	2-Methyl	358	71
3	2-Methoxy	369	61
4	2-Nitro	385	16
5	2-Chloro	354	35
6	2-Fluoro	356	33
7	2-Iodo	361	46
8	2-Bromo	362	32
9	3-Nitro	349	0
10	3-Chloro	359	78
11	3-Fluoro	352	50
12	3-Bromo	360	82
13	3-Iodo	368	83
14	2,3-Dimethyl	362	100
15	2,6-Dimethyl	359	71
16	2,3-Dimethoxy	362	77
17	2,3-Dichloro	420	81
18	2,3-Difluoro	374	26
19	2,3,5-Trimethyl	351	10
20	2,3,6-Trimethyl	366	100

Table 4.1B Reduction of 2-(4'-sulfophenylazo)-phenol dyes by NADH

No.	Substituent	λ_{\max} (nm)	Dye decolorized* (%)
1	4-Methyl	326	67
2	4-Methoxy	324	74
3	4-Chloro	318	47

Table 4.1C Reduction of commercial azo dyes by NADH

No.	Azo dye	λ_{\max} (nm)	Dye decolorized* (%)
1	Orange I	476	93
2	Orange II	484	44
3	4-Hydroxyazobenzene	348	31
4	Allura Red	500	77
5	Sunset Yellow FCF	484	58

* Quantitated by HPLC

4.2.6 Kinetics of azo dye reduction

Orange I (50 μ M) and NADH (10 mM) were mixed in 20 mM succinate (pH 3.5) at 25°C. Dye reduction was monitored by following the decrease in absorbance at 476 nm.

4.2.7 Analytical methods

The reduction of azo dyes was quantitated by monitoring the decrease in absorbance at the maximum wavelength for each azo dye with a UV-visible spectrophotometer (Model UV-265, Shimadzu Corporation, Kyoto, Japan). Dye reduction and product formation were also quantitated using HPLC. A C-18 reverse phase column described in Chapter 3 was used. The reductive products were eluted with a gradient containing 100 mM phosphate buffer (pH 7.0) and a mixture of deionized water and methanol (1:1). The reaction mixture was monitored at 254 nm using a UV-visible detector. The flow rate of eluent was 1 ml/min. Initially, the phosphate buffer concentration was maintained at 100% for 5 min. Then the water-methanol mixture was increased from 0 to 100% over 10 min and maintained at 100% concentration for an additional 10 min. For gas chromatography-mass spectrometry (GC-MS), the reduction product was extracted with ethyl acetate, purified using HPLC, and acetylated with pyridine and acetic anhydride (1:2). Analyses were carried out as described in Chapter 3.

4.3 Results and Discussion

The white-rot fungus *P. chrysosporium* completely oxidizes azo dyes to CO₂ (Spadaro et al., 1992). It is possible that this degradation is initiated by the reduction of azo linkage. To further understand this process, reduction of Orange II by intracellular extracts of *P. chrysosporium* was tested. Surprisingly, control experiments which contained either no enzyme or heat-inactivated enzyme showed high levels of azo dye reduction in the presence of NAD(P)H. This suggested that azo dyes can be non-enzymatically reduced by NAD(P)H.

4.3.1 pH effect on azo dye reduction

To evaluate pH effects on azo dye, Orange I reduction was examined at different pH values. Orange I was reduced up to 63% by 0.8 mM NADH in the pH range of 3.5 to 8.0 during a 15-min reaction (Figure 4.1). Reduction of Orange I was measured only in the pH range of 3.5 to 6.0, and maximum reduction was determined at the lowest pH.

Wuhrmann et al. (1980) observed a similar pH dependence on azo dye reduction by reduced flavin nucleotide. Reduction of azobenzene to aniline by abiotic reduction of an anaerobic sediment was also a pH-dependent process (Weber & Wolfe, 1987). The low pH optimum for azo dye reduction indicates the requirement for protons in the reductive process.

4.3.2 Effect of NADH levels on azo dye reduction

A series of Orange I reductions was performed at different NADH concentrations (0.3–1.5 mM) under identical experimental conditions at pH 4.0. The amount of azo dye reduced increased with increasing NADH concentration (Figure 4.2). These results are in agreement with second-order kinetics, indicating that the rate of disappearance of a reactant increases with the increasing concentration of another reactant.

4.3.3 Product analysis

The products of Orange I and 4-hydroxyazobenzene reduction by NADH were analyzed by HPLC and GC-MS. HPLC analysis showed that the reduction of Orange I via cleavage of the azo linkage generates 4-aminobenzenesulfonic acid ($t_R = 4.0$ min) (Figure 4.3B). β -Aminonaphthol, the second product of Orange II reduction, was not found because that product was unstable. Prior to GC-MS analysis, the reduction product was acetylated. The mass spectra of the acetylated 4-hydroxyazobenzene reduction product indicated the presence of an aniline derivative. Thus, the reduction product was identified as an aniline. MS (m/z): 135 (30%); 93 (100%); 77 (8%) (Figure 4.4). These findings suggest that NADH can reduce azo dyes by four electrons to generate two aromatic amines.



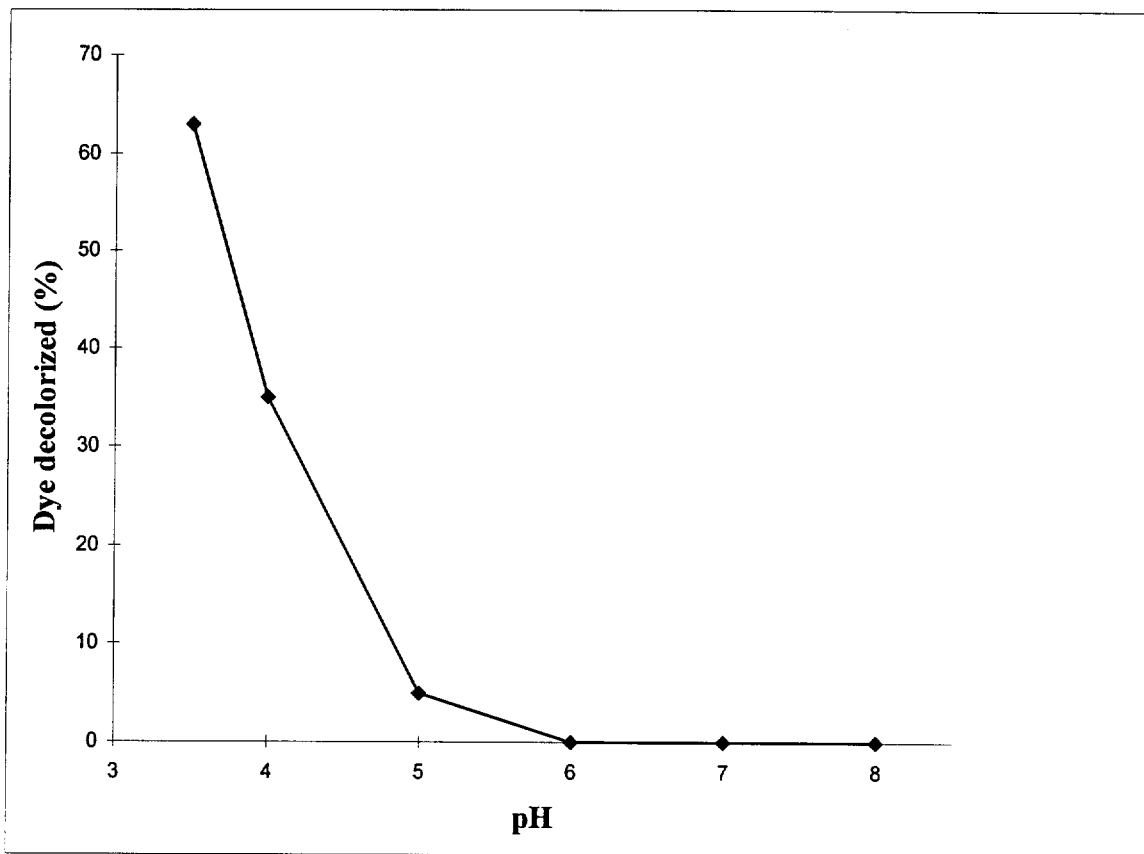


Figure 4.1 Effect of pH on the reduction of Orange I by NADH. $[\text{Dye}]_0 = 10 \mu\text{M}$ and $[\text{NADH}] = 0.8 \text{ mM}$. Reaction time was 15 min at 25°C .

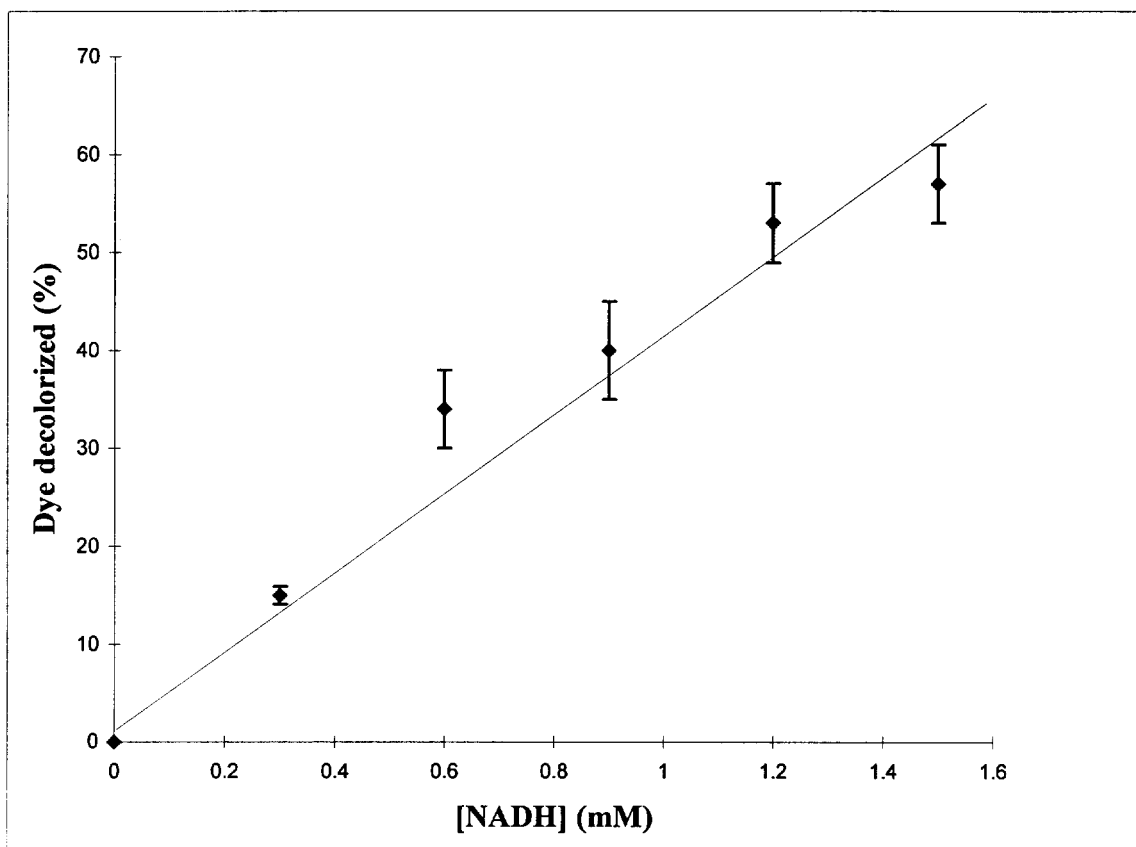


Figure 4.2 Effect of different NADH concentrations on the reduction of Orange I. Reaction conditions: $[\text{Dye}]_0 = 100 \mu\text{M}$ and $[\text{NADH}] = 0.3\text{--}1.5 \text{ mM}$ in the presence of 20 mM succinate (pH 4.0) at 25°C for 1 h.

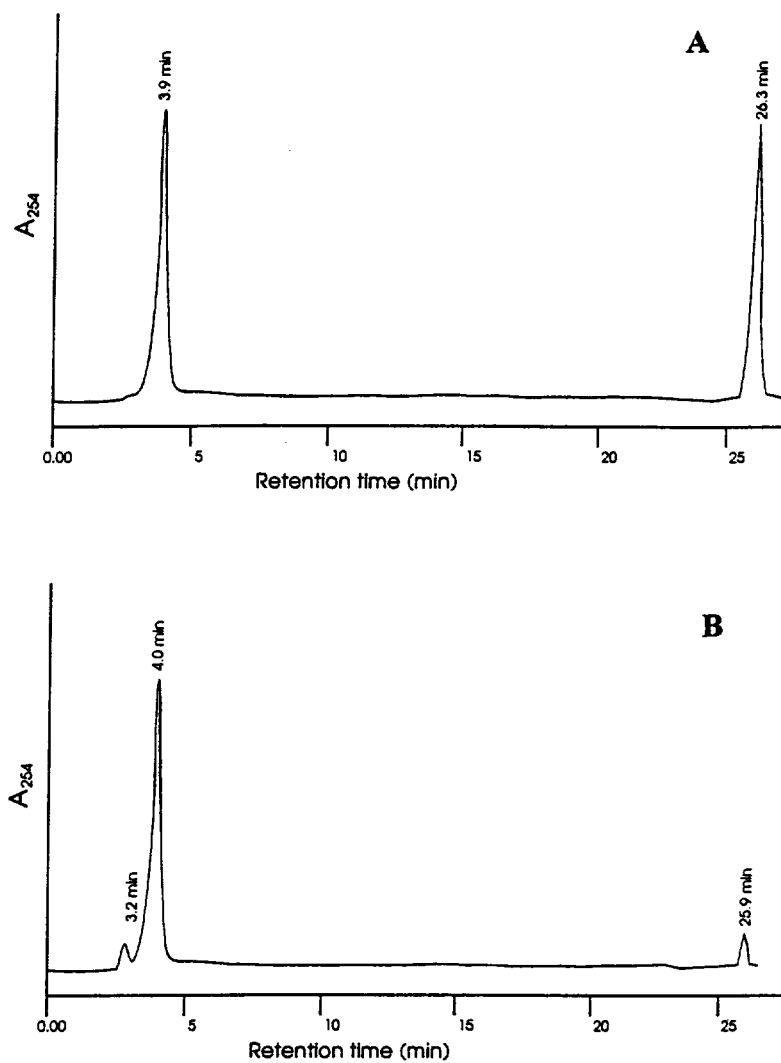


Figure 4.3 HPLC analysis of Orange I reduction products by NADH. (A) Standard of 4-aminobenzenesulfonic acid ($t_R = 3.9$ min) and Orange I ($t_R = 26.3$ min). (B) Reaction products. 4-Aminobenzenesulfonic acid ($t_R = 4.0$ min) and Orange I ($t_R = 25.9$ min).

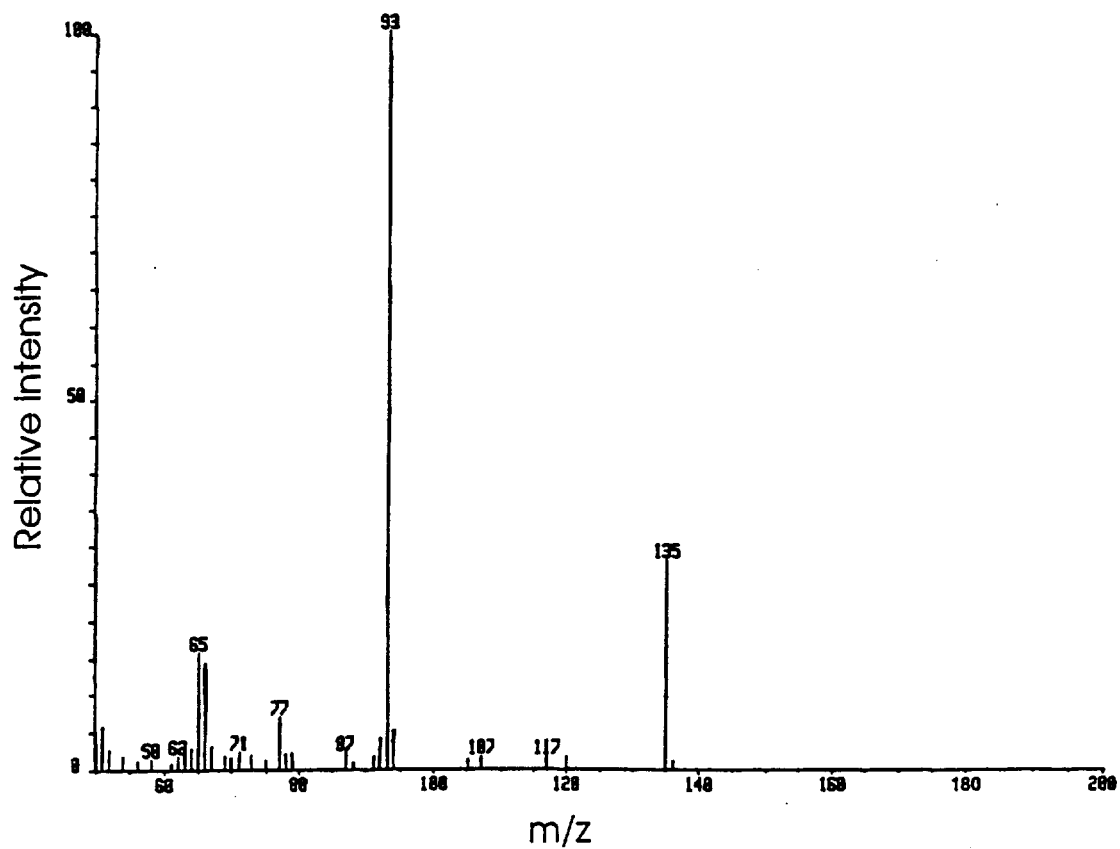


Figure 4.4 The mass spectrum of 4-hydroxyazobenzene reduction product acetylated with pyridine and acetic anhydride (1:2). This product was identified as aniline.

4.3.4 Kinetics of azo dye reduction

The rate of disappearance of a reactant in a second-order reaction is described by equation 4.2 in which A and B are the two reactants.

$$d[A] / dt = -k[A][B] \quad (4.2)$$

If the concentration of reactant B is in great excess with respect to reactant A, the rate law might be approximated by a pseudo first-order rate law assuming a constant concentration of B (Morris, 1990) as in equation 4.3:

$$d[A] / dt = -k_{\text{obs}}[A] \quad (4.3)$$

where k is the second-order constant, t is time, and k_{obs} ($k_{\text{obs}} = k[B]$) indicates the observed pseudo first-order rate constant.

The non-enzymatic reduction of Orange I by NADH was used as a model for the kinetic study. In this study, the initial concentration of dye was 50 μM , and that of NADH was 10 mM. The concentration of dye decreased with respect to time as shown in Figure 4.5. The plot of $\log [Dye] / [Dye]_0$ versus time was linear (Figure 4.6). Therefore, in this system, the disappearance of Orange I is characterized as a pseudo-first order reaction with respect to the dye concentration. k_{obs} was $0.110 \pm 0.004 \text{ min}^{-1}$ ($n = 5$, $s = 0.020$, $r^2 = 0.997$). However, at low concentrations of NADH, this kinetic reaction might change to a true second-order overall, first-order with respect to azo dye and NADH. Since k_{obs} is equal to $k[B]$ (equation 4.3), the second-order rate constant (k) in this system can be approximated as $0.183 \pm 0.007 \text{ M}^{-1} \text{ s}^{-1}$.

4.3.5 Proposed mechanism for azo dye reduction by NADH

Azo dye reduction occurred only under acidic conditions, indicating that dye reduction increased with decreasing pH. This suggests two probable pathways for azo dye reduction (Figure 4.7). Initially, a hydride of NADH may be added to nitrogen that is connected to the sulfonated benzene ring. This nitrogen is expected to be electron-deficient, because it is linked to a sulfophenyl group. Addition of a proton to the negatively charged nitrogen would create a hydrazo intermediate. Addition of one more hydride and one more proton would lead to cleavage of N–N bond to produce two aromatic amines. The second pathway involves initial protonation of the azo

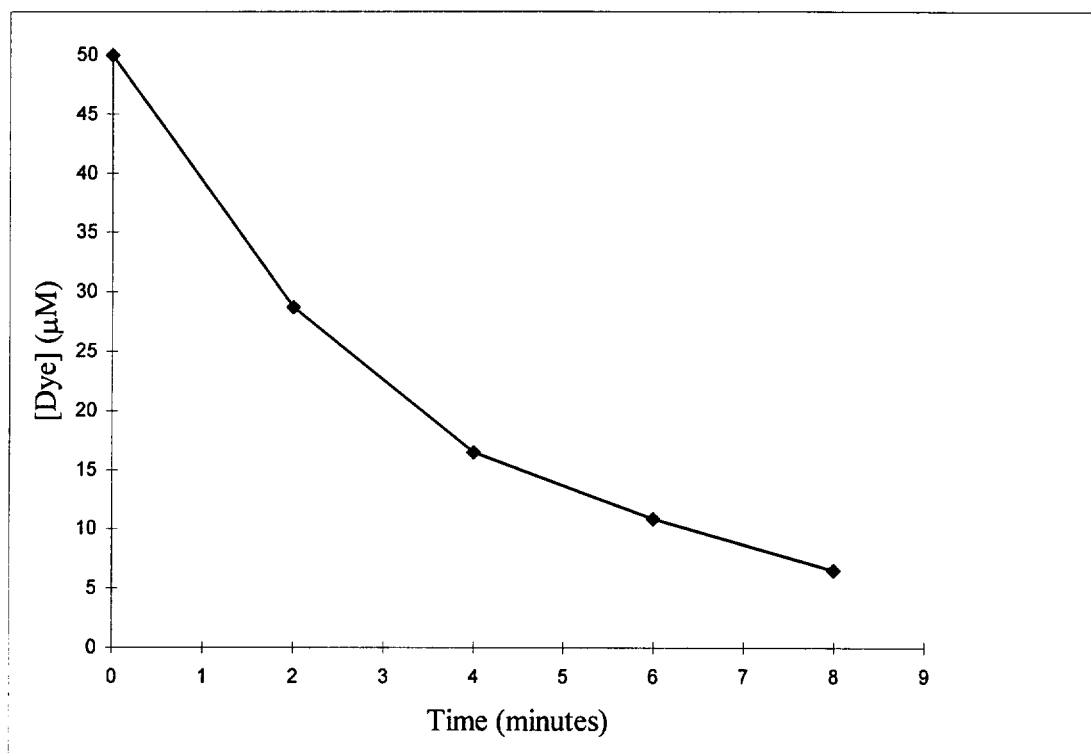


Figure 4.5 The reduction of Orange I by NADH. Reaction conditions: $[\text{Dye}]_0 = 50 \mu\text{M}$ and $\text{NADH} = 10 \text{ mM}$ in the presence of 20 mM succinate (pH 3.5) at 25°C .

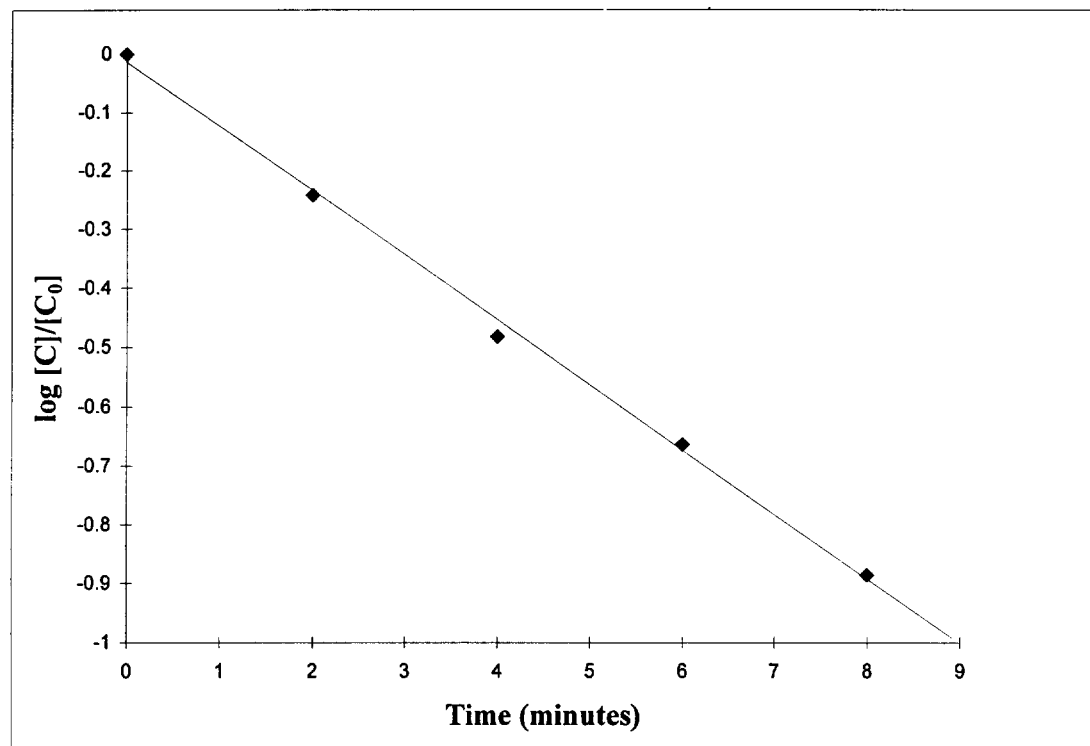


Figure 4.6 Linear regression of $\log C/C_0$ versus time (minutes) for same data shown in Figure 4.5, showing pseudo first-order disappearance of Orange I. The slope of the regression line gives $k_{\text{obs}} = 0.110 \pm 0.004 \text{ min}^{-1}$.

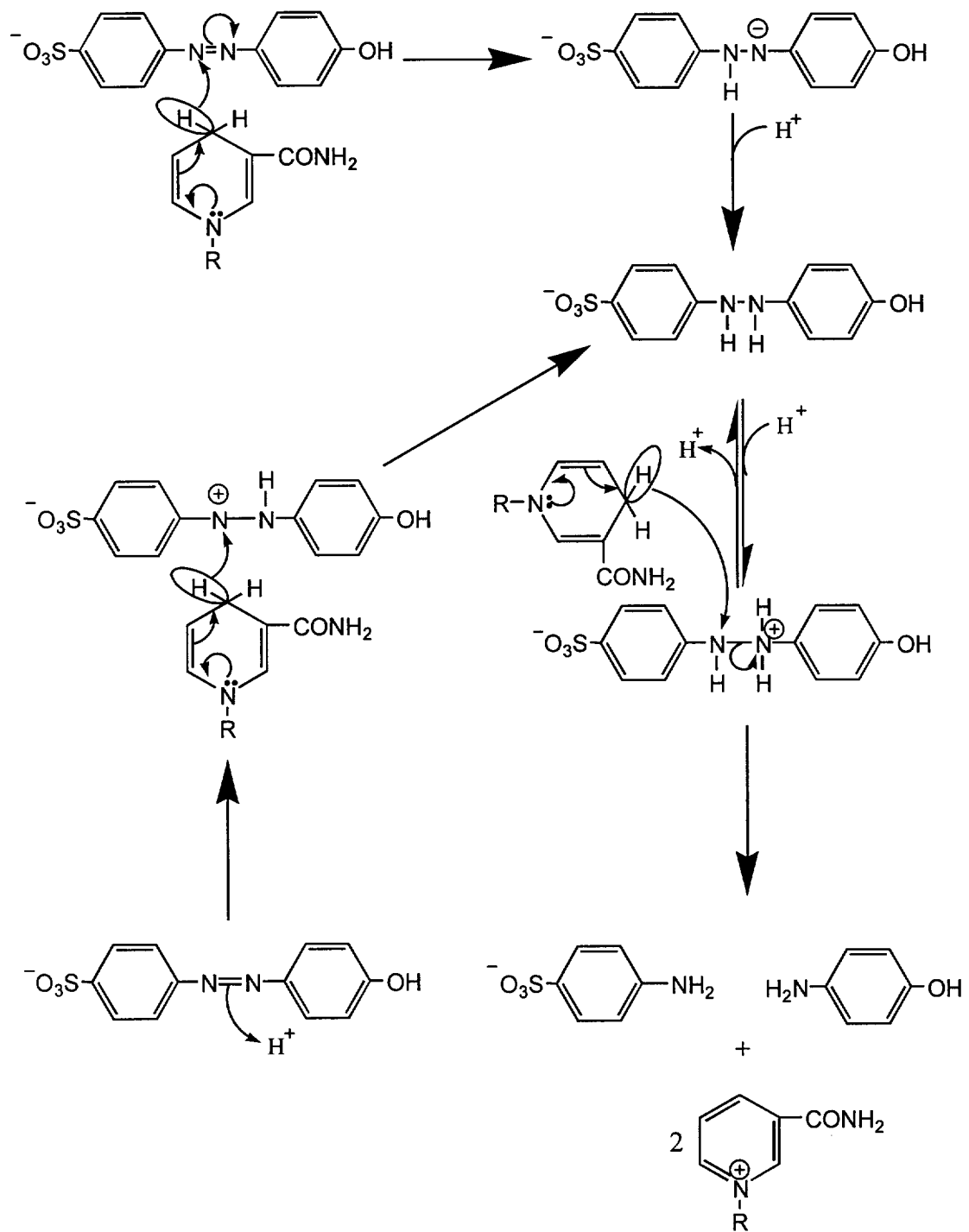


Figure 4.7 A probable mechanism for azo dye reduction by NADH.

linkage, followed by a hydride transfer to form the corresponding hydrazo compound. Alternatively, reduction might be initiated by proton addition to the azo linkage followed by a hydride transfer from NAD(P)H.

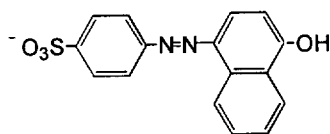
4.3.6 Effect of dye structures on azo dye reduction

To further understand the reductive process, reduction of Orange I, Orange II, 4-hydroxyazobenzene, Allura Red, and Sunset Yellow FCF was examined. Allura Red and Sunset Yellow FCF are used in foods. With the exception of 4-hydroxyazobenzene, all other dyes are naphthol-based dyes with one or two sulfonic acid groups. The amount of dye decolorized ranged from 31 to 93% (Table 4.1C). This suggested that there is some selectivity in the reduction of azo dyes by NAD(P)H. To further understand this selectivity, reduction of a variety of 4-(4'-sulfophenylazo)-phenol and 2-(4'-sulfophenylazo)-phenol dyes was examined. All substituent alterations were made only in the phenolic ring of azo dyes. The percentage of decolorization of these dyes at pH 3.5 in the presence of 1 mM NADH is presented in Table 4.1A and B. Structures of dyes studied are shown in Figure 4.8.

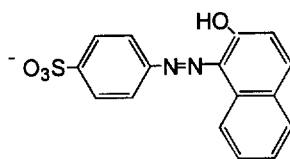
Among the mono-substituted dyes examined, all dyes except the 3-nitro substituted dye were reduced. In general, 3-substituted dyes appeared to be preferred over 2-substituted dyes. Introduction of electron-withdrawing substituents such as halogens in the 2-position decreased azo dye reduction. Introduction of halogens in the 3-position enhanced azo dye reduction. Introduction of di-methyl substitution in the 2,3-position or tri-methyl in the 2,3,6-position lead to complete reduction of those azo dyes. In general, introduction of an identical second substituent did not appear to significantly affect reduction. However, the 2,3-difluoro analog was an exception to this observation, in which reduction actually decreased compared to 2- or 3-fluoro substituted azo dye.

Substrate selectivity study favors the mechanism involving initial hydride transfer. Any substituent that decreases the electron density of azo linkage should increase the rate of hydride transfer; in contrast, a substituent which increases the electron density of azo linkage will retard hydride transfer. For example, a strong

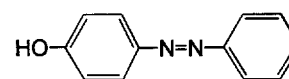
Orange I



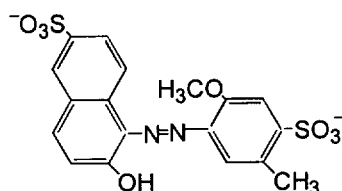
Orange II



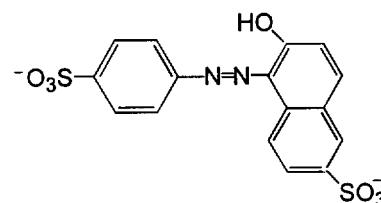
4-Hydroxyazobenzene



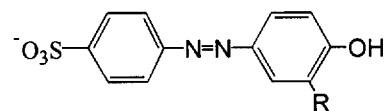
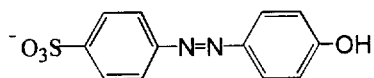
Allura Red



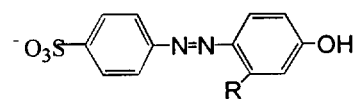
Sunset Yellow FCF



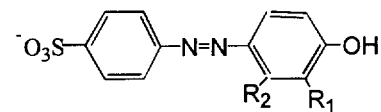
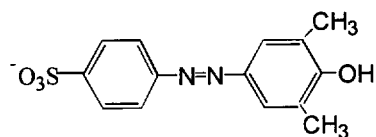
4-(4'-Sulfophenylazo)-phenol derivatives



R = CH₃, OCH₃, NO₂, or X.

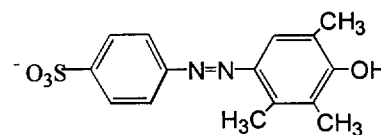
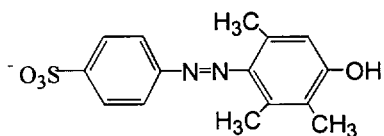


R = NO₂ or X.

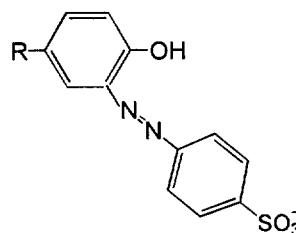


R₁ = CH₃, OCH₃, or X.

R₂ = CH₃, OCH₃, or X.



2-(4'-Sulfophenylazo)-phenol derivatives



R = CH₃, OCH₃, or Cl.

Figure 4.8 Structures of axo dyes.

electron-withdrawing substituent such as a halogen will make the phenol more acidic and lower its pK_a . When pK_a is low, the phenoxide form will predominate. The phenoxide via resonance can enrich the electron density of the azo linkage. This should reduce the rate of azo reduction. In accordance with this argument, 2-halogen substituted dyes are reduced at a slower rate compared to unsubstituted dyes. However, introduction of a 3-halogen substituent increases azo dye reduction. This might be because a 3-halogen substituent can withdraw electron density from the azo linkage by inductive effects. In addition to electronic effects, steric effects might also be important. Reduction of 2,3,5- and 2,3,6-trimethyl exemplifies this effect. Reduction of the 2,3,5-trimethyl analog is at least 10-fold lower than that of the 2,3,6-trimethyl analog. Since the electronic nature of the two analogs is expected to be similar, the observed differences are most probably due to steric effects.

The amount of reduction of 2-(4'-sulfophenylazo)-phenol dyes is comparable to that of 4-(4'-sulfophenylazo)-phenol dyes. 2-(4'-Sulfophenylazo)-phenol dyes are oxidized very slowly by peroxidases and the Fe^{III}/H_2O_2 system only, compared to 4-(4'-sulfophenylazo)-phenol dyes (see Chapters 2 and 3). This suggests that the former class of dyes is more susceptible to reduction than oxidation.

In summary, this study suggests that all the dyes tested, except the 3-nitro substituted dye, can be non-enzymatically reduced by NADH. Introduction of methyl and methoxy substituents into the 2-, 2,3-, 2,6-, or 2,3,6-position of the aromatic ring accelerates the reduction of phenolic azo dyes by NADH, compared to that of unsubstituted dye. In addition, halogenation on the 3-position renders phenolic azo dyes more susceptible to reduction than halogenation on the 2-position. The position of the azo linkage with respect to the hydroxyl group does not significantly influence the reduction of phenolic azo dyes.

Azo dye reduction by NADH has certain implications on the mammalian metabolism and degradation of azo dyes. In mammalian metabolism, sulfonated water-soluble azo dyes such as food dyes are primarily reduced only by intestinal anaerobic bacteria, and no reduction occurs in the mammalian liver (Brown & DeVito, 1993). The aromatic amine metabolites are suggested to be excreted from the body. However, this study suggests that non-enzymatic reduction might occur in

the stomach, where the environment is maintained in the pH range of 1.0 to 1.5 (Brady, 1990) and possibly from food sources when NAD(P)H is available.

One of the reasons bacteria are unable to oxidize azo dyes readily is attributed to the azo linkage, which does not occur in nature. However, aerobic bacteria can degrade aromatic amines. Thus, non-enzymatic reduction of azo dyes to amines could facilitate further degradation by bacteria. For example, sulfanilic acid, which could be formed from the reduction of a variety of azo dyes, can be degraded by an activated sludge (Brown & Hamburger, 1987). Hammer et al. (1996) also demonstrated that a mixed bacterial culture of *Hydrogenophaga palleronii* strain S1 and *Agrobacterium radiobacter* strain S2 can degrade sulfanilic acid. A drawback of this reduction is that it could also generate potentially carcinogenic aromatic amines.

CHAPTER 5

KINETICS OF AZO DYE REDUCTION BY ZERO-VALENT IRON

5.1 Introduction

Reduction of azo dyes can occur in biological, chemical, and photochemical systems. Some bacteria can reduce the azo linkages of azo dyes under both aerobic and anaerobic conditions (Chung & Stevens, 1992; Brown & DeVito, 1993). In mammals, the azo linkages of azo dyes are reduced by azo reductases in intestinal microflora and liver (Huang et al., 1979; Rafii et al., 1990; Chung & Cerniglia, 1992). Reduction of azo dyes appears to be mediated by a chemical redox process in anaerobic sediments at the bottom of stagnant or brackish waterways (Weber & Wolfe, 1987; Weber & Adams, 1995). Though the aromatic amine products generated by the dye reduction are toxic to mammals, they are more susceptible to biodegradation compared to the parent dye compounds (Zollinger, 1987).

Recently the remediation of contaminants by granular iron metal has been extensively studied. Zero-valent iron (Fe^0) is a mild reductant, which is readily oxidized to ferrous iron (Tratnyek, 1996). The direct role of Fe^0 as a reducing agent implies the involvement of reactive sites on the metal surface (Matheson & Tratnyek, 1994). The area and condition of the Fe^0 surface strongly affect the rate of reduction of organic pollutants including chlorinated aliphatics and nitro aromatics. The mechanism of these reactions appears to be electrochemical. Oxidation of Fe^0 to Fe^{II} could be the anodic reaction at the interface between Fe^0 and H_2O , and the reduction of compounds from solution could be the cathodic reaction (Agrawal & Tratnyek, 1996). The cathodic reaction varies with the reactivity of available electron acceptors. In pure anoxic aqueous systems, the acceptors include H^+ and H_2O , which yield OH^- and H_2 :



In oxic aqueous systems, O_2 is the preferred electron acceptor at the cathodic site:



Other strong electron acceptors (oxidants), both inorganic and organic, may offer additional cathodic reactions that contribute to iron corrosion (Agrawal & Tratnyek, 1996). For example, a recent study showed that the reduction of 4-aminoazobenzene by Fe^0 in an aqueous system resulted from a reaction mechanism involving a surfaced-mediated process (Weber, 1996). Hydrogen peroxide (H_2O_2) also reacts readily with Fe^0 at low pH (Tang & Chen, 1996). In this system, Fe^0 is oxidized to Fe^{+2} , which subsequently produces hydroxyl radicals via Fenton reaction.

In this study, we investigated the reduction of azo dyes by zero-valent iron metal in HEPES [N-(2-hydroxyethyl)-piperazine-N'-(2-ethanesulfonic acid)] buffer. The objective was to characterize the kinetics of azo dye reduction by Fe^0 . The findings in this study should help assess the possible use of Fe^0 in waste water treatment technologies for azo dyes.

5.2 Materials and Methods

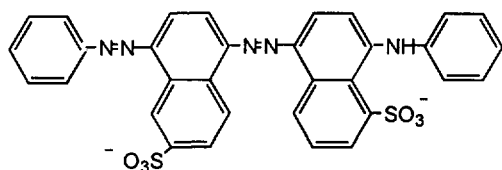
5.2.1 Chemicals

Food dyes such as Allura Red (FD&C Red # 40), Tartrazine (FD&C Yellow # 5), Brilliant Blue FCF (FD&C Blue # 1), and Sunset Yellow FCF (FD&C Yellow #6) were obtained from Warner Jenkinson (St. Louis, MO). Orange I was purchased from TCI America (Portland, OR). Amaranth, Naphthol Blue Black, Crocein Orange G, Orange II, and Acid Blue 113 were obtained from Aldrich (Milwaukee, WI). The dyes and their structures are summarized in Table 5.1 and Figure 5.1. All dyes were purchased in the highest purity that was commercially available and used as received without further purification. Zero-valent iron filings (>99.9%, Fluka, Cat. No. 44905) were sieved to obtain the 16–32 mesh size grains and then used without any further treatment. The surface area of this iron was $1.42 \text{ m}^2 \text{ L}^{-1}$, as determined by BET gas adsorption with krypton (Johnson et al., 1996).

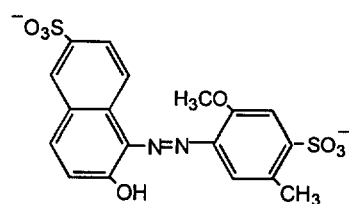
Table 5.1 Dyes used and their physical properties

No.	Name	Synonyms	CI No.	CAS No.	M.W. (g/mol)	λ_{\max} (nm)
1	Acid Blue 113	N/A	26360	3351-05-1	637.68	566
2	Allura Red	FD&C Red # 40	16035	25956-17-6	452.45	500
3	Amaranth	Acid Red 27	16185	915-67-3	538.52	521
4	Brilliant Blue FCF	FD&C Blue # 1	42092	3844-45-9	751.90	610
5	Crocein Orange G	Acid Orange 12	15970	1934-20-9	328.34	484
6	Naphthol Blue Black	Acid Black 1	20470	1064-48-8	574.54	618
7	Orange I	N/A	14600	523-44-4	328.34	476
8	Orange II	Acid Orange 7	15510	633-96-5	328.34	484
9	Sunset Yellow FCF	FD&C Yellow # 6	15985	2783-94-0	408.40	482
10	Tartrazine	FD&C Yellow # 5	19140	1934-21-0	468.41	424

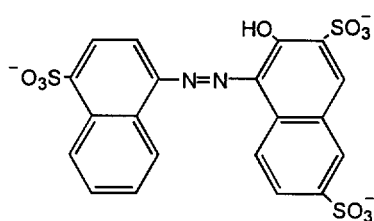
1. Acid Blue 113



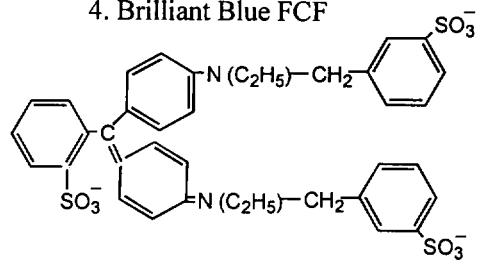
2. Allura Red



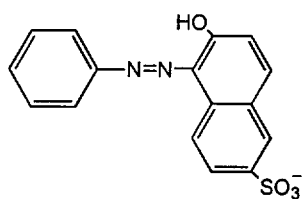
3. Amaranth



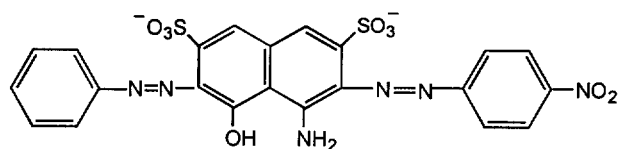
4. Brilliant Blue FCF



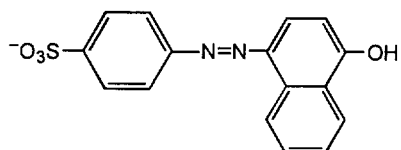
5. Crocein Orange G



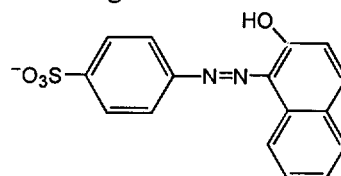
6. Naphthol Blue Black



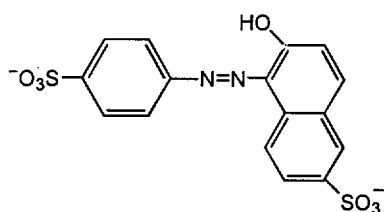
7. Orange I



8. Orange II



9. Sunset Yellow FCF



10. Tartrazine

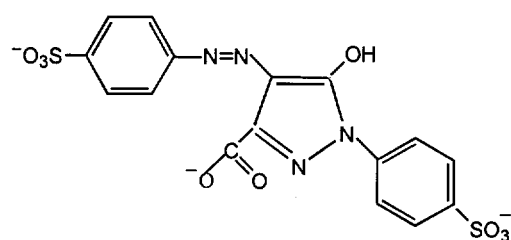


Figure 5.1 Dye structures.

5.2.2 Batch system

All experiments were buffered with HEPES (pH 7.0, 10 mM) from Sigma. Buffer was prepared with deionized and deoxygenated water. All dye reduction kinetics were determined in 7-ml scintillation vials containing 1.000 ± 0.002 g Fe^0 , resulting in a surface area concentration $\rho_a = 1.42$ m² L⁻¹. In an anaerobic glove box, dye solutions of 60 μM , 300 μM , and 3 mM were combined with HEPES buffer and sealed with Teflon-lined caps and Parafilm. The final reaction volume was 5 ml. Reaction was performed by shaking the iron filings with the dye solution on an orbital shaker at room temperature. The solution phase was routinely sampled at specified time intervals, and the amount of dye remaining was determined using a spectrophotometer.

5.2.3 Analytical methods

Samples were diluted 2–10 times with deionized water to obtain spectrophotometrically measurable absorbances. Decolorization of each dye was quantitated by monitoring the decrease in absorbance at the λ_{max} (Table 5.1) for each dye using a UV-visible spectrophotometer (Model UV-265, Shimadzu Corporation, Kyoto, Japan). In the experiments with textile waste water, decolorization was followed by collecting absorbance spectra from 350 to 700 nm at specified time intervals.

5.3 Results and Discussion

5.3.1 Characterization of reduction products

Fe^0 decolorized Orange II and produced sulfanilic acid (HPLC retention time 3.8 min) from Orange II (Figure 5.2). The color of Orange II ($\lambda_{\text{max}} = 484$ nm) disappeared completely in 6 min, and was accompanied by the appearance of sulfanilic acid. After 6 min, the mass balance between decolorized Orange II and sulfanilic acid produced approached 90%, suggesting that Orange II disappearance was due to dye reduction by Fe^0 . β -Aminonaphthol was not analyzed, but is presumed to be the other product of cleavage of the azo linkage. Thus, the overall

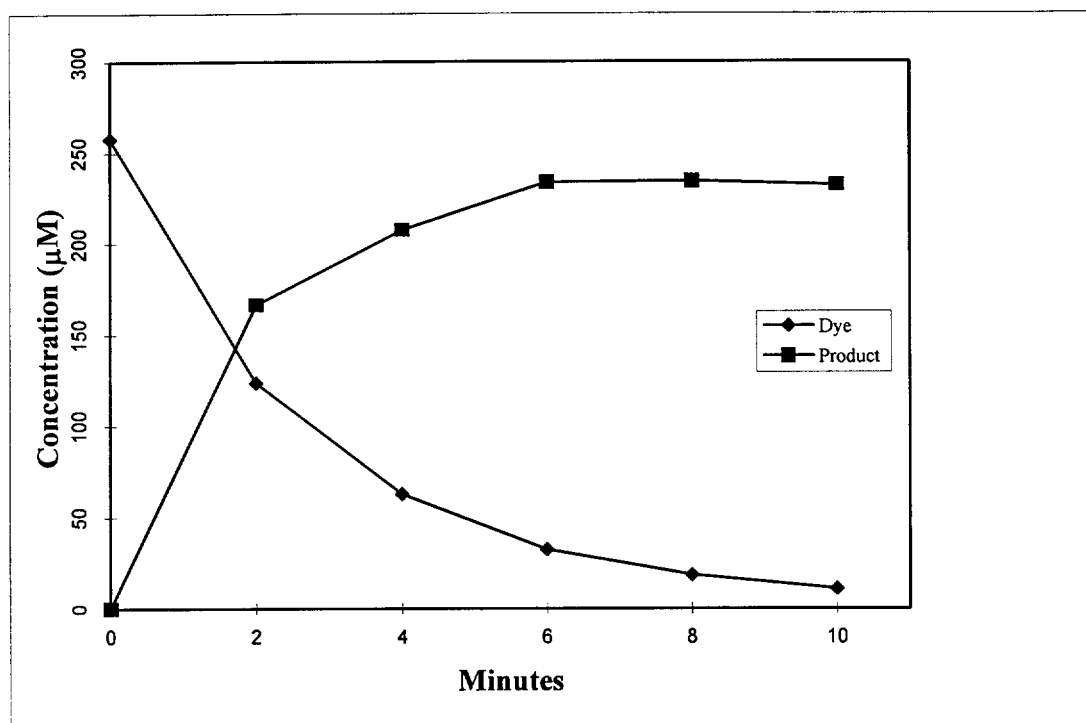
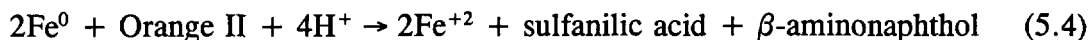


Figure 5.2 Time course of decolorization of Orange II by Fe⁰ (16–32 mesh, Fluka) and formation of 4-aminobenzenesulfonic acid.

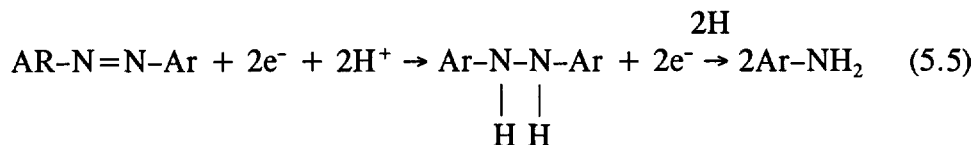
reaction can be summarized:



Based on HPLC analysis, all other azo dyes tested in this study also produced substituted anilines from dye reduction by Fe^0 .

Our results with Orange II are consistent with previously reported results for azobenzene reduction (Weber, 1996). Weber reported that the dissolved 4-aminoazobenzene (4-AAB) was readily reduced with the formation of aniline which is stable in a $\text{Fe}^0\text{-H}_2\text{O}$ system. Reduction of dissolved 4-AAB by Fe^0 resulted in the complete loss of 4-AAB in 2 h, which generated the rapid formation of aniline with good mass balance (Weber, 1996).

Azo linkage reduction involves transfer of four electrons from zero-valent iron. The reaction might proceed in a stepwise fashion; initially azo dye might be transformed into a hydrazo intermediate by the transfer of two electrons, and then azo linkage might be further reduced with two electrons to generate a substituted aniline (equation 5.5).



5.3.2 Kinetics

5.3.2.1 Characterization of azo dye reduction. First-order kinetics apply when reduction rates decrease linearly with substrate concentration. The first-order rate law for the disappearance of a reactant is

$$-d[\text{C}] / dt = k_{\text{obs}}[\text{C}] \quad (5.6)$$

which integrates to

$$\ln[\text{C}] / [\text{C}_0] = -k_{\text{obs}}t \quad (5.7)$$

where C_0 is the initial concentration of reactant, t is time, and k_{obs} indicates the first-order rate constant.

First-order rate constants (k_{obs}) should be characteristic of a particular contaminant but not dependent on its concentration (Johnson et al., 1996). In the reduction of Orange II by Fe^0 , the concentration of dye decreased exponentially with respect to time (Figure 5.2) and linearly on a $\ln[\text{C}] / [\text{C}_0]$ versus t plot (Figure 5.3).

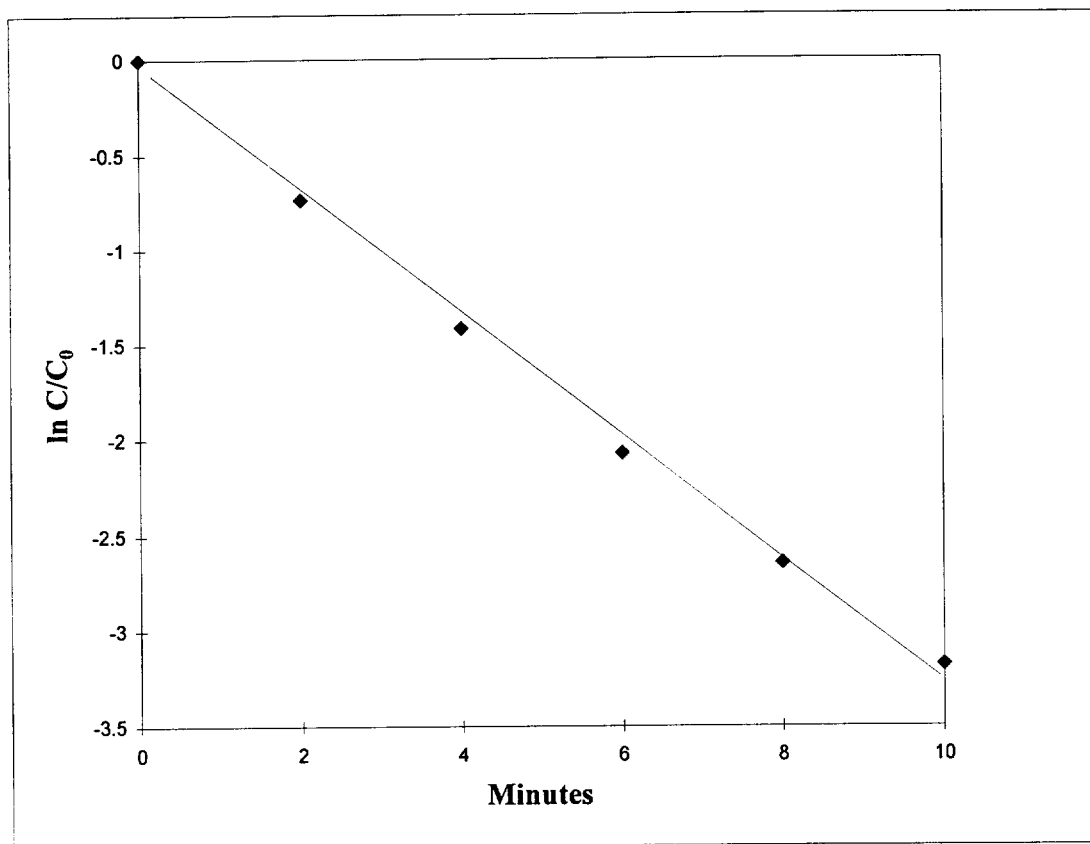


Figure 5.3 C_0 and C are the Orange II concentrations at time 0 and time t , respectively. First-order rate constant k_{obs} was determined to be $0.306 \pm 0.009 \text{ min}^{-1}$.

Thus, the disappearance of the azo dye proceeds by kinetics that are first-order with respect to azo dye concentration.

Reduction with Fe^0 is also dependent on the amount of iron present, as represented in the following model from Johnson et al. (1996):

$$-d[C] / dt = k_{SA} \alpha_s \rho_m [C] \quad (5.8)$$

or

$$-d[C] / dt = k_{SA} \rho_a [C] \quad (5.9)$$

Where k_{SA} = the specific reaction rate constant ($\text{L h}^{-1} \text{m}^{-2}$),

α_a = the specific surface area of Fe^0 ($\text{m}^2 \text{g}^{-1}$),

ρ_m = the mass concentration of Fe^0 (g L^{-1}), and

ρ_a = the surface area concentration of Fe^0 ($\text{m}^2 \text{L}^{-1}$).

The rearrangement of equations 5.6 and 5.9 gives a useful equation:

$$k_{obs} = k_{SA} \times \rho_a \quad (5.10)$$

where ρ_a is $\alpha_s \rho_m$. In equation 5.10, the specific reaction rate constant (k_{SA}) could be determined by the slope of a plot of k_{obs} versus ρ_a .

Forty experiments for the kinetic study of azo dye reduction were performed with $\rho_a = 1.42 \text{ m}^2 \text{L}^{-1}$ of Fluka iron turnings. The experimental details and kinetic data are summarized in Table 5.2. Most azo dyes were more than 90% reduced in about 10 min. In all cases, $\ln[C] / [C_0]$ versus time plots were linear, as exemplified by Figure 5.3. Therefore, rates of azo reduction by zero-valent iron in an anaerobic $\text{Fe}^0\text{-H}_2\text{O}$ system appear to be first-order reactions. Linear regression on Figure 5.3 gives $k_{obs} = 0.306 \pm 0.009$ ($n = 5$, $r^2 = 0.997$). k_{obs} for a variety of dyes was determined using similar linear regression analyses of kinetic data (Table 5.2).

5.3.2.2 Effect of mixing on kinetics (rpm dependent kinetics). The reaction of azo dyes by Fe^0 could proceed by the following steps: (i) initial transport of the azo dye from the bulk solution to the iron metal surface, (ii) adsorption of the azo dye to the iron surface to generate a surface complex, (iii) reduction of the surface complex, (iv) desorption of the products, and (v) mass transport of the product to the bulk solution (Spiro, 1989; Stumm, 1992). One or more of these steps might be slow enough to influence k_{obs} values.

Table 5.2 Summary of kinetic data

Exp. #	Dye	C ₀ (μM)	rpm	k _{obs} (min ⁻¹)
1	Acid Blue 113	300	100	0.064 ± 0.002
2	Allura Red	300	100	0.144 ± 0.004
3	Allura Red	300	100	0.141 ± 0.027
4	Allura Red	300	120	0.159 ± 0.007
5	Allura Red	300	140	0.226 ± 0.017
6	Amaranth	300	100	0.149 ± 0.004
7	Amaranth	300	100	0.137 ± 0.003
8	Amaranth	300	120	0.194 ± 0.008
9	Amaranth	300	140	0.279 ± 0.000
10	Brilliant Blue FCF	300	140	0.010 ± 0.000
11	Crocein Orange G	60	90	0.174 ± 0.012
12	Crocein Orange G	60	100	0.197 ± 0.000
13	Crocein Orange G	60	120	0.291 ± 0.011
14	Crocein Orange G	60	140	0.356 ± 0.010
15	Crocein Orange G	60	160	0.530 ± 0.015
16	Crocein Orange G	300	90	0.167 ± 0.016
17	Crocein Orange G	300	100	0.207 ± 0.006
18	Crocein Orange G	300	100	0.177 ± 0.007
19	Crocein Orange G	300	120	0.276 ± 0.007
20	Crocein Orange G	300	140	0.380 ± 0.007
21	Crocein Orange G	300	160	0.458 ± 0.002
22	Crocein Orange G	1000	120	0.239 ± 0.009
23	Crocein Orange G	1000	140	0.303 ± 0.006
24	Crocein Orange G	1000	160	0.393 ± 0.010
25	Crocein Orange G	3000	100	0.119 ± 0.014
26	Crocein Orange G	3000	100	0.104 ± 0.006
27	Crocein Orange G	3000	124	0.167 ± 0.013
28	Crocein Orange G	3000	160	0.225 ± 0.015
29	Naphthol Blue Black	300	100	0.023 ± 0.002
30	Orange I	300	100	0.138 ± 0.005
31	Orange I	300	120	0.218 ± 0.002
32	Orange I	300	140	0.274 ± 0.013
33	Orange II	300	100	0.161 ± 0.003
34	Orange II	300	120	0.245 ± 0.011
35	Orange II	300	130	0.306 ± 0.009
36	Orange II	300	140	0.380 ± 0.011
37	Sunset Yellow FCF	300	100	0.148 ± 0.006
38	Sunset Yellow FCF	300	120	0.241 ± 0.004
39	Sunset Yellow FCF	300	140	0.304 ± 0.018
40	Tartrazine	300	100	0.116 ± 0.038

One common criterion for assessing the contribution of mass transport in reaction kinetics is the effect of mixing. Generally, aggressive mixing increases diffusion-controlled rates by narrowing the diffusion layer at particle surfaces (Spiro, 1989). The mixing method used in this study was orbital shaking, so the most convenient measure of mixing rate is rpm of the orbital table. Different mixing rates were applied to reduction for Crocein Orange G (Figure 5.4A and B). In this series of experiments, k_{obs} values and reduction rates at all initial dye concentrations tested increased with increasing rpm (Figure 5.4A and B).

These results are similar to those for reduction of nitrobenzene by Fe^0 (Agrawal & Tratnyek, 1996). Nitro reduction rate constants show a linear correlation to mixing rates, even though the mixing method applied was 360° rotation around a fixed-length axis. In that study, Agrawal & Tratnyek concluded that the reaction rate was dominated by mass transport effects.

Current findings also suggest that mixing velocity directly affects the rate of azo dye reduction and that azo dye reduction rates under the experimental conditions used are influenced by mass transport. It is possible that k_{obs} might not change at higher rpm as the reaction system moves from mass-transport control to diffusion control. In addition, mixing rates on k_{obs} values and reaction rates at different initial concentrations provide the non-zero intercepts.

5.3.2.3 Effect of initial concentration on reduction kinetics.

Reduction of Crocein Orange G at 100 rpm was studied at initial concentrations ranging from $60 \mu\text{M}$ to 3 mM . Rate constants (k_{obs}) increased with decreasing initial dye concentrations at the same mixing rate (Figure 5.4A), whereas reaction rates indicated a reverse trend (Figure 5.4B). This series of experiments provided evidence for deviations from simple first-order kinetics, because k_{obs} values decreased 45% as initial concentration increased (Figure 5.5A). These results are similar to those for dechlorination of CCl_4 by Fe^0 (Johnson et al., 1996). These deviations might be due to limited reaction sites at the iron surface. These deviations are often observed in heterogeneous systems where the surface and the surface complex affect disappearance rates (Scherer & Tratnyek, 1995; Johnson et al., 1996).

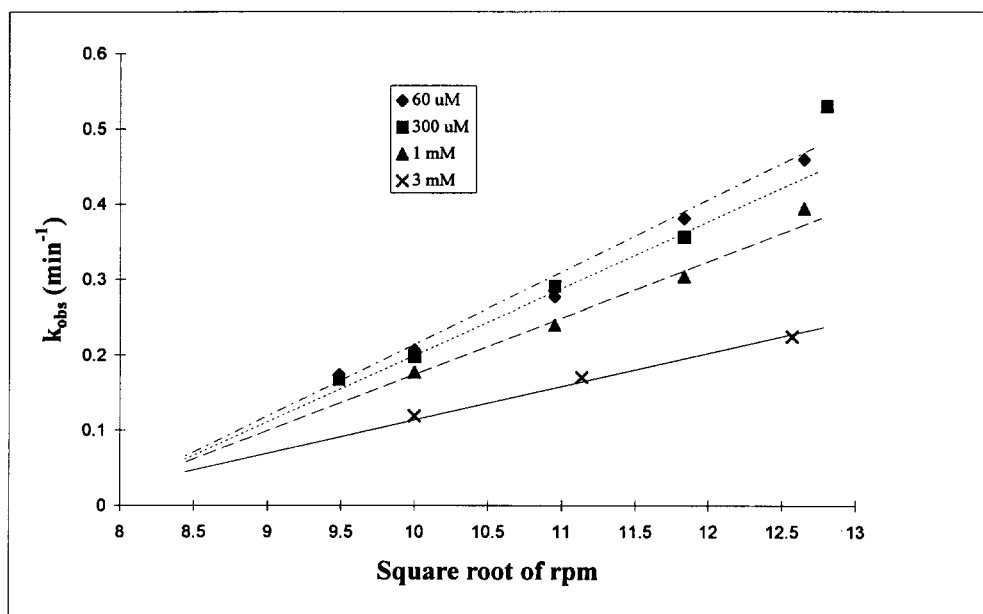


Figure 5.4A Effect of mixing rate (square root of rpm) on the pseudo first-order rate constant for Crocein Orange G reduction. Initial Crocein Orange G concentrations are indicated in the insert. Dye in HEPES buffer (pH 7.0, 10 mM) was shaken with Fe^0 (16–32 mesh, $\rho_a = 1.42 \text{ M}^2 \text{ L}^{-1}$, Fluka) at specified rpm rates on an orbital shaker at room temperature.

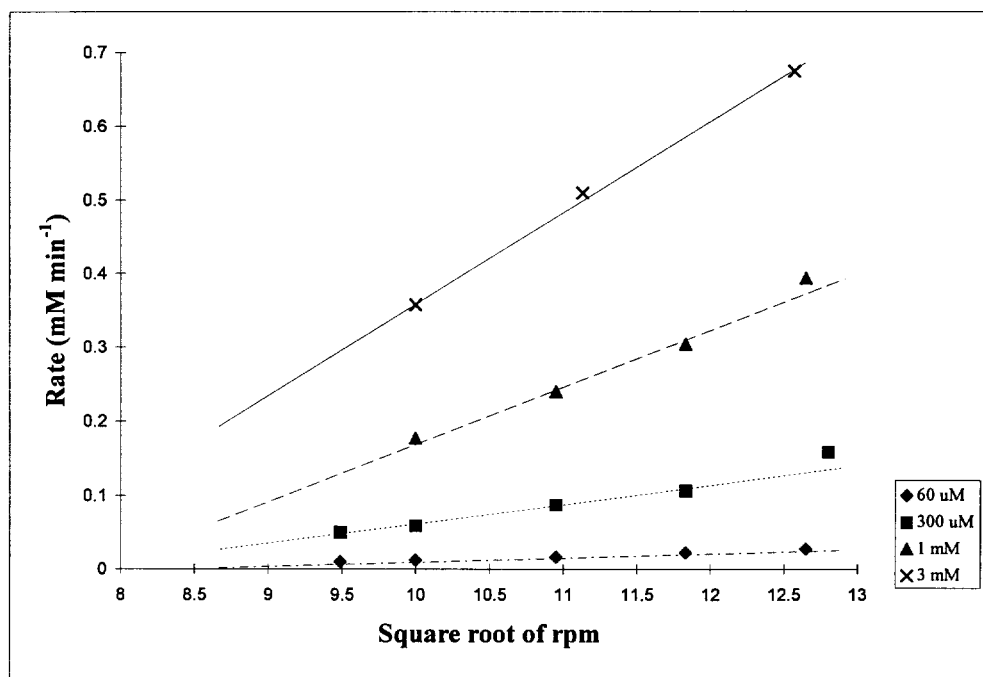


Figure 5.4B A plot of rate of Crocein Orange G reduction (mM min^{-1}) versus square root of rpm for the data shown in Figure 5.4A.

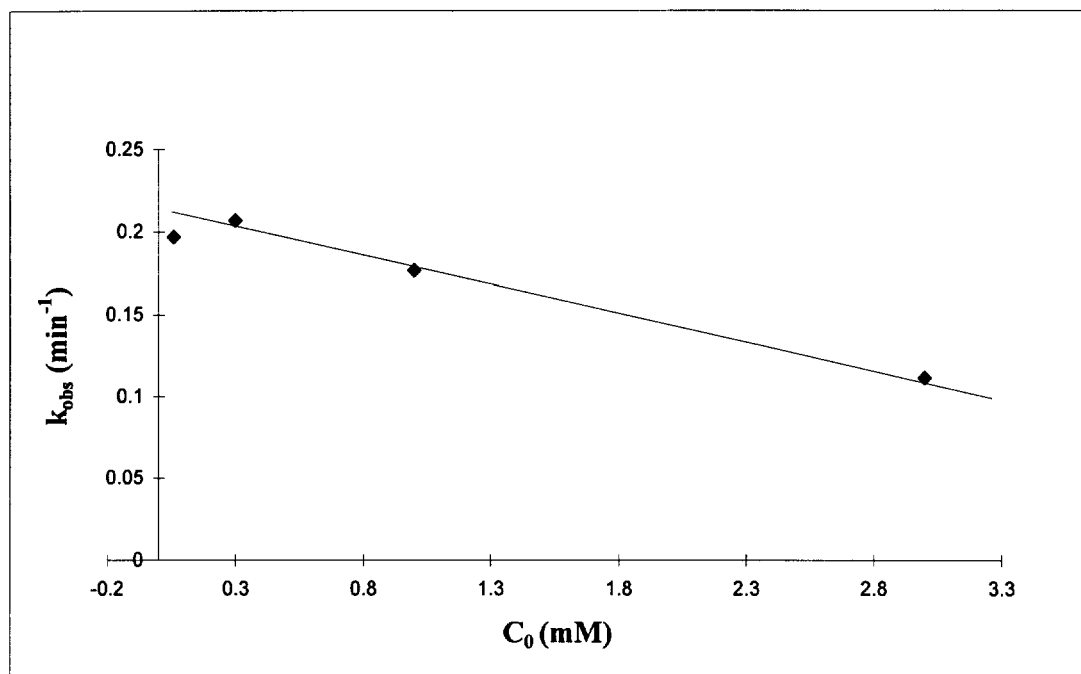


Figure 5.5A Effect of initial dye concentration on the pseudo first-order rate constant for Crocein Orange G reduction at 100 rpm on an orbital-shaker. $[\text{Dye}]_0 = 1.0 \times 10^{-4}$ M, 3.0×10^{-4} M, 1.0×10^{-3} M, and 3.0×10^{-3} M. Dye was reacted with untreated Fe^0 (16–32 mesh, $\rho_a = 1.42 \text{ m}^2 \text{ L}^{-1}$, Fluka) in the presence of HEPES buffer (pH 7.0, 10 mM) at room temperature.

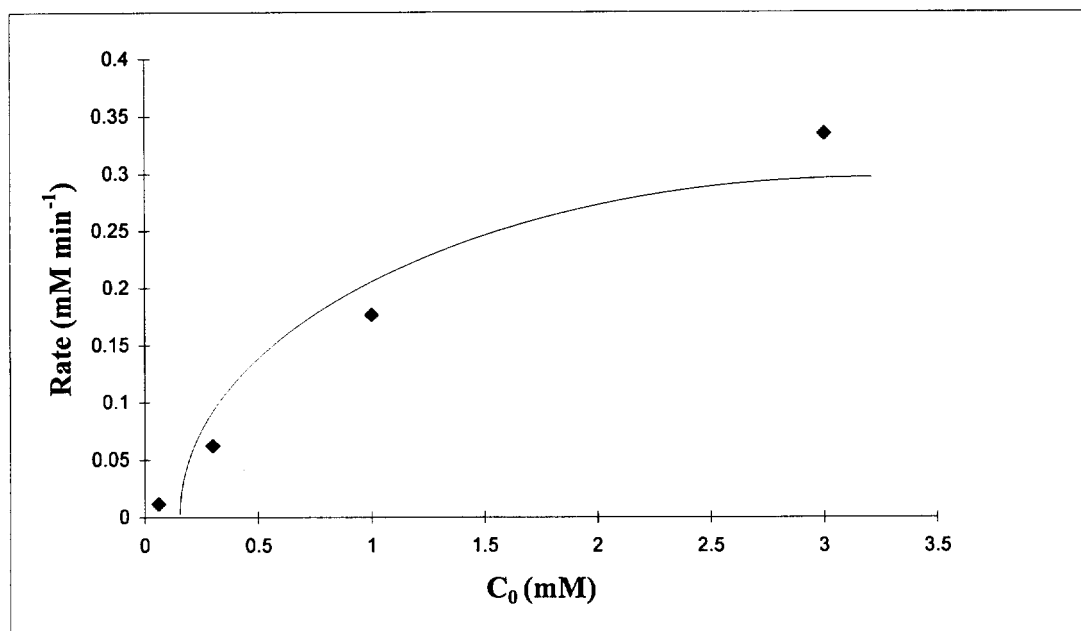


Figure 5.5B A plot of rate of Crocein Orange G reduction (mM min^{-1}) versus initial dye concentration (mM) for the data shown in Figure 5.5A. The curve is from a fit to an exponential function.

Reduction rates of Crocein Orange G increased with increasing initial dye concentration and then leveled out at higher dye concentration, showing a hyperbolic curve (Figure 5.5B). Generally, deviations from the kinetic model (equation 5.6) are generated through changes in reactivity of the metal surface due to adsorption or other reactions on the metal surface (Johnson et al., 1996). In addition, reaction sites on the iron surface are limited, so the rate of azo dye reduction increases with increasing dye concentration until the saturation of these sites occurs, and then this saturation results in these deviations. Heterogeneous systems such as the Fe^0 reduction system often exhibit a hyperbolic relationship between the rate of reduction and the initial reactant concentration. Scherer et al. (1998) found Michaelis–Menten-type kinetic behavior in the reduction of carbon tetrachloride by Fe^0 . A similar behavior was observed in the reduction of azo dyes by Fe^0 . At low dye concentration, the rate of reduction linearly increased with increasing dye concentration. However, at high levels of dye concentration, the rate of reduction did not change with dye concentration.

5.3.3 Effects of azo dye structure on k_{obs} values

Quantitative structure–activity relationships (QSARs) are powerful tools for analysis of properties of many important organic substances in environmental chemistry. QSARs provide the possibility of estimating properties that have not been previously measured (Tratnyek, 1998).

In this study, except for Brilliant Blue FCF, all of the dyes tested were azo dyes which included one or two azo linkages. All of the dyes contained at least one sulfonate group, which makes the dyes water-soluble. Except for Brilliant Blue, all of the dyes included one hydroxyl group. The structure of azo dyes (Figure 5.1) apparently influences the rate of reduction (Table 5.2).

Many descriptor variables are available for correlation analysis (Eriksson et al., 1993). Typical descriptors for reductive reactions include substituent constants (σ) and some molecular descriptors such as energy of the lowest unoccupied molecular orbital (E_{LUMO}). Substituent constants (σ), which indicate electronic effects of substituents on the reaction, are used in correlations such as the Hammett equation

and its various extensions (Tratnyek, 1998). E_{LUMO} refers to the energy gained when an electron is added to the lowest unoccupied molecular orbital (LUMO).

In this study, the LUMO energy of each azo dye was calculated in order to estimate the potential for azo dye decolorization. The calculation was done with the CAChe computer program (Oxford Molecular, Beaverton, OR) after optimizing the molecular geometry using MOPAC with PM3 parameters. The properties and descriptors of azo dyes used for a QSAR are presented in Table 5.3.

In this study, regression of k_{obs} versus E_{LUMO} shows a linear correlation with some deviations in QSAR (Figure 5.6):

$$\text{For 100 rpm, } k_{obs} = (0.078 \pm 0.040) \times E_{LUMO} + (0.263 \pm 0.025) \quad (5.11)$$

where $n = 10$, $s = 0.022$, and $r = 0.572$.

$$\text{For 120 rpm, } k_{obs} = (0.156 \pm 0.080) \times E_{LUMO} + (0.448 \pm 0.043) \quad (5.12)$$

where $n = 6$, $s = 0.035$, and $r = 0.664$.

$$\text{For 140 rpm, } k_{obs} = (0.257 \pm 0.106) \times E_{LUMO} + (0.681 \pm 0.060) \quad (5.13)$$

where $n = 7$, $s = 0.044$, and $r = 0.734$.

In the correlation between k_{obs} and E_{LUMO} , steepness of the slope decreases as the rpm is decreased from 140 to 100. k_{obs} values showed a positive correlation with E_{LUMO} in all three rpm experiments. This finding suggests that dye reduction could be influenced by its reduction potential.

5.4 Conclusions

All azo dyes tested were readily reduced by Fe^0 . This reduction followed first-order kinetics with respect to initial azo dye concentration. Decolorization rates of azo dyes were proportional to the mixing rates, suggesting a dependence on mass transport. In addition, the correlation between k_{obs} values and E_{LUMO} suggests that the reaction could be influenced by azo dye reduction potential. Investigation of the effect of initial dye concentration on dye reduction by Fe^0 at fixed rpm suggested a hyperbolic relationship between initial dye concentration and the rate of reduction. This behavior resembles the Michaelis-Menten kinetics of enzymatic reaction.

Table 5.3 LUMO energy of azo dyes

No.	Name	LUMO energy (eV) w/ AM1 no H ₂ O	LUMO energy (eV) w/ PM3 no H ₂ O	LUMO energy (eV) w/ AM1 H ₂ O	LUMO energy (eV) w/ PM3 H ₂ O
1	Acid Blue 113	2.139	2.083	-1.702	-1.493
2	Allura Red	3.189	3.039	-1.462	-1.365
3	Amaranth	5.045	4.932	-1.701	-1.533
4	Brilliant Blue FCF	-5.044	-5.355	-1.862	-2.090
5	Crocein Orange G	0.999	0.874	-1.180	-1.307
6	Naphthol Blue Black	2.339	2.291	-1.857	-1.631
7	Orange I	0.967	0.890	-1.503	-1.208
8	Orange II	0.891	0.766	-1.327	-1.424
9	Sunset Yellow FCF	3.066	2.918	-1.504	-1.391
10	Tartrazine	5.526	5.448	-1.327	-1.174

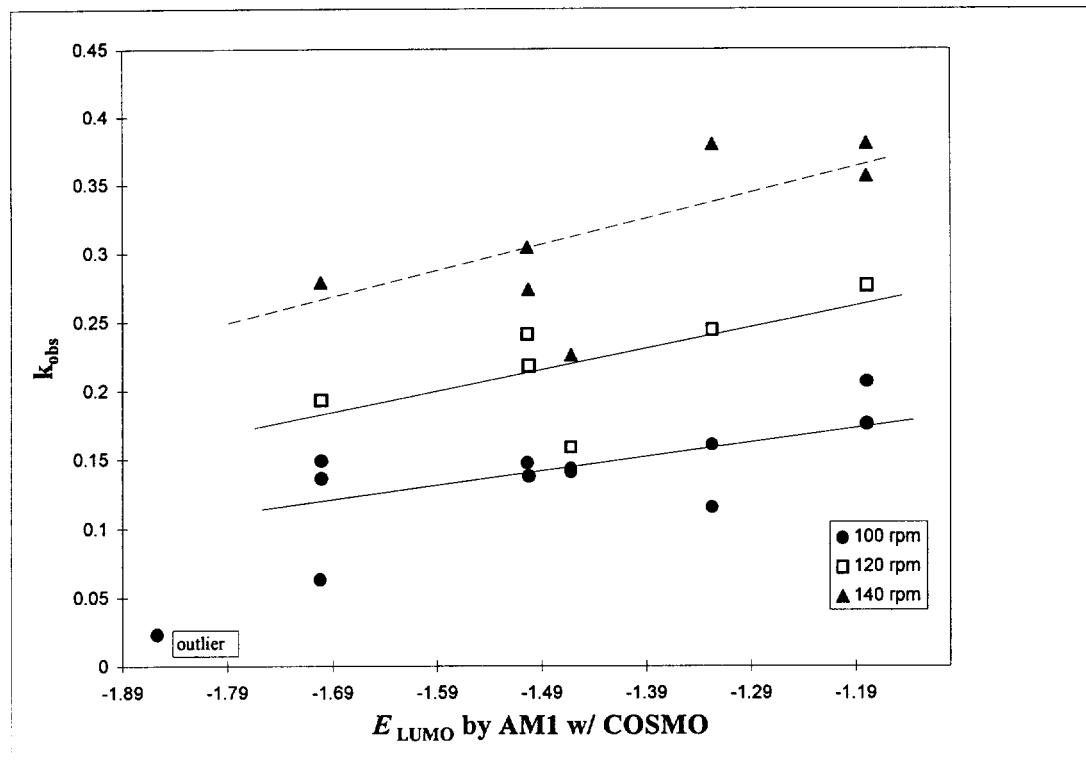


Figure 5.6 Correlation between k_{obs} and E_{LUMO} for data shown in Table 5.3. E_{LUMO} was calculated at an optimizing geometry in H_2O using CAChe computer program. AM1 w/ COSMO indicates an optimized geometry with AM1 parameters and the Conductor-like Screening Model (COSMO) in water.

CHAPTER 6

FINAL COMMENTS

Azo dyes constitute more than 50% of all dyes produced in the world (Betowski et al., 1987; Zollinger, 1987). It is estimated that 10–15% of the dye utilized in the dyeing process is not bound to fabric (Brown et al., 1981), and that much of it is apparently released into waste streams (Clarke & Anliker, 1980). Currently dye effluents are treated by physical, chemical, and biological methods (Park & Shore, 1984). Physical methods, such as adsorption and chemical precipitation, do not degrade dyes and require disposal of the dye-adsorbed precipitates (Davis et al., 1994). Chemical methods include chlorination, ozonation, and reduction. Chlorination might produce toxic chlorinated dyes and their by-products (Riefe, 1992; Davis et al., 1994). Ozonation is limited by its efficiency and cost (Matsui et al., 1981; Park & Shore, 1984). Reduction might produce aromatic amines which are potentially toxic or carcinogenic (Brown & DeVito, 1993). Bacterial degradation might be economical, but isolation of dye-degrading bacteria is difficult; furthermore bacteria generally do not non-specifically degrade dyes (Zimmerman et al., 1982). The white-rot fungus *P. chrysosporium* can mineralize sulfonated or non-sulfonated azo dyes (Paszczyński et al., 1992; Spadaro et al., 1992), but these organisms are not suitable for remediating the dye effluent. Thus, it appears that more fundamental research will be needed to develop viable alternate treatment technologies.

Some peroxidases can oxidatively degrade azo dyes. Bacteria genetically engineered to express these peroxidases might be useful in dye waste treatment. To further understand peroxidase-catalyzed azo dye degradation, we studied the substrate specificity of HRP, MnP, and LiP using 4-(4'-sulfophenylazo)-phenol and 2-(4'-sulfophenylazo)-phenol dyes. HRP, MnP, and LiP oxidized variously substituted 4-

(4'-sulfophenylazo)-phenol dyes. All 2-(4'-sulfophenylazo)-phenol dyes were poor substrates or non-substrates for all peroxidases examined. HRP was the most active among the three peroxidases. MnP was comparatively specific in dye oxidation, and it was particularly ineffective for halogenated dyes. LiP oxidized dyes at very low rates. In a Hammett correlation analysis, HRP and MnP preferred dyes with electron-donating substituents. Correlations for HRP and MnP oxidation were weak and strong, respectively. No correlation with Hammett factors was observed for LiP oxidation. These findings suggested that MnP oxidation is primarily controlled by electronic effects of substituents, and HRP oxidation might be controlled by electronic and other factors. In the case of HRP oxidation, steric hindrance might affect the dye oxidation. In particular, steric hindrance of *ortho*-substituents may influence the dye oxidation. Steric effects of substituents might be assessed in a QSAR study. Steric parameters, such as steric substituent constants or van der Waals radii, may be useful for assessing steric effects of substituents.

Peroxidases require hydrogen peroxide for azo dye degradation, but laccases, which are copper-dependent enzymes, oxidize azo dye in the presence of oxygen (Bollag, 1992; Thurston, 1994). Thus, laccase-catalyzed azo dye oxidation might be more suitable for remediating the dye effluent than peroxidase-catalyzed oxidation. Many white-rot fungi produce extracellular laccases which are involved in lignin degradation (Hatakka, 1994). Chivukula and Reganathan (1995) suggested a probable mechanism for the degradation of phenolic azo dyes by laccase from *Pyricularia oryzae*. The mechanism was similar to that of peroxidase-catalyzed azo dye oxidation. A QSAR study of laccase-catalyzed dye oxidation could provide further understanding of oxidative dye degradation. Xu (1996) performed a QSAR study of phenol oxidation by several fungal laccases. In that study, a good correlation between laccase activity and redox potentials was discovered. It was suggested that the one-electron redox potential difference between laccase and its substrate is an important factor in phenol oxidation. A similar QSAR study of laccase-catalyzed oxidation of azo dyes might be useful.

Hydroxyl radical-generating systems might be suitable for remediating the dye effluent because $\cdot\text{OH}$ is non-specific and can completely degrade dyes. Since $\cdot\text{OH}$ is

very reactive and non-specific in its reactions, we expected all dyes to be degraded at the same rate. However, we found a weak correlation between the amount of dye decolorized and the charge density of the phenolate anion species of the dye, indicating that dye oxidation by the $\text{Fe}^{\text{III}}/\text{H}_2\text{O}_2$ system (Fenton chemistry) might be limited by $\cdot\text{OH}$ attack on the phenolate anion. One of the problems of advanced oxidation processes (AOPs) is that additives, such as inorganic anions, organic solvents, and detergents, could slow dye oxidation by competing for the $\cdot\text{OH}$. Surprisingly, we found that nitrate can greatly enhance dye oxidation. We believe that AOPs might be applicable to treating effluent-containing low levels of additives or to effluent which is pretreated to eliminate organic and inorganic additives. The $\text{Fe}^0/\text{H}_2\text{O}$ system readily reduces and decolorizes azo dyes. However, this may not be a useful process, because the product amines are potentially toxic or carcinogenic and they can also be reoxidized to generate azo dyes. A two-stage process consisting of Fe^0 reduction followed by biodegradation is possible. Whereas bacteria are unable to degrade azo dyes, they seem to be capable of degrading sulfonated and non-sulfonated aromatic amines. Brown and Hamburger (1987) have demonstrated that sulfanilic acid is readily degraded by activated sludge. Hammer et al. (1996) also demonstrated that a mixed bacterial culture of *Hydrogenophaga palleronii* strain S1 and *Agrobacterium radiobacter* strain S2 can degrade sulfanilic acid. Haug et al. (1991) used a two-stage biodegradation process, anaerobic followed by aerobic, to degrade Mordant Yellow 3. Yet another advantage of reduction followed by aerobic biodegradation is that, though dyes are structurally complex, they are usually produced by combining a few dozen aromatic amines and phenols. Thus, only a few bacterial isolates might be sufficient to degrade aromatic amines completely.

LITERATURE CITED

- Agrawal, A., and Tratnyek, P. G. (1996) Reduction of nitro aromatic compounds by zero-valent iron metal. *Environ. Sci. Technol.* **30**, 153–160.
- Anbar, M., Baruch, Z., and Meyerstein, D. (1996) The synthesis of ^{18}O -labelled hydrogen peroxide in H_2O -16. *Int. J. Appl. Radiat. Isot.* **17**, 256.
- Arvanitoyannis, L., Eleftheriadis, I., and Kavlentis, E. (1987) Treatment of dye-containing effluents with different bentonites. *Chemosphere* **16**, 2523–2529.
- Atlas, R. L., and Bartha, R. (1993) *Microbial Ecology Fundamentals and Applications*, 3rd Edn., Benjamin/Cummings, Redwood City, CA, pp. 360–382.
- Bahorsky, M. S. (1997) Textiles. *Water Environ. Res.* **69**, 658–664.
- Baozhen, W., and Jun, Y. (1986) Removal of aromatic nitro-compounds from water by ozonation. *Aquaculture* **2**, 86–96.
- Berry, D. F., Francis, A. J., and Bollag, J.-M. (1987) Microbial metabolism of homocyclic and heterocyclic aromatic compounds under anaerobic conditions. *Microbiol. Rev.* **51**, 43–59.
- Betowski, L. D., Pyle, S. M., Ballard, J. M., and Shaul, G. M. (1987) Thermospray LC/GC/MS/ analysis of wastewater for disperse azo dyes. *Biomed. Environ. Mass Spectrom.* **14**, 343–354.
- Bigda, R. J., and Elizardo, K. P. (1992) Destruction of TOC's in industrial waste water using Fenton chemistry. *Abstract of Papers, 204th ACS National Meeting*, Vol. 32(2), American Chemical Society, Washington, DC, pp. 259–262.
- Blake, R. C., and Coon, M. J. (1981) On the mechanism of action of cytochrome P-450. Evaluation of homolytic and heterolytic mechanisms of oxygen-oxygen bond cleavage during substrate hydroxylation by peroxides. *J. Biol. Chem.* **256**, 12127–12133.
- Blée, E., and Schuber, F. (1989) Mechanism of S-oxidation reactions catalyzed by a soybean hydroperoxide-dependent oxygenase. *Biochemistry* **28**, 4962–4967.

- Bollag, J.-M. (1992) Enzymes catalyzing oxidative coupling reactions of pollutants. *Met. Ions Biol. Syst.* **28**, 205-217.
- Bollag, J.-M., Shuttleworth, K. L., and Anderson, D. H. (1988) Laccase-mediated detoxification of phenolic compounds. *Appl. Environ. Microbiol.* **54**, 3086-3091.
- Brady, J. E. (1990) *General Chemistry: Principle and Structure*, 5th Edn., Wiley and Sons, New York, pp. 516-520.
- Brezonik, P. L. (1990) Reaction rates of process in natural waters. In *Aquatic Chemical Kinetics* (Stumm, W., Ed.), Wiley-Interscience, New York, pp. 113-143.
- Brown, D., and Hamburger, B. (1987) The degradation of dyestuffs. Part III. Investigation of their ultimate degradability. *Chemosphere* **16**, 1539-1552.
- Brown, D., Laboureur, P. (1983) The aerobic biodegradability of primary aromatic amines. *Chemosphere* **12**, 405-414.
- Brown, D. H., Hitz, H. R., and Schafer, L. (1981) The assessment of the possible inhibitory effect of dye-stuffs on aerobic waste-water. Experience with a screening test. *Chemosphere* **10**, 245-261.
- Brown, M. A., and DeVito, S. C. (1993) Predicting azo dye toxicity. In *Critical Reviews in Environmental Science and Technology*, Vol. 23(3) (Logan, T. J., ed.), CRC Press, Boca Raton, FL, pp. 249-324.
- Bumpus, J. A., and Brock, B. J. (1988) Biodegradation of crystal violet by the white-rot fungus *Phanerochaete chrysosporium*. *Appl. Environ. Microbiol.* **54**, 1143-1150.
- Bumpus, J. A., Tien, M., Wright, D., and Aust, S. D. (1985) Oxidation of persistent environmental pollutants by a white-rot fungus. *Science* **228**, 1434-1436.
- Cartwright, R. A. (1983) Historical and morden epidemiological studies on populations exposed to *N*-substituted aryl compounds. *Environ. Health Perspect.* **49**, 13.
- Cha, D. K., Song, J. S., Sarr, D., and Kim, B. J. (1996) Hazardous waste treatment technologies. *Water Environ. Res.* **68**, 575-586.
- Chance, B. (1952) The transition from the primary to the secondary peroxidase-peroxide complex. *Arch. Biochem. Biophys.* **37**, 235-237.
- Chen, L. C., and Chou, T. C. (1993) Photobleaching of methyl orange in titanium dioxide suspended in aqueous solution. *J. Mol. Catal.* **85**, 201-214.

- Chivukula, M., and Renganathan, V. (1995) Phenolic azo dye oxidation by laccase from *Pyricularia oryzae*. *Appl. Environ. Microbiol.* **61**, 4374-4377.
- Chivukula, M., Spadaro, J. T., and Renganathan, V. (1995) Lignin peroxidase-catalyzed oxidation of sulfonated azo dyes generates novel sulfophenyl hydroperoxides. *Biochemistry* **34**, 7765-7772.
- Chudgar, R. J. (1992) Azo dyes. In *Kirk-Othmer Encyclopedia of Chemical Technology*, 4th Edn., Vol. 3 (Howe-Grant, M., ed.), John Wiley and Sons, New York, pp. 821-825.
- Chung, K.-T., and Cerniglia, C. E. (1992) Mutagenicity of azo dyes: structure-activity relationships. *Mutat. Res.* **277**, 201-220.
- Chung, K.-T., and Stevens, S. E., Jr. (1992) Degradation of azo dyes by environmental microorganisms and helminths. *Environ. Toxicol. Chem.* **12**, 2121-2132.
- Chung, N.-H., and Aust, S. D. (1995) Veratryl alcohol-mediated indirect oxidation of phenol by lignin peroxidase. *Arch. Biochem. Biophys.* **316**, 733-737.
- Clarke, E. A., and Anliker, R. (1980) Anthropogenic compounds. In *The Handbook of Environmental Chemistry*, Vol. 3, Part A (Hutzinger, O., ed.), Springer-Verlag, Berlin, pp. 181-211.
- Cotton, M. L., and Dunford, H. B. (1973) Nature of compounds I and II as determined from the kinetics of the oxidation of ferrocyanide. *Can. J. Chem.* **51**, 582-587.
- Cripps, C., Bumpus, J. A., and Aust, S. D. (1990) Biodegradation of azo and heterocyclic dyes by *Phanerochaete chrysosporium*. *Appl. Environ. Microbiol.* **56**, 1114-1118.
- Czapski, G., Samuni, A., and Meisel, D. (1971) The reactions of organic radicals formed by some Fenton reagents. *J. Phys. Chem.* **75**, 3271-3280.
- Davis, R. J., Gainer, J. L., O'Neal, G., and Wu, I.-W. (1994) Photocatalytic decolorization of wastewater dyes. *Water Environ. Res.* **66**, 50-53.
- De Jong, E., de Vries, F. P., Field, J. A., van der Zwan, R. P., and de Bont, A. M. (1992) Isolation and screening of basidiomycetes with high peroxidase activity. *Mycol. Res.* **96**, 1098-1104.

- De Long, M. J., Prochaska, H. J., and Talalay, P. (1986) Induction of NAD(P)H:quinone reductase in murine hepatoma cells by phenolic antioxidants, azo dyes, and other chemoprotectors: a model system for the study of anticarcinogens. *Proc. Nat. Acad. Sci. U.S.A.* **83**, 787-791.
- Dieckmann, M. S., Gray, K. A., and Zepp, R. G. (1994) The sensitized photocatalysis of azo dyes in a solid system: a feasibility study. *Chemosphere* **28**, 1021-1034.
- Dietrich, D., Hickey, W. J., and Lamar, R. (1995) Degradation of 4,4'-dichlorobiphenyl, 3,3',4,4'-tetrachlorobiphenyl, 2,2',4,4',5,5',-hexachlorobiphenyl by the white-rot fungus *Phanerochaete chrysosporium*. *Appl. Environ. Microbiol.* **61**, 3904-3909.
- Dolfing, J., and Tiedje, J. (1991) Influence of substituents on reductive dehalogenation of 3-chlorobenzoate analogs. *Appl. Environ. Microbiol.* **57**, 820-824.
- Donlon, B., Razo-Flores, E., Luijten, M., Swarts, H., Lettinga, G., and Field, J. (1997) Detoxification and partial mineralization of the azo dye mordant orange 1 in a continuous upflow anaerobic sludge-blanket reactor. *Appl. Microbiol. Biotechnol.* **47**, 83-90.
- Dorn, E., and Knackmuss, H.-J. (1978) Chemical structure and biodegradability of halogenated aromatic compounds. Substituent effects on 1,2-dioxygenation of catechol. *Biochem. J.* **174**, 85-94.
- Dunford, H. B., and Adeniran, A. J. (1986) Hammett $\rho\sigma$ correlation for reactions of horseradish peroxidase compound II with phenols. *Arch. Biochem. Biophys.* **251**, 536-542.
- Eaton, D. C. (1985) Mineralization of polychlorinated biphenyls by *Phanerochaete chrysosporium*: a ligninolytic fungus. *Enzyme Microb. Technol.* **7**, 194-196.
- Eaton, D., Chang, H.-M., and Kirk, T. K. (1980) Fungal decolorization of kraft bleach plant effluents. *Tappi* **63**, 103-106.
- Elovitz, M. S., and Fish, W. (1994) Redox interactions of Cr(VI) and substituted phenols: kinetic investigation. *Environ. Sci. Technol.* **28**, 2161-2169.
- Eriksson, K.-E. L., Blanchette, R. A., and Ander, P. (1990) *Microbial and Enzymatic Degradation of Wood and Wood Components*. Springer-Verlag, Berlin, pp. 1-72, 225-332.

- Eriksson, L., Verhaar, H. J. M., Sjöström, M., and Hermens, J. L. M. (1993) Multivariate characterization and modeling of the chemical reactivity of epoxides. Part II: Extension to di- and trisubstitution. *Quant. Struct.-Act. Relat.* **12**, 357-366.
- Exner, O. (1978) A critical compilation of substituent constants. In *Correlation Analysis in Chemistry: Recent Advances* (Chapman, N. B., and Shorter, J., eds.), Plenum Press, New York, pp. 439-530.
- Fenton, H. J. H. (1894) Oxidation of tartaric acid in the presence of iron. *J. Chem. Soc.* **65**, 899-910.
- Fernando, T. J., Bumpus, J. A., and Aust, S. D. (1990) Biodegradation of TNT (2,4,6-trinitrotoluene) by *Phanerochaete chrysosporium*. *Appl. Environ. Microbiol.* **56**, 1666-1671.
- Ferrey, M. L., Koskinen, W. C., Blanchette, R. A., and Burnes, T. A. (1994) Mineralization of alachlor by lignin-degrading fungi. *Can. J. Microbiol.* **40**, 795-798.
- Fujita, T., and Nishioka, T. (1976) The analysis of the ortho effect. *Progr. Phys. Org. Chem.* **12**, 49-89.
- Fujita, S., and Peisach, J. (1977) Electron transfer between liver microsomal cytochrome b₅ and cytochrome P-450 in the azo reductase reaction. *Biochem. Biophys. Res. Commun.* **78**, 328-335.
- Fujita, S., and Peisach, J. (1982) The stimulation of microsomal azoreduction by flavins. *Biochim. Biophys. Acta* **719**, 178-189.
- Fytianos, K., Vasilikiotis, T., Agelidis, P., Kofos, P., and Stefanidis, K. (1985) Color removal from dye containing effluents by treatment with manganese solid waste. *Chemosphere* **14**, 411-416.
- Givaudan, A., Effosse, A., Faure, D., Potier, P., Bouillant, M., and Bally, R. (1993) Polyphenol oxidase from *Azospirillum lipoferum* isolated from the rhizosphere: evidence for a laccase in non-motile strains of *Azospirillum lipoferum*. *FEMS Microbiol. Lett.* **108**, 205-210.
- Glenn, J. K., and Gold, M. H. (1983) Decolorization of several polymeric dyes by the lignin-degrading basidiomycete, *Phanerochaete chrysosporium*. *Appl. Environ. Microbiol.* **45**, 1741-1747.
- Glenn, J. K., and Gold, M. H. (1985) Purification and characterization of an extracellular Mn(II)-dependent peroxidase from the lignin-degrading basidiomycete, *Phanerochaete chrysosporium*. *Arch. Biochem. Biophys.* **242**, 329-341.

- Glenn, J. K., Morgan, M. A., Mayfield, M. B., Kuwahara, M., and Gold, M. H. (1983) An extracellular H_2O_2 -requiring enzyme preparation involved in lignin biodegradation by the white rot basidiomycete *Phanerochaete chrysosporium*. *Biochem. Biophys. Res. Commun.* **114**, 1077-1083.
- Glenn, J. K., Akileswaran, L., and Gold, M. H. (1986) Mn(II) oxidation is the principle function of the extracellular Mn-peroxidase from *Phanerochaete chrysosporium*. *Arch. Biochem. Biophys.* **251**, 688-696.
- Glover, B. (1992) Dyes, application and evaluation. In *Kirk-Othmer Encyclopedia of Chemical Technology*, 4th Edn. Vol. 8 (Howe-Grant, M., ed.), Wiley and Sons, New York, pp. 678-679.
- Gold, M. H., Kuwahara, M., Chiu, A. A., and Glenn, J. K. (1984) Purification and characterization of an extracellular H_2O_2 -requiring diarylpropane oxygenase from the white rot basidiomycete, *Phanerochaete chrysosporium*. *Arch. Biochem. Biophys.* **234**, 353-362.
- Gold, M. H., Wariishi, H., and Valli, K. (1989) Extracellular peroxidases involved in lignin degradation by the white-rot basidiomycete *Phanerochaete chrysosporium*. *ACS Symp. Ser.* **389**, 127-140.
- Goldstein, S., Meyerstein, D., and Czapski, G. (1993) The Fenton reagents. *Free Radical Biol. Med.* **15**, 435-445.
- Goszczyński, S., Paszczyński, A., Pasti-Grigsby, M. B., Crawford, R. L., and Crawford, D. L. (1994) New pathway for degradation of sulfonated azo dyes by microbial peroxidases of *Phanerochaete chrysosporium* and *Streptomyces chromofuscus*. *J. Bacteriol.* **176**, 1339-1347.
- Gregory, P. (1990) The classification of dyes by chemical structure. In *The Chemistry and Application of Dyes* (Waring, D. R., Hallas, G., eds.), Plenum Publishing, New York, pp. 17-47.
- Grüber, C., and Bub, V. (1989) Quantum-mechanically calculated properties for the development of quantitative structure-activity relationships (QSAR's). pKA-values of phenols and aromatic and aliphatic carboxylic acids. *Chemosphere* **19**, 1595-1609.
- Gunten, U. V., and Oliver, Y. (1997) Kinetics of the reaction between hydrogen peroxide and hypobromous acid: implication on water treatment and natural systems. *Water Res.* **31**, 900-906.
- Haag, W. R., and Yao, C. C. D. (1992) Rate constants for reaction of hydroxyl radicals with several drinking water contaminants. *Environ. Sci. Technol.* **26**, 1005-1013.

Haber, F., and Weiss, J. J. (1934) The catalytic decomposition of H_2O_2 by iron salts. *Proc. R. Soc. London, A* **147**, 332–351.

Halliwell, B., and Gutteridge, J. M. C. (1981) Formation of a thiobarbituric acid-active substrates from deoxyribose and hydroxyl radicals. *FEBS Lett.* **128**, 347–352.

Hammel, K. E. (1989) Organopollutant degradation by ligninolytic fungi. *Enzyme Microb. Technol.* **11**, 776–777.

Hammel, K. E., and Moen, M. A. (1991) Depolymerization of a synthetic lignin in vitro by lignin peroxidase. *Enzyme Microb. Technol.* **13**, 15–18.

Hammel, K. E., Green, B., and Gai, W. Z. (1991) Ring fission of anthracene by a eukaryote. *Proc. Natl. Acad. Sci. U.S.A.* **88**, 10605–10608.

Hammel, K. E., Gai, W. Z., Green, B., and Moen, M. A. (1992) Oxidative degradation of phenanthrene by the ligninolytic fungus *Phanerochaete chrysosporium*. *Appl. Environ. Microbiol.* **58**, 1832–1838.

Hammer, A., Stolz, A., and Knackmuss, H.-J. (1996) Purification and characterization of a novel type of protocatechuate 3,4-dioxygenase with the ability to oxidize 4-sulfocatechol. *Arch. Microbiol.* **166**, 92–100.

Hansch, C., and Gao, H. (1997) Comparative QSAR: radical reactions of benzene derivatives in chemistry and biology. *Chem. Rev.* **97**, 2995–3059.

Hatakka, A. (1994) Lignin-modifying enzymes from selected white-rot fungi: production and role in lignin degradation. *FEMS Microbiol. Rev.* **13**, 125–135.

Haug, W., Schmidt, A., Nörtemann, B., Hempel, D. C., and Stolz, D. C., Knackmuss, H.-J. (1991) Mineralization of the sulfonated azo dye Mordant Yellow 3 by a 6-aminonaphthalene-2-sulfonate-degrading bacteria consortium. *Appl. Environ. Microbiol.* **57**, 3144–3149.

Heckman, R. A., and Espenson, J. A. (1979) Kinetics and mechanism of oxidation of cobalt(II) macrocycles by iodide, bromide, and hydrogen peroxide. *Inorg. Chem.* **18**, 38–43.

Heinfling, A., Bergbauer, M., and Szewzyk, U. (1997) Biodegradation of azo and phthalocyanine dyes by *Trametes versicolor* and *Bjerkandera adusta*. *Appl. Microbiol. Biotechnol.* **48**, 261–266.

Higson, F. K. (1991) Degradation of xenobiotics by white rot fungi. *Rev. Environ. Contam. Toxicol.* **122**, 111–141.

- Ho, P. C. (1986) Photooxidation of 2,4-dinitrotoluene in aqueous solution in the presence of hydrogen peroxide. *Environ. Sci. Technol.* **20**, 260–267.
- Hoff, T., Liu, S.-Y., and Bollag, J.-M. (1985) Transformation of halogen-, alkyl-, and alkoxy-substituted anilines by a laccase of *Trametes versicolor*. *Appl. Environ. Microbiol.* **49**, 1040–1045.
- Hoigné, J., and Bader, H. (1993) Kinetics of reactions involving chlorine dioxide (OClO) in water. *Water Res.* **28**, 185–194.
- Hoigné, J., Faust, B. C., Haag, W. R., Scully, F. E., Jr., and Zepp, R. G. (1989) Aquatic humic substances as sources and sink of photochemically produced transient reactants. In *Aquatic Humic Substances: Influence on Fate and Treatment of Pollutants* (Suffet, I., and MacCarty, P., eds.) American Chemical Society, Washington, DC, pp. 362–381.
- Hong, A., Zappi, M. E., Kuo, C. H., and Hill, D. (1996) Modeling kinetics of illuminated and dark advanced oxidation processes. *J. Environ. Eng.* **122**, 58–62.
- Hsuanyu, Y., and Dunford, H. B. (1992) Prostaglandin H synthase kinetics: the effect of substituted phenols on cyclooxygenase activity and the substituent effect on phenolic peroxidatic activity. *J. Biol. Chem.* **267**, 17649–17657.
- Huang, M.-T., Miwa, G. T., and Lu, A. Y. H. (1979) Rat liver cytosolic azoreductase. Purification and characterization. *J. Biol. Chem.* **254**, 3930–3935.
- Hustert, K., Zepp, R. G. (1992) Photocatalytic degradation of selected azo dyes. *Chemosphere* **24**, 335–342.
- Idaka, E., Horitsu, H., and Ogawa, T. (1987) Some properties of azoreductase produced by *Pseudomonas cepacia*. *Bull. Environ. Contam. Toxicol.* **39**, 982–989.
- Ince, N. H., and Goenenc, D. T. (1997) Treatability of a textile azo dye by UV/H₂O₂. *Environ. Technol.* **18**, 179–185.
- Jayson, G. G., Parsons, B. J., and Swallow, A. J. (1973) Simple, highly reactive, inorganic chlorine derivatives in aqueous system. Formation using pulses of radiation and their role in the mechanism of the Fricke dosimeter. *J. Chem. Soc. Faraday Trans. 1*, 1597–1607.
- Job, D., and Dunford, H. B. (1976) Substituent effect on the oxidation of phenols and aromatic amines by horseradish peroxidase compound I. *Eur. J. Biochem.* **66**, 607–614.

- Johnson, T. L., Scherer, M. M., and Tratnyek, P. G. (1996) Kinetics of halogenated organic compound degradation by iron metal. *Environ. Sci. Technol.* **30**, 2634–2640.
- Joshi, D. K., and Gold, M. H. (1993) Degradation of 2,4,5-trichlorophenol by the lignin-degrading basidiomycete, *Phanerochaete chrysosporium*. *Appl. Environ. Microbiol.* **59**, 1779–1785.
- Jungclaus, G. A., Games, L. M., and Hites, R. A. (1976) Identification of trace organic compounds in tire manufacturing plant wastewater. *Anal. Chem.* **48**, 1894–1896.
- Kadlubar, F. F. (1987) ISI Atlas of Science. *Pharmacology* **1**, 129–132.
- Kersten, P. J., and Kirk, T. K. (1987) Involvement of a new enzyme, glyoxal oxidase, in extracellular H₂O₂ production by *Phanerochaete chrysosporium*. *J. Bacteriol.* **169**, 2195–2201.
- Kirk, T. K., and Farrell, R. L. (1987) Enzymatic “combustion”: the microbial degradation of lignin. *Annu. Rev. Microbiol.* **41**, 465–505.
- Kirk, T. K., Schultz, E., Connors, W. J., Lorenz, L. F., and Zeikus, J. G. (1978) Influence of culture parameters on lignin metabolism by *Phanerochaete chrysosporium*. *Arch. Microbiol.* **117**, 277–285.
- Kirk, T. K., Tien, M., Kersten, P. J., Mozuch, M. D., and Kalyanaraman, B. (1986) Ligninase of *Phanerochaete chrysosporium*. Mechanism of its degradation of the non-phenolic arylglycerol β -aryl ether substructure of lignin. *Biochem. J.* **236**, 279–287.
- Kobayashi, S., Nakano, M., Kimura, T., and Schaap, P. (1987) On the mechanism of the peroxidase-catalyzed oxygen-transfer reaction. *Biochemistry* **26**, 5019–5022.
- Kormann, C., Bahnemann, D. W., and Hoffmann, M. R. (1988) Photocatalytic production of H₂O₂ and organic peroxides in aqueous suspensions of TiO₂, ZnO, and desert sand. *Environ. Sci. Technol.* **22**, 798–806.
- Krishna, G., Xu, J., and Nath, J. (1986) Comparative mutagenicity studies of azo dyes and their reduction products in *Salmonella typhimurium*. *J. Toxicol. Environ. Health* **18**, 111–119.
- Kuan, I.-C., Johnson, K. A., and Tien, M. (1993) Kinetics analysis of manganese peroxidase: the reaction with manganese complexes. *J. Biol. Chem.* **268**, 20064–20070.
- Kubinyi, H. (1997) QSAR and 3D QSAR in drug design part 1: methodology. *Drug Discovery Today* **2**, 457–467.

- Kulla, H. G., Klausener, F., Meyer, U., Ludeke, B., and Leisinger, T. (1983) Interference of aromatic sulfo groups in the microbial degradation of the azo dyes Orange I and Orange II. *Arch. Microbiol.* **135**, 1-7.
- Kunai, A., Hata, S., Ito, S., and Sasaki, K. (1986) The role of oxygen in the hydroxylation reaction of benzene with Fenton's reagent. ^{18}O tracer study. *J. Am. Chem. Soc.* **108**, 6012-6016.
- Kuo, W. G. (1992) Decolorizing dye wastewater with Fenton's reagent. *Water Res.* **26**, 881-886.
- Laat, J. D., Tace, E., Dore, M. (1994) Degradation of chloroethanes in dilute aqueous solution by $\text{H}_2\text{O}_2/\text{UV}$. *Water Res.* **28**, 2507-2519.
- Langlais, B., Reckhow, D. A., and Brink, D. R. (1991) *Ozone in Water Treatment: Application and Engineering*, 2nd Edn., Lewis Publishers, Chelsea.
- Laszlo, J. (1997) Regeneration of dye-saturated quaternized cellulose by bisulfite-mediated borohydride reduction of dye azo groups: an improved process for decolorization of textile wastewaters. *Environ. Sci. Technol.* **31**, 3647-3653.
- Legrini, O., Oliveros, E., and Braun, A. M. (1993) Photochemical processes for water treatment. *Chem. Rev.* **93**, 671-698.
- Leung, S. W., Watts, R. J., and Miller, G. C. (1992) Degradation of perchloroethylene by Fenton's reagent: speciation and pathway. *J. Environ. Qual.* **21**, 377-381.
- Lin, S. H., and Chen, M. L. (1997) Treatment of textile wastewater by chemical methods for reuse. *Water Res.* **31**, 868-876.
- Lipczynska-Kochany, E. (1991) Degradation of aqueous nitrophenols and nitrobenzene by means of the fenton reaction. *Chemosphere* **22**, 529-536.
- Maguire, R. J., and Tkacz, R. J. (1991) Occurrence of dyes in the Yamaska River, Quebec. *Water Pollut. Res. J. Can.* **26**, 145-161.
- Mallett, A. K., King, L. J., and Walker, R. (1982) A continuous spectrophotometric determination of hepatic microsomal azoreductase activity and its dependence on cytochrome P-450. *Biochem. Pharmacol.* **201**, 589-595.
- Mason, R. P., Peterson, F. J., and Holtman, J. L. (1978) Inhibition of azoreductase by oxygen. The role of the azo anion free radical metabolite in the reduction of oxygen to superoxide. *Mol. Pharmacol.* **14**, 665-671.

- Masten, S. J., and Davies, S. H. (1994) The use of ozonation to degrade organic contaminants in wastewaters. *Environ. Sci. Technol.* **28**, 180A–185A.
- Matheson, L. J., and Tratnyek, P. G. (1994) Reductive dehalogenation of chlorinated methanes by iron metal. *Environ. Sci. Technol.* **28**, 2045–2053.
- Matsui, M., Kobayashi, K., Shibata, K., and Takase, Y. (1981) Ozonation of dyes. II-Ozone treatment of 4-phenylazo-1-naphthol. *J. Soc. Dyers Colourists* **97**, 210–213.
- Matthews, E. J., Spalding, J. W., and Tennant, R. W. (1993) Transformation of BALB/c-3T3 cells. V. transformation responses of 168 chemicals compared with mutagenicity in *Salmonella* and Carcinogenicity in rodent bioassays. *Environ. Health Perspect.* **101**(Suppl. 2), 347–482.
- Matthews, R. W. (1991) Photooxidative degradation of coloured organics in water using supported catalysis TiO₂ on sand. *Water Res.* **25**, 1169–1176.
- McCann, J., Ames, B. N. (1975) Detection of carcinogens and mutagens in the *Salmonella*/microsome test. Assay of 300 chemicals: discussion. *Proc. Natl. Acad. Sci. U.S.A.* **73**, 950–954.
- McCann, J., Choi, E., Yamasaki, E., Ames, B. N. (1975) Detection of carcinogens as mutagens in the *Salmonella*/microsome test. Assay of 300 chemicals. *Proc. Natl. Acad. Sci. U.S.A.* **72**, 5135–5139.
- Morris, J. G. (1990) *A Biologist's Physical Chemistry*, Chapman and Hall, New York, pp. 236–277.
- Muralikrishna, C., and Renganathan, V. (1993) Peroxidase-catalyzed desulfonation of 3,5-dimethyl-4-hydroxy and 3,5-dimethyl-4-aminobenzenesulfonic acids. *Biochem. Biophys. Res. Commun.* **197**, 798–804.
- Murphy, A. P., Boegli, W. J., Price, M. K., and Moody, C. D. (1989) A Fenton-like reaction to neutralize formaldehyde waste solutions. *Environ. Sci. Technol.* **23**, 166–169.
- Nelson, C. R., and Hites, R. A. (1980) Aromatic amines in and near the Buffalo River. *Environ. Sci. Technol.* **14**, 1147–1149.
- Pagga, U., and Brown, D. (1986) The degradation of dye stuffs in aerobic biodegradation tests. *Chemosphere* **15**, 479–491.
- Paris, D. F., Wolfe, N. L., and Steen, W. C. (1982) Structure–activity relationships in microbial transformation of phenols. *Appl. Environ. Microbiol.* **44**, 153–158.

- Park, J., and Shore, J. J. (1984) Water for the dyehouse: supply, consumption, recovery and disposal. *J. Soc. Dyers Colourists* **100**, 383–399.
- Pasti-Grigsby, M. B., Paszczynski, A., Goszczynski, S., Crawford, D. L., and Crawford, R. L. (1992) Influence of aromatic substitution patterns on azo dye degradability by *Streptomyces* spp. and *Phanerochaete chrysosporium*. *Appl. Environ. Microbiol.* **58**, 3605–3613.
- Paszczynski, A., and Crawford, R. L. (1991) Degradation of azo compounds by ligninase from *Phanerochaete chrysosporium*: involvement of veratryl alcohol. *Biochem. Biophys. Res. Commun.* **178**, 1056–1063.
- Paszczynski, A., Pasti-Grigsby, M. B., Goszczynski, S., Crawford, D. L., and Crawford, R. L. (1991) New approach to improve degradation of recalcitrant azo dyes by *Streptomyces* spp. and *Phanerochaete chrysosporium*. *Enzyme Microb. Technol.* **13**, 378–384.
- Paszczynski, A., Pasti-Grigsby, M. B., Goszczynski, S., Crawford, R. L., and Crawford, D. L. (1992) Mineralization of sulfonated azo dyes and sulfanilic acid by *Phanerochaete chrysosporium* and *Streptomyces chromofuscus*. *Appl. Environ. Microbiol.* **58**, 3598–3604.
- Pignatello, J. J. (1992) Dark and photoassisted Fe⁺³-catalyzed degradation of Chlorophenoxy herbicides by hydrogen peroxide. *Environ. Sci. Technol.* **31**, 944–951.
- Prat, C., Vecente, M., and Esplugas, S. (1988) Treatment of bleaching waters in the paper industry by hydrogen peroxide and ultraviolet radiation. *Water Res.* **22**, 663–668.
- Rafii, F., Franklin, W., and Cerniglia, C. E. (1990) Azoreductase activity of anaerobic bacteria isolated from human intestinal microflora. *Appl. Environ. Microbiol.* **56**, 2146–2151.
- Reineke, W., and Knackmuss, H.-J. (1978) Chemical structure and biodegradability of halogenated aromatic compounds. Substituent effects on 1,2-dioxygenation of benzoic acid. *Biochim. Biophys. Acta* **542**, 412–423.
- Renganathan, V., and Gold, M. H. (1986) Spectral characterization of the oxidized states of lignin peroxidase, an extracellular heme enzyme from the white rot basidiomycete *Phanerochaete chrysosporium*. *Biochemistry* **25**, 1626–1631.
- Riefe, A. (1992) Dyes, environmental chemistry. In *Kirk-Othmer Encyclopedia of Chemical Technology*, 4th Edn., Vol. 8 (Howe-Grant, M., ed.), Wiley and Sons, New York, pp. 753–783.

Ritchie, C. D. (1990) *Physical Organic Chemistry*, 2nd Ed, Marcel Dekker, New York, pp. 85–115.

Roe, J. A., and Goodin, D. V. (1993) Enhanced oxidation of aniline derivatives by two mutants of cytochrome *c* peroxidase at Tryptophan 51. *J. Biol. Chem.* **268**, 20037–20045.

Ruppert, G., Bauer, R., and Heisler, G. (1994) UV-O₃, UV-H₂O₂, UV-TiO₂ and the photo-Fenton reaction-comparison of advanced of oxidation processes for wastewater treatment. *Chemosphere* **28**, 1447–1454.

Ryan, T. P., and Bumpus, J. A. (1989) Biodegradation of 2,4,5-trichlorophenoxyacetic acid in liquid culture and soil by the white-rot fungus *Phanerochaete chrysosporium*. *Appl. Microbiol. Biotechnol.* **31**, 302–307.

Ryu, K., and Dordick, J. S. (1992) How do organic solvents affect peroxidase structure and function? *Biochemistry* **31**, 2588–2598.

Sandhu, P., and Chipman, J. K. (1990) Bacterial mutagenesis and hepatocyte unscheduled DNA synthesis induced by chrysoidine azo-dye components. *Mutation Res.* **240**, 227–236.

Sanglard, D., Leisola, M. S. A., and Fiechter, A. (1986) Role of extracellular ligninases in biodegradation of benzo[a]pyrene by *Phanerochaete chrysosporium*. *Enzyme Microb. Technol.* **8**, 209–212.

Scheline, R. R., Nygaard, R. T., and Longberg, B. (1970) Enzymatic reduction of the azo dye, acid yellow, by extracts of *Streptococcus faecalis* isolated from rat intestine. *Food Cosmet. Toxicol.* **8**, 55–58.

Scherer, M. M., and Tratnyek, P. G. (1995) Dechlorination of carbon tetrachloride by iron metal: effect of reactant concentrations. In *209th National Meeting ACS. Preprint Extended Abstracts, Division of Environmental Chemistry*. Anaheim, CA, **35**, 805–806.

Scherer, M. M., Balko, B. A., and Tratnyek, P. G. (1998) The role oxides in reduction reactions at the metal water interface. *ACS Symp. Ser.*, in press.

Schliephake, K., and Lonergan, G. T. (1997) Laccase variation during dye decolourisation in a 200 L packed-bed bioreactor. *Biotechnol. Lett.* **18**, 881–886.

Sedlak, D. L., and Andren, A. W. (1991) Oxidation of chlorobenzene with Fenton's reagent. *Environ. Sci. Technol.* **25**, 777–782.

- Shaul, G. M., Holdsworth, T. J., Dempsey, C. R., and Dostal, K. A. (1991) Fate of water soluble azo dyes in the activated sludge process. *Chemosphere* **22**, 107-119.
- Shin, K.-S., OH, I.-K., and Kim, C.-J. (1997) Production and purification of Remazol Brilliant Blue R decolorizing peroxidase from the culture filtrate of *Pleurotus ostreatus*. *Appl. Environ. Microbiol.* **63**, 1744-1748.
- Shorter, J. (1982) *Correlation Analysis of Organic Reactivity with Particular Reference to Multiple Regression*, John Wiley & Sons, Chichester, England, p. 235.
- Shu, H.-Y., and Huang, C.-R. (1995) Degradation of commercial azo dyes in water using ozonation and UV enhanced ozonation process. *Chemosphere* **31**, 3813-3825.
- Shu, H.-Y., Huang, C.-R., and Chang, M.-C. (1994) Decolorization of mono-azo dyes in wastewater by advanced oxidation process: a case study of Acid Red 1 and Acid Yellow 23. *Chemosphere* **29**, 2597-2607.
- Solozhenko, E. G., Soboleva, N. M., and Goncharuk, V. V. (1995) Decolorization of azodye solutions by Fenton's oxidation. *Water Res.* **29**, 2206-2210.
- Spadaro, J. T., and Renganathan, V. (1994) Peroxidase-catalyzed oxidation of azo dyes: mechanism of Disperse Yellow 3 degradation. *Arch. Biochem. Biophys.* **312**, 301-307.
- Spadaro, J. T., Gold, M. H., and Renganathan, V. (1992) Degradation of azo dyes by the lignin-degrading fungus *Phanerochaete chrysosporium*. *Appl. Environ. Microbiol.* **58**, 2397-2401.
- Spadaro, J. T., Isabelle, L., and Renganathan, V. (1994) Hydroxyl radical mediated degradation of azo dyes: evidence for benzene generation. *Environ. Sci. Technol.* **28**, 1389-1393.
- Spiro, M. (1989) Heterogeneous catalysis of solution reactions. In *Chemical Kinetics: Reactions at the Liquid-Solid Interface*, Vol. 28 (R. G. Compton, ed.), Elsevier, Amsterdam, pp. 69-166.
- Stumm, W. (1992) *Chemistry of the Solid-Water Interface: Progress at the Mineral-Water and Particle-Water Interface of Natural Systems*, Wiley & Sons, New York, p. 428.
- Tang, W. Z., and An, H. (1995) UV/TiO₂ photocatalytic oxidation of commercial dyes in aqueous solutions. *Chemosphere* **31**, 4157-4170.
- Tang, W. Z., and Chen, R. Z. (1996) Decolorization kinetics and mechanism of commercial dyes by H₂O₂/iron powder system. *Chemosphere* **32**, 947-958.

- Thurston, C. F. (1994) The structure and function of fungal laccases. *Microbiology* **140**, 19–26.
- Tien, M. (1987) Properties of ligninase from *Phanerochaete chrysosporium* and their possible applications. *Crit. Rev. Microbiol.* **15**, 141–168.
- Tien, M., and Kirk, T. K. (1983) Lignin-degrading enzyme from the hymenomycete *Phanerochaete chrysosporium* burds. *Science* **221**, 661–663.
- Tien, M., and Kirk, K. T. (1984) Purification, characterization, catalytic properties of a unique H₂O₂-requiring oxygenase. *Proc. Natl. Acad. Sci. U.S.A.* **81**, 2280–2284.
- Tincher, W. C., and Robertson, J. R. (1982) Analysis of dyes in the textile dyeing wastewater. *Textile Chem. Colorist* **14**, 269–275.
- Tratnyek, P. G. (1996) Putting corrosion to use: remediation of contaminated groundwater with zero-valent metals. *Chem. Ind. (London)* **13**, 499–503.
- Tratnyek, P. G. (1998) Correlation analysis of environmental reactivity of organic substances. In *Perspectives in Environmental Chemistry* (Macalady, D. L., ed.), Oxford University Press, New York, pp. 167–194.
- United States International Trade Commission. *Synthetic Organic Chemicals, U.S. Production and Sales, 1994*. Investigation 332–135, Publication 2933, November, 1995.
- Vaidya, A. A., and Datye, K. V. (1982) Environmental pollution during chemical processing of synthetic fibers. *Colourage* **14**, 3–10.
- Valli, K., and Gold, M. H. (1991) Degradation of 2,4-dichlorophenol by the lignin-degrading fungus *Phanerochaete chrysosporium*. *J. Bacteriol.* **173**, 345–352.
- Valli, K., Wariishi, H., and Gold, M. H. (1990) Oxidation of monomethoxylated aromatic compounds by lignin peroxidase: role of veratryl alcohol in lignin biodegradation. *Biochemistry* **29**, 8535–8539.
- Valli, K., Brock, B. J., and Gold, M. H. (1992a) Degradation of 2,4-nitrotoluene by the lignin-degrading fungus *Phanerochaete chrysosporium*. *Appl. Environ. Microbiol.* **58**, 221–228.
- Valli, K., Wariishi, H., and Gold, M. H. (1992b) Degradation of 2,7-dichlorodibenzo-*p*-dioxin by the lignin-degrading basidiomycete *Phanerochaete chrysosporium*. *J. Bacteriol.* **174**, 2131–2137.

- Vinodgopal, K., and Kamat, P. (1995) Enhanced rates of photocatalytic degradation of an azo dye using SnO₂/TiO₂ coupled semiconductor thin films. *Environ. Sci. Technol.* **29**, 841–845.
- Wade, L. G. (1991) *Organic Chemistry*, Prentice-Hall, Englewood Cliffs, NJ, p. 861.
- Walker, R. (1970) The metabolism of azo compounds: a review of the literature. *Food Cosmet. Toxicol.* **8**, 659–676.
- Walker, R., Gingell, R., and Murrels, D. F. (1971) Mechanism of azo reduction by *Streptococcus faecalis*. I. Optimization of assay conditions. *Xenobiotica* **1**, 221–229.
- Walling, C. (1975) Fenton's reagent revisited. *Acc. Chem. Res.* **8**, 125–131.
- Walling, C., and Kato, S.-I. (1971) Oxidation of alcohols by Fenton's reagent: the effect of copper ion. *J. Am. Chem. Soc.* **93**, 4275–4281.
- Wariishi, H., and Gold, M. H. (1990) Lignin peroxidase compound III. Mechanism of formation and decomposition. *J. Biol. Chem.* **265**, 2070–2077.
- Wariishi, H., Akileswaran, L., and Gold, M. H. (1988) Manganese peroxidase from the basidiomycete *Phanerochaete chrysosporium*: spectral characterization of the oxidized states and catalytic cycle. *Biochemistry* **27**, 5365–5370.
- Wariishi, H., Dunford, H. B., MacDonald, I. D., and Gold, M. H. (1989a) Manganese peroxidase from the lignin-degrading basidiomycete *Phanerochaete chrysosporium*. *J. Biol. Chem.* **264**, 3335–3340.
- Wariishi, H., Valli, K., and Gold, M. H. (1989b) Oxidative cleavage of a phenolic diarylpropane lignin model dimer by manganese peroxidase from *Phanerochaete chrysosporium*. *Biochemistry* **28**, 6017–6023.
- Wariishi, H., Valli, K., and Gold, M. H. (1992) Manganese(II) oxidation by manganese peroxidase from the basidiomycete *Phanerochaete chrysosporium*. *J. Biol. Chem.* **267**, 23688–23695.
- Watts, R. J., Udell, M. D., Rauch, P. A., and Leung, S. W. (1990) Treatment of pentachlorophenol-contaminated soils using Fenton's reagent. *Haz. Waste Haz. Mater.* **7**, 335–354.
- Weber, E. J. (1996) Iron-mediated reductive transformation: investigation of reaction mechanism. *Environ. Sci. Technol.* **30**, 716–719.
- Weber, E. J., and Adams, R. L. (1995) Chemical- and sediment-mediated reduction of the azo dye Disperse Blue 79. *Environ. Sci. Technol.* **29**, 1163–1170.

Weber, E. J., and Wolfe, N. L. (1987) Kinetic studies of the reduction of aromatic azo compounds in anaerobic sediment/water systems. *Environ. Toxicol. Chem.* **6**, 911-919.

Wuhrmann, K., Mechsner, K., and Kappeler, T. (1980) Investigation on rate-determination factors in the microbial reduction of azo dyes. *European J. Appl. Microbiol. Biotechnol.* **9**, 325-338.

Xu, F. (1996) Oxidation of phenols, anilines, and benzenethiols by fungal laccases: Correlation between activity and redox potentials as well as halide inhibition. *Biochemistry* **35**, 7608-7614.

Yadav, J. S., and Reddy, C. A. (1992) Non-involvement of lignin peroxidase and manganese peroxidase in a 2,4,5-trichlorophenoxyacetic acid degradation by *Phanerochaete chrysosporium*. *Biotechnol. Lett.* **14**, 1089-1092.

Yang, Y., Ladisch, C. M., and Ladisch, M. R. (1988) Cellulosic adsorbents for treating textile mill effluents. *Enzyme Microb. Technol.* **10**, 632-636.

Yatome, C., Matsufuru, H., Taguchi, T., and Ogawa, T. (1993) Degradation of 4'-dimethylaminoazobenzene-2-carboxylic acid by *Pseudomonas stutzeri*. *Appl. Microbiol. Biotechnol.* **39**, 778-781.

Young, L., and Yu, J. (1997) Ligninase-catalysed decolorization of synthetic dyes. *Water Res.* **31**, 1187-1193.

Zimmerman, T., Kulla, H. G., and Leisinger, T. (1982) Properties of purified Orange II azoreductase, the enzyme initiating azo dye degradation by *Pseudomonas* KF46. *Eur. J. Biochem.* **129**, 197-203.

Zollinger, H. (1987) *Color Chemistry-Syntheses, Properties and Applications of Organic Dyes and Pigments*, VCH Publishers, New York, pp. 92-102.

BIOGRAPHICAL SKETCH

Sangkil Nam was born January 15, 1960, in Taejon, Korea. He earned a B.S. in Chemistry from the University of Kansas in 1994 and began his graduate studies in the Department of Biochemistry and Molecular Biology at the Oregon Graduate Institute of Science and Technology in 1994.